

FOUNDATION EFFECT FROM PIONEER SPECIES AFTER PHYSICAL  
DISRUPTION OF THE FISH SKIN MICROBIOME OF *GAMBUSIA AFFINIS*

---

A Thesis

Presented to

The Faculty of the Department of Biological Sciences

Sam Houston State University

---

In Partial Fulfillment

of the Requirements for the Degree of

Master of Science

---

by

Javier Angel Gomez

August, 2020

FOUNDATIONAL EFFECT FROM PIONEER SPECIES AFTER PHYSICAL  
DISRUPTION OF THE FISH SKIN MICROBIOME OF *GAMBUSIA AFFINIS*

by

Javier Angel Gomez

---

APPROVED:

Todd P. Primm, PhD  
Committee Director

Anne A. Gaillard, PhD  
Committee Member

Madhusudan Choudhary, PhD  
Committee Member

Carmen Montana, PhD  
Committee Member

John Pascarella, PhD  
Dean, College of Biological Sciences

## ABSTRACT

Gomez, Javier Angel, *Foundation Effect from Pioneer Species After Physical Disruption of the Fish Skin Microbiome of Gambusia affinis*. Master of Science (Biology), August, 2020, Sam Houston State University, Huntsville, Texas.

Multicellular organisms provide an important ecosystem for bacteria to live and thrive upon, and in return, they support the host in many aspects, like protection from pathogens and enhancing digestion. The microbiome has been found to have profound effects on host health. A complex problem to tackle is understanding how the microbial community fails to recover after a disruption, such as antibiotic-associated enterocolitis in patients. Temporary domination of the community after disruption by one pioneer species is commonly observed, but the impact of this is unclear. Application of ecological theories may lead to more accurate prediction of such negative side effects. In this study, the fish skin microbiome of *Gambusia affinis* was physically disrupted and three different pioneer species were seeded. A pioneer is the first organism dominant in abundance after a community disturbance during community succession. Community biochemical profiles were measured by 25 different tests and community composition was observed by 16S rRNA gene sequencing. At 240 hours in recovery, community composition was different for all three treatments, suggesting a foundation effect for each of the pioneers. These results suggest pioneer species may act as foundation species by modulating the ecosystem, and thus affect the final recovery community structure. This suggests application of selected probiotics after disruption allow prevention of negative side effects by changing climax community composition.

**KEY WORDS:** Microbiome, Pioneer species, Foundation species, Disruption, Natural pioneer, Introduced pioneer, Succession, Microbial ecology, Resilience.

## TABLE OF CONTENTS

	Page
ABSTRACT.....	iii
TABLE OF CONTENTS.....	iv
LIST OF TABLES .....	v
LIST OF FIGURES .....	vii
CHAPTER I: INTRODUCTION .....	1
Theories .....	2
Hypothesis/Objectives .....	8
CHAPTER II: PROOF OF PRINCIPLE ( <i>E.COLI</i> CHAPTER).....	11
Materials and Methods .....	11
K12 May act as a Foundation Species .....	18
Results.....	18
Discussion.....	43
Conclusion .....	47
CHAPTER III: PIONEER SPECIES TESTED AS FOUNDATION .....	48
Fish Skin Pioneers .....	48
Materials and Methods .....	55
Results.....	58
Discussion.....	102
Conclusion .....	113
REFERENCES .....	117
VITA.....	133

## LIST OF TABLES

	Page
1 Tracking of introduced pioneer K12 by plating CFU.....	21
2 Good's coverage of the sequenced 16S V3-V4 for each sample.....	27
3 Shannon's Index of each sample at ESV level. ....	28
4 Mean and standard deviation of Shannon's Index of groups at the ESV level.....	29
5 Shannon's Index of each sample at genus level.....	30
6 Average Shannon's Diversity Index at genus level by time (hours). ....	31
7 Biochemical activity of fish skin microbiota at major sampling points. ....	34
8 Averages of core taxa at the genus level in every sample. ....	39
9 Environmental characteristics collected at major sampling points using API Freshwater Master Test Kit and Tetra EasyStrips 6-in-1 Aquarium Test Strips. ....	41
10 Correlation of water chemistry with community changes over time by regression. ..	41
11 FMI1B biochemical profile.....	50
12 FBI408 biochemical profile. ....	52
13 FSI38B biochemical profile. ....	54
14 Tracking of introduced pioneer S.rhizophilia by plating CFU. ....	62
15 Tracking of introduced pioneer A.hydrophilia by plating CFU. ....	63
16 Tracking of introduced pioneer Brevibacterium by plating CFU.....	64
17 Biochemical activity of fish skin microbiota at major sampling times. ....	66
18 Sequence coverage for all samples. ....	72
19 Sequence coverage per group. ....	74
20 Identification of dominant ESVs. ....	84

21	Environmental characteristics collected at major sampling points using API Freshwater Master Test Kit and Tetra EasyStrips 6-in-1 Aquarium Test Strips. ....	98
22	Correlation of water chemistry with community changes over time. ....	99

## LIST OF FIGURES

	<b>Page</b>
1 Experimental design of foundation species experiment. ....	16
2 Flowchart summarizing the major concepts of the study. ....	16
3 Normalized fish skin CFU by fish weight over time. ....	20
4 CFU comparison of total counts on NA and XLD44 selective for E.coli K12. Symbols represent mean and error bars represent standard deviation. ....	22
5 Boxplot of CFU normalized by fish weight showing Pre-treatment and Post-Rinse treatments. ....	23
6 Boxplot comparing pre-treatment samples and 240-hour samples of normalized CFU counts per fish weight. ....	24
7 Rarefaction curve of samples showing sampling depth. ....	26
8 Strip chart of alpha diversity (# of genera) at 240 hours per treatment. ....	32
9 Strip chart of Shannon diversity index at 240 hours per group. ....	33
10 Principal components analysis of biochemical profiles across the major sampling points. ....	35
11 Bar graphs of relative abundance of ten most abundant genera across all samples gathered by groups. ....	37
12 Boxplots showing relative abundance of the five most abundant genera across samples. ....	38
13 NMDS of all genera comparing composition of communities across major sampling times. ....	40

14	NMDS of all genera showing the correlation of fish skin community composition and water chemistry across major sampling times. ....	42
15	FMI1B morphology. ....	50
16	FBI408 morphology.....	52
17	FSI38B morphology.....	54
18	Experimental design of BCE experiments.....	56
19	Line plot of CFU by group across time (hours).....	60
20	Scatterplot of CFU across the major sampling times.....	61
21	Line plot of CFU of PAIN and NA plates tracking <i>S.rhizophilia</i> .....	62
22	Line plot of CFU of TCBSAN and NA plates tracking <i>A.hydrophilia</i> . ....	63
23	Line plot of CFU of PAIN and NA plates tracking <i>Brevibacterium</i> . ....	64
24	Fish skin microbiome biochemical profile. ....	69
25	Rarefaction curves showing sampling depth of all samples .....	71
26	Mean observed number of ESVs across groups. ....	75
27	Shannon Diversity Index of groups, calculated at the ESV level. ....	77
28	Average evenness index including all ESVs. ....	79
29	Richness of groups at the level of genus.....	80
30	Simpson's evenness of groups at the level of genus.....	82
31	Abundance of dominant ESVs across major sampling times for all samples.....	83
32	Abundance of dominant genera across major sampling times across all samples.....	85
33	Strip plot of the five most abundant genera across all groups. ....	89
34	Strip plot of the next five most abundant genera (6 through 10-most) across all groups.....	91



35	Relative abundance of core ESVs in all groups.....	93
36	NMDS of all ESVs. Non-metric multidimensional scaling visualization of the similarity (Bray-Curtis dissimilarity matrix calculated from all ESVs) between the communities, with each symbol representing one fish community. ....	94
37	NMDS of abundant ESVs. Analysis includes only ESVs that are above 0.1% abundance in each sample using Bray-Curtis distance. ....	95
38	NMDS of all genera using Bray-Curtis distance. ....	96
39	NMDS of all ESVs using Bray-Curtis distance, and the correlation of water chemistry and samples. ....	100
40	Homogeneity of pre-treatment, drift and treatments at 240 hours.....	101
41	Foundation effect recovery pathway after pioneer species inoculation.....	115

## **CHAPTER I**

### **Introduction**

All living organisms interact closely among each other, and a specific type of interaction of increased recent scientific interest is the interaction between multicellular organisms and bacteria. Multicellular organisms provide an important ecosystem for bacteria to live and thrive upon, and in return, they help the host in many aspects, such as protection from pathogens, and enhancing digestion (Aidy et al., 2013; Mach et al., 2015; Theriot & Young, 2013). The microbiome (i.e., microbial community, or microbiota) refers to both the microorganisms in the environment and the gene pool of the microorganisms in the environment. The importance of these microorganisms and the interactions between them and the host are critical in many aspects of the development of the host (D'Argenio & Salvatore, 2015; Van et al., 2015). Bacteria and the host benefit from each other in a symbiosis. Currently, the microbiome is a highly active and expanding area of research, with over 12,000 publications between 2013 and 2017 on just the gut microbiome (Cani, 2018).

To gain a better understanding of the close interactions between humans and microbiomes, the National Institutes of Health (NIH) funded the Human Microbiome Project (HMP, 2012), with the primary task to categorize and generate a “map” of the composition of the microbiome of healthy individuals. Initially, the HMP (2012) reported minimal information of the intricate interaction of the human host and the bacteria living on them, yet it gave insights into the complex symbiotic relationship between humans and bacteria. One of the most important findings of the HMP (2012) was the conserved “core” of metabolic pathways across bacterial communities within one

body location (such as the tongue) and how gene copy numbers representing pathways are stable even when the variance of bacterial composition is dramatic. These findings suggest that the metabolism (such as lactose fermentation) of community members is more important than the species identification. Also, the data indicate how the community composition of samples from body sites cluster together, such as communities from the intestine are more related to each other than to skin (Gilbert et al., 2018, HMP, 2012). Through quality inquiry and research over time, the HMP reported important information that expanded the human microbiome project, which focuses on understanding the variation of microbes among healthy individuals to find signature species in their respective microbiomes. The findings of the original HMP (2012) allowed researchers to understand the importance of these symbiotes and how crucial these organisms are for daily body functions. Although microbiomes can be quite complex and have a close relationship with their hosts, examining microbiomes from an ecological perspective and using ecological theories could help researchers discover patterns to understand the system on a broader level.

## **Theories**

### ***Disruption***

One complex problem is understanding the effects a disruption has on the microbiome community. The stability of the microbiome plays an important role in the host, and many researchers have reported that disruption of the microbiome can cause disease of the host. A common form of disruption of the microbiome is the use of antibiotics. Rising problems with the use of antibiotics are *Clostridium difficile* infections (CDI) and post-antibiotic enterocolitis (Cammarota et al., 2015). Researchers

have reported that antibiotics can significantly shift the microbiome community structure by lowering overall diversity and losing rare species of bacteria that could irreversibly affect the host's microbiome (Dethlefsen et al., 2008; Rebecca et al., 2018; Simon et al., 2015; Zaura et al., 2015). Certain species of bacteria are targets of the antibiotic, allowing other species the advantage by decreasing competition within the environment. The exact mechanisms by which these problems arise are not well understood because of the variability of the microbiome from human to human (Dethlefsen et al., 2011). Clearly, antibiotics can have a large effect on the host because microbiome dynamics remain poorly understood.

A consistent trend following disruption of the microbiome is loss of microbiome diversity, and more intriguingly, often a bloom of one specific taxon dominates the community temporarily (Brumlow et al., 2019). A credible theory on how microbiome communities recover after disruption is still lacking. Shaw et al. (2019) suggested examining microbiomes using a stability landscape framework where microbiome communities are not fixed, but dynamic. Forces (disruptions) can act on microbiome communities, shifting communities from equilibrium into a different position on the landscape. The type of disruption is continuous (presses) or sudden (pulses) and affects where the microbiome will shift on the landscape because presses and pulses create different degrees of disturbance. A course of antibiotics can be thought of as a press disturbance that affects the microbiome. Antibiotic treatment can have a range of effects on the host because host heterogeneity is another factor that adds complexity to the system (Gibson et al., 2016). Antibiotics are valuable tools, yet understanding antibiotic-

associated microbiome disruptions can be challenging and complex because of the overall effects on the microbes and the host.

***Succession (predictable changes of species composition over time due to disruption or disturbance)***

The process of primary succession refers to an event where organisms first colonize a virgin habitat (Walker et al., 2011). Primary succession is an important event because the pioneer species that first colonize the habitat could modulate the successions until the shifting communities stabilize (Walker et al., 2011). In mammals, primary succession begins shortly after birth with inoculation from the birth canal (Pantoja et al., 2013), and during breast-feeding (Van et al., 2015). However, controversy over first succession in mammals with the discovery of the maternal microbiome and its effects on development exists (Gritz and Bhandari et al., 2015; Macpherson et al., 2017, Pronovost et al., 2018). Primary succession is important because the pioneer species that colonize the community help shape the environment, but researchers have reported that microbiomes display large shifts in their abundances and compositions in the early stages of weaning (Koenig et al., 2011). When established microbial communities are disrupted, the process of secondary succession occurs.

In secondary succession, a **pioneer species** is defined as one that better adapts and dominates after the disturbance. Recovery of microbiomes after disruptions is difficult to predict given the complexity of the communities and host/microbe interactions. A potential complication in humans after antibiotic treatment is CDI, and this infection can be seen as a pioneer species effect because *C. difficile* is pre-existing in the patient gut at low abundance and then blooms after the antibiotic depletes other taxa. The host

microbiome composition does not return to normal during CDI, and typically the host becomes more susceptible to future CDI, suggesting persistent abnormalities of the community (Theriot & Young, 2015).

As described by Collen and Slatyer (1977), disruptions or disturbances that affect the community can make prior occupied spaces available by lowering total richness. Following disruption of the microbiome, domination by one taxon is common and in many mammalian gut models, a transient *Enterobacteriaceae* bloom has been noted, which reduces the alpha diversity (the total number of species present) of the gut microbiome (Zhu et al., 2018). The mechanisms driving these taxa blooms are not well understood, nor is how the climax community remains susceptible after disruption. However, a current theory by Winter et al. (2013) and confirmed by other researchers is that gut inflammation drives an increase in reactive oxygen and nitrogen species, such as hydrogen peroxide or nitrate (Spees et al., 2013; Zheng et al., 2017). Further increase of these chemicals serve as alternate electron acceptors to give *Enterobacteriaceae* more efficient metabolism than other gut taxa (mostly obligate anaerobes that only ferment) and thus a survival advantage. Further Zhu et al., (2018) has provided a possible treatment based on Winter's theory. Tungstate, which blocks usage of these electron acceptors by inhibiting the electron transport chain, prevented the *Enterobacteriaceae* bloom in mice following induction of gut inflammation by dextran sulfate sodium. An increase in abundance of certain bacteria in the environment drives a specific set of pathways that generate or degrade a specific set of metabolites (El et al., 2013; Nobel et al., 2015). Furthermore, even short-term use of antibiotics can possibly promote conditions such as diabetes, yeast overgrowth, inflammatory bowel disease,

cardiovascular disease, and immune dysregulation (Buffie et al., 2012; Lau et al., 2017; Ni et al., 2017).

### ***Resilience***

Many researchers have published on the importance of maintaining a balance between the host and its microbiome to maintain the host's health (Greenblum et al., 2012; Scher et al., 2015; Singh et al., 2017; Wu et al., 2011). These findings strongly support the importance of maintaining stability in the microbiome composition as disruptions can have adverse effects and impact the host's health. Interestingly, a high degree of functional redundancy has been reported in microbiome studies (Jorth, 2014; Lozupone et al., 2012) and even some researchers have argued to apply Waddington's (1942) view of an epigenetic landscape (Moya & Ferrer et al., 2016) to the microbiome with phenotypic changes from birth to death. Unlike mammals and plants, bacteria have the ability to dramatically change their "food source" based on their environment, which makes microbiomes even a more complicated and intricate system to study. In ecology, the resilience refers to the capacity of the community to resist change in composition and function from a disruption and the speed of recovery from the disruption of the disturbance (Folke et al., 2014; Holling, 1973; Tilman & Downing, 1994).

Many questions remain when trying to apply community ecology to understand what happens in microbiome disruption. What effects the transient bloom of pioneer taxa have on the future microbiome is still unclear. In ecology, the term **foundation species** refers to a species that has a strong role in structuring a community. Their role in the community is defined by: 1) being numerically abundant and dominating the biomass of the community, 2) having a "base" connection or central role in the network of the

community, with many interactions with multiple other species and 3) having interactions that usually reflect non-trophic or mutualistic relationships (Ellison, 2019). By having a central role in the community and numerous interactions (directly or indirectly) with other species, foundation species should heavily affect nutrient cycling in the ecosystem. Thus, the presence or absence of a foundation species would strongly affect community composition and function.

In this study, I used the freshwater species Western mosquitofish from the Poeciliidae family, *Gambusia affinis*, as a model organism to investigate the microbiome mucosal surfaces. This model allows for easy manipulation of the skin mucosal microbiome, thus allowing me to experimentally introduce selected pioneer species and observe the effects. The fish are vertebrates and, thus, have acquired immunity like humans, which strongly affects host-microbiome interactions (Gaulke et al., 2019; Kayama & Takeda, 2016; Shi et al., 2017; Wang et al., 2019). I was interested in mucosal surfaces because these surfaces harbor larger numbers of bacteria and more closely interact with the host. In humans, mucosal microbiomes include the gut, lung, urinary, and reproductive tracts.

Historically, *Gambusia* was introduced and spread in North America by humans to aid with control of mosquito population by eating larva (Pyke, 2008). This fish has been used to study the evolution of mating behavior (Chen et al., 2018; Hou et al., 2018), biology of aquatic invasive species (Bickerton et al., 2018; Gao et al., 2019), and toxicology of small fish (Hou et al., 2017; Lee et al., 2017), and with its genome published to facilitate genetic studies (Hoffberg et al., 2018). In this study, the *Gambusia* skin microbiota was disrupted using a pulse disruption called the rinsing method, which



has no residual effect, unlike antibiotics. The ability to challenge the fish mucosal microbiome with a selected pioneer species after rinse disruption provides a rather unique vertebrate system which could be useful to follow specific trends and shed light on how the pioneer species may act as foundational to affect climax community composition and function. Further, understanding this principle may allow researchers to take a more accurate approach on choosing probiotics to restore disrupted microbiomes.

## **Hypothesis/Objectives**

### ***Hypothesis #1***

*Climax community composition is affected by the pioneer species, i.e. the pioneer acts as a foundation species.*

After disruption of the stable microbiome community, specific bacteria species can take advantage of the open niches and proliferate because of the lack of competition. When *Gambusia* were treated with the broad-spectrum antibiotic rifampicin, one Operational Taxonomic Unit (OTU) (identified as genus *Myroides*) became more than 60% of the abundance of the skin microbiome on day two of recovery, and then fell to 1.2% abundance after one week (Carlson et al., 2017). The pioneer species temporarily dominated the bacterial community, which suggested that it could be a major driving force in the overall environment. Certain biological functions or pathways could be enhanced during this pioneer effect, possibly bringing different successions, depending on the pioneer functional role. Specific metabolic pathways could be possible key factors that determine the climax community composition, suggesting that similar microbiome composition will not recover equally, depending on the functions of the particular pioneer, (i.e., depleting certain nutrients or generating certain metabolic byproducts). For

example, in the human vagina, *Lactobacillus* can colonize, which then generate lactic acid from glycogen secreted by the human epithelium, which in turn drives down the pH to allow only certain species to later thrive (Tachedjian, et al., 2017). Thus, *Lactobacillus* acts as a foundation species based on this metabolism. Alternatively, because the high abundance of the pioneer is transient, it may not have a strong effect on the climax, recovered community composition.

### ***Hypothesis #2***

*The climax community biochemical functions are affected by the pioneer species.*

Stable bacterial communities tend to have a high diversity of species of bacteria with some abundant “dominant” species. Once this community is disturbed, the pioneer species has the ability to thrive in the environment, and it could be imposing a driving set of metabolic activities in the environment. For example, a nitrate-reducing pioneer may significantly change nitrogen metabolism in the recovering microbiome as it removes nitrate and generates nitrite, which would then benefit bacteria that utilize nitrite. Because the pioneer species has specific metabolic capabilities, it could control succession and be a selective factor in the resulting biochemical composition of the climax community.

Again, alternatively, because the high abundance of the pioneer is temporary, the community may be resilient, and the pioneer may have little effect.

### ***Hypothesis #3***

*Pioneer effects on the climax community composition and function will be predictable, based on the metabolic capabilities of that pioneer.*

If hypotheses one and two are supported, then hypothesis three becomes probable.

Biochemical activities of each pioneer will be determined and used to predict effects.

Climax community composition and function will confirm or deny these effects.

## CHAPTER II

### Proof of Principle (*E.coli* Chapter)

Understanding foundation species effect is quite challenging. A widely used tool in microbiology is *Escherichia coli* (*E.coli*). In this study, we used *E.coli* strain K-12 MG1655 because it is non-pathogenic, widely used in laboratories across the world, is a primary model for basic bacterial biology, has many strains with whole genomes sequenced, and has available a full collection of knockout strains from the “*E.coli* Genome Project” (Blattner et al., 1996). The genus *Escherichia* is in the class *Gammaproteobacteria* and is rarely present in low abundance in the skin microbiome of *G. affinis* (Brumlow et al., 2019; Carlson et al., 2015; Carlson et al., 2017). By artificially introducing and making K12 a pioneer after disruption of the fish microbiome community, we tested the principle of foundation species, and so directly experimentally asked the question: does our selected K12 pioneer act as a foundational species during recovery?

### Materials and Methods

#### *Animal Model*

*Gambusia affinis* has been used as a model organism for mating behavior in other studies, but in this study, we used the fish, *G. affinis*, to model a mucosal microbiome because fish naturally have a mucus layer on their skin that can be easily manipulated (Brumlow et al., 2019; Carlson et al., 2015; Carlson et al., 2017). Fish were obtained from a pond in Walker County, Texas and identified by eye. In several previous studies, researchers have utilized this pristine field (low human impact) site (Brumlow et al., 2019; Carlson et al., 2015; Carlson et al., 2017). Careful precautions were taken using a

dip net during capture to ensure that the natural skin microbiome was minimally disturbed. Fish were acclimated to the lab in buckets where they were kept for 2-3 days with a feeding pattern of 5 mg/fish to get them acclimated to the food. Afterwards, the fish were maintained in 20-gal aquaria with 12 h light/12 h dark cycles at 23–25 °C. Before the start of any experiment, the fish were acclimated for at least 12 days in the aquarium, which results in highly similar skin microbiomes between fish (Carlson et al., 2015). Fish were fed daily with 5 mg per fish of TetraFin flake food. During experiments, fish were held in artificial pond water (APW) that consisted of 0.33 g/L CaCl<sub>2</sub>, 0.33 g/L MgSO<sub>4</sub>, 0.19 g/L NaHCO<sub>3</sub> in deionized water, which was sterilized by autoclaving prior to usage. All animal experiments were under approved SHSU IACUC protocol 18-09-25-1018-3-01.

### ***Fish Microbiome Extraction and Culture***

To extract the skin microbiome, using a VWR® Standard Heavy-Duty Vortex Mixer (catalog#: 97043-562), the fish were vortexed at maximum speed (3200 rpm) in a sterile 15 mL conical tube in 2 mL of PBST (137 mM NaCl, 10 mM phosphate, and 0.1% Tween 20, pH 7.4) for 1 minute, pausing shortly every 10 seconds (Brumlow et al., 2019; Carlson et al., 2015, Carlson et al., 2017). For colony counts, tenfold serial dilutions of skin extract were made in PBST, and then 100 µL aliquots were spread onto Nutrient Agar (NA) (7.5 g/L of Bacto agar, 2.5 g/L of peptone, and 1.5 g/L of beef extract) plates. In a previous comparison of ten types of media, NA displayed the highest counts and the most consistent numbers from fish skin. Selective and differential plates were used to count pioneer persistence in the fish mucosal microbiome. The plates were checked after 48 h of incubation at 25°C.

### ***Rinsing Method***

For physical removal of the skin microbiome of *G. affinis*, a rinsing method was used as a strong disturbance. This method consists of a series of rinses, which mechanically removes the microbiome from the mucus layer on the fish skin (Brumlow et al., 2019). Using a VWR® Standard Heavy-Duty Vortex Mixer (catalog#: 97043-562), each fish was vortexed at maximum speed (3200 rpm) serially four times in a sterile 15 mL conical tube in sterile 2 mL PBST (137 mM NaCl, 10 mM phosphate, and 0.1% Tween 20, pH 7.4) for 20 seconds, pausing shortly second at 10 seconds, and then placed in their corresponding APW bucket. (Brumlow et al., 2019). This rinsing method of disturbance was used because it is a strong disruption that has no residual effects. Also, after disruption, the researcher will be able to introduce selected pioneer species in the water column. Each experimental fish was rinsed and placed in sterile APW for recovery where they were sampled later. Mortality is low during this procedure as derived by examining previous experiments (Brumlow et al., 2019).

### ***K12 Inoculation***

K12 was grown in nutrient broth (NB) at 25°C overnight. K12 overnight growth was quantified by measuring the optical density at 650 nm. Then, a clean 2.5-qt. polyethylene bucket (HDX Model # 05M3HDX) containing 2 L of sterile APW was inoculated with K12 at a calculated OD<sub>650</sub> of 0.05. After rinsing, the fish were exposed to K12 in the water column for 8 hours to allow the pioneer species to invade the skin microbiome. Afterward, the fish were transferred to fresh APW for recovery where they were sampled at later time points. Mortality was low, as expected, during this procedure because the pioneer species K12 is non-pathogenic.

### ***K12 Enumeration***

Differentiation of the pioneer species was a crucial component of this experiment in order to track persistence in the microbiome community. Differential and selective media were used to count pioneer species apart from the rest of the microbiome community. Preliminary data to selectively grow the potential pioneer *E. coli* from a fish microbiome sample suggest that xylose-lysine-deoxycholate agar (XLD) plates incubated at 44 °C will grow *E. coli*, but it does grow not any background fish skin bacteria. This is highly selective for K12 because XLD contains high levels of three sugars, totaling 18.75 g/L, along with 5 g/L of NaCl and 2.5 g/L of the bile salt deoxycholate. Adding in the high incubation temperature, this media is very stressful to membranes, and few bacteria can adapt to it and grow. Also, metabolic tests were used to further confirm presence of the chosen pioneer species. For K12, this meant random selection of suspected colonies from plates, and confirming they were Gram negative, rod-shaped, and lactose positive.

### **Biochemical Analysis**

To determine the microbiome function profile, using a VWR® Standard Heavy-Duty Vortex Mixer (catalog#: 97043-562), skin microbiome communities were extracted by placing a one fish per time point in a 15 mL conical tube with 5 mL of sterile saline water (0.85% NaCl). Each fish was vortexed at maximum speed (3200 rpm) for 1-minute pausing shortly for 1 second every 10 seconds, then the fish was removed aseptically from the tube and placed in a recovery aquarium where the fish was not resampled. Fish skin extract was inoculated into the Microgen A+B system. A total of 100µL were placed into each well, and wells 1, 2, 3, 9, and 24 were overlaid with 100µL of sterile immersion oil. Wells were read according to manufacturer's instructions. A limitation of

this method is that while a positive result in this test indicates that the community has a certain biochemical capability, it does not prove that this function is active while the community is actually on the fish skin. So, it demonstrates possibility, not *in situ* results.

### ***Experimental Design***

All fish were collected from the same aquarium tank to ensure minimal starting community variance (homogeneity). A total of ~80 fish were used for this study, where 20 fish were required per group. Experimental and control groups were rinsed and transferred to the appropriate APW bucket (with bacteria and with no bacteria) as groups. The experimental group was incubated for 8-hours (Fig. 1 Experimental group [E]) with pioneer species and then transferred to a clean APW bucket for recovery. The control group [C] was incubated for the same amount of time in sterile APW, then transferred into a clean APW bucket for recovery. As a further comparison, one group of fish was not rinsed (in figure labeled as “Not Rinsed [NR]”), but these fish went through the same transfers as the experimental and control groups. Major samples were collected pre-treatment (PT), post-rinse (PR), after an 8-hour incubation, which confirms levels of pioneer introduction, 48-hours in recovery (to represent mid-recovery), and 240-hours in recovery (to represent final recovery). Comparing the microbiome composition and function of the 240-hour experimental group to the 240-hour control group should confirm or deny hypotheses one and two. Comparison across multiple experiments with different pioneer species should confirm or deny hypothesis three.



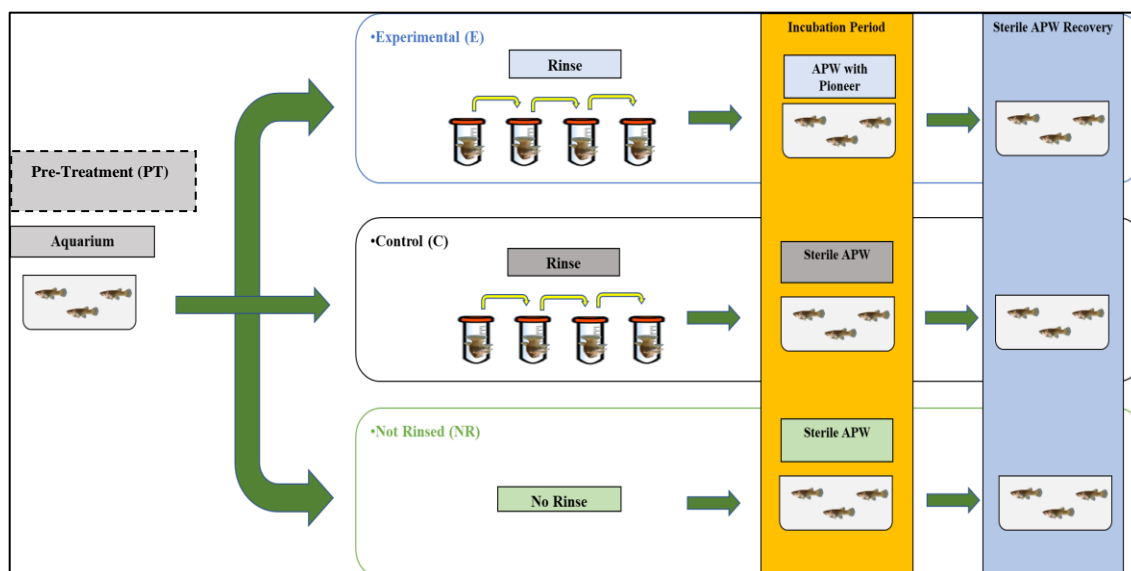


Figure 1 Experimental design of foundation species experiment.

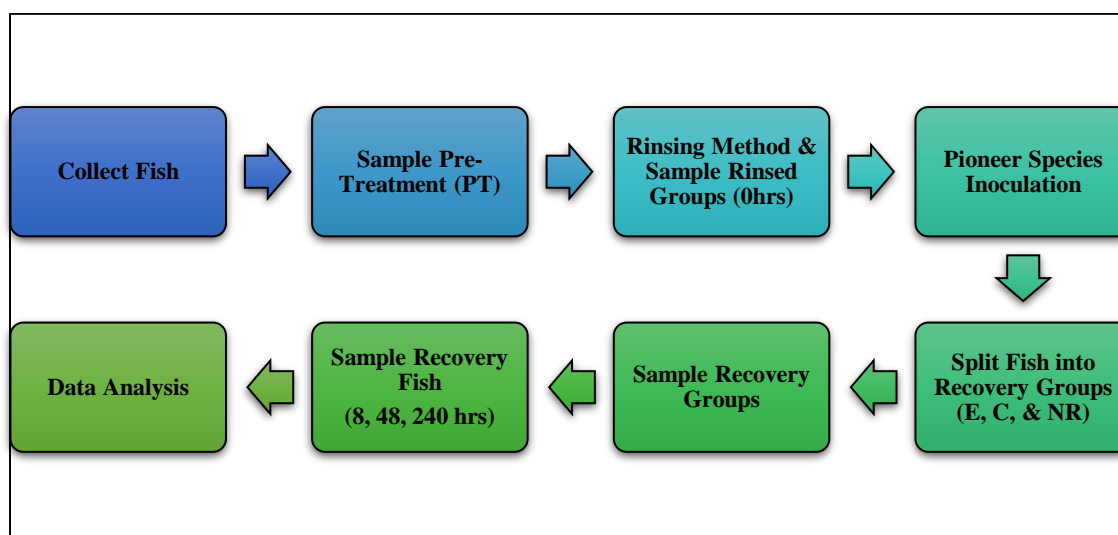


Figure 2 Flowchart summarizing the major concepts of the study.

### **Microbiome 16S rRNA Extraction and Amplification**

For 16S rRNA gene profile analysis, microbiome was extracted from the fish using the protocol above, then bacteria were pelleted by a 2-minute spin in a centrifuge at room temperature at top speed (14,000 rpm). The pellet was frozen and stored at  $-80^{\circ}\text{C}$  until all were ready for DNA extraction. Total DNA was extracted using

the PowerSoil DNA isolation kit (MO BIO Laboratories) following manufacturer's instructions. The company Mr.DNA (www.mrdnalab.com, Shallowater, TX) was used for 16S gene sequencing using PCR primers 515F/806R (5'-GTGCCAGCMGCCGCGGTAA-3'/5'-GGACTACHVHHHTWTCTAAT-3') on the sequencing platform Ion Torrent PGM Ion S5/XL.

### **Data Analysis**

R version 3.6.3 (2020-02-29) was used with R Studio version 1.2.5033. All figures were generated using ggplot2 package version 3.2.1 (Whickman, 2016). Exact Sequence Variants (ESV) were generated using the dada2 package version 1.14.0 (Callahan et al., 2016) for a total of 692 of ESVs. Rarefaction curves were generated using *ggrare* from *ranacapa* package version 0.1.0 (Gaurasv, 2019). Taxonomic classifications were assigned by *IdTaxa* using the Ribosomal Database Project (Cole et al., 2014) release version 16 released March 2018 by the DECIPHER package version 2.14.0 (Wright, 2016). Before analysis was performed, ESVs that matched Archaea, Eukarya, or unidentified at the level of domain (no database match) were filtered out, for a total of 502 ESVs.

The phyloseq package version 1.30.0 (McMudie & Holmes, 2013) and the microbiome package version 1.9.95 (Lahti et al., 2017) were used to generate multiple measures. Observed and Shannon Diversity Indices (SDI) for all samples and all groups at the ESV level and genus level were generated through the *estimate\_richness* function in the microbiome package. NMDS using Bray-Curtis dissimilarity was generated using *ordinate* function in the phyloseq package to visualize differences between the composition (beta diversity) of skin communities at different times points. Statistical

analysis of Bray-Curtis diversity among groups was analyzed by the *adonis* function in the vegan package version 2.5-6 (Oksanen et al., 2019). Furthermore, SIMPER analysis via *simper* function from vegan package was used to assess taxon driving community differences. Normality was measured by *shapiro.test* function; a significant p-value indicates a non-normal distribution and variables were tested based on normality.

## **K12 May act as a Foundation Species**

### **Results**

#### ***Total Bacterial Load Counts Throughout the Experiment***

Total bacterial load was obtained by plating on nutrient agar (NA) plates to assess a baseline for initial community composition. Baseline carrying capacity of the fish skin was determined by pre-treatment sampling of CFU. As shown in Figure 3, the total bacterial load trend of overgrowth is consistent with previous experiments (Brumlow et al., 2019, Carlson et al., 2017). Bacterial load peaks at around 48 hours after microbiome disruption and bacterial CFU returns to pre-treatment levels at around 240 hrs. The effect the rinse protocol had on composition of the fish skin microbiome was quantified by CFU numbers immediately after disruption. As shown in Figure 5, the fish skin microbiota is severely depleted after the rinse protocol by lowering counts from  $2.40 \pm 0.16 \times 10^5$  CFU/g fish weight to  $9.14 \pm 2.69 \times 10^4$ . The rinse protocol depleted the fish skin microbiome by ~ 97% of pre-treatment levels which is consistent with previous experiments (Brumlow et al., 2019), showing a major disruption of the fish skin microbiome.

As shown by Figure 3, fish skin bacterial load peaks after disruption at around 48 to 72 hours into recovery, which is consistent with previous experiments (Brumlow et al.,

2019). The bacterial load at pre-treatment CFU level was  $2.40 \pm 1.63 \times 10^5$  and the experimental CFU level was  $5.97 \pm 5.63 \times 10^7$ . CFUs number increased by ~2500% from the baseline. In the control group the average at 48 hours was  $2.95 \pm 3.78 \times 10^8$ , which is ~ 12,300% increase in the carrying capacity of the fish skin microbiome. Final community composition was determined based on pre-treatment bacterial load at the beginning of the experiment. There was no difference among pre-treatment and experimental, control and not rinsed treatment at 240 hours (Figure 6). After 240 hours of recovery after rinse disruption, the CFU counts returned to pre-treatment levels indicating the carrying capacity of the fish skin mucosa had returned to normal condition, which is consistent with previous experiments (Brumlow et al., 2019, Carlson et al., 2015, Carlson, et al., 2017).

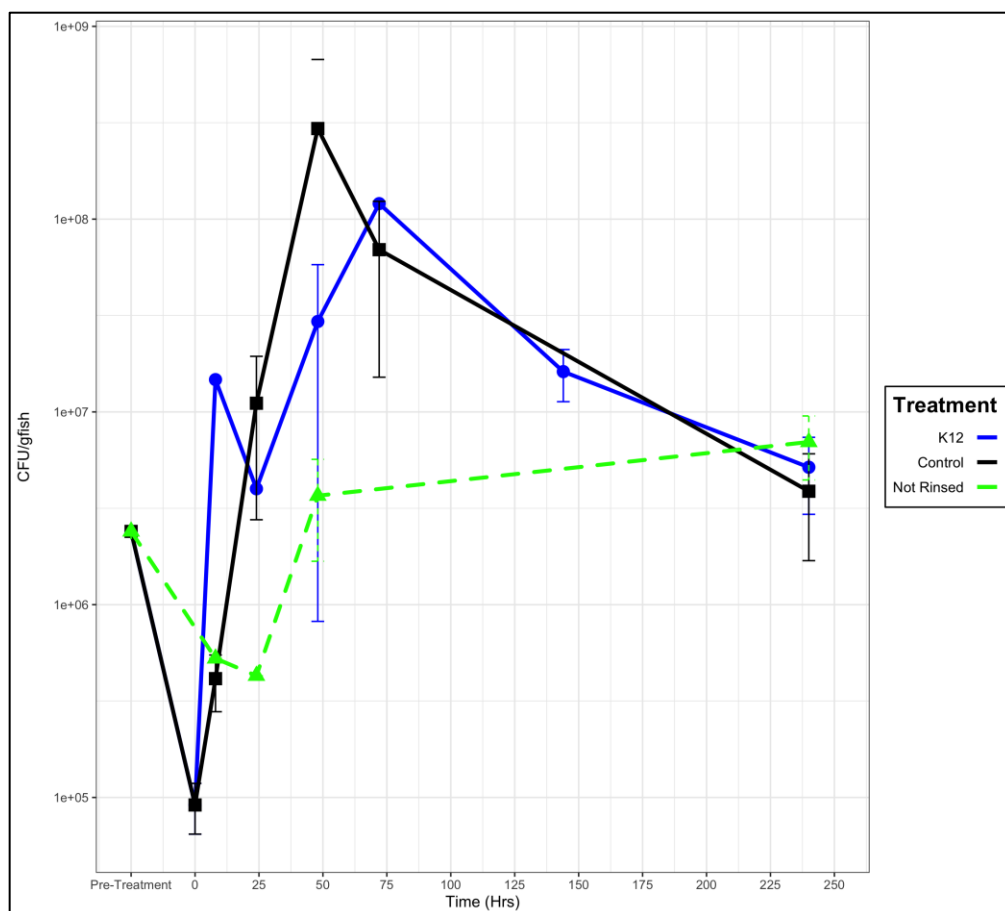


*Figure 3 Normalized fish skin CFU by fish weight over time.*

n = 15 per treatment, and each data point is the mean with standard deviation of a group of 3 fish.

*Table 1 Tracking of introduced pioneer K12 by plating CFU.*

<b>Treatment</b>	<b>Time</b>	<b>CFU/gfish Average</b>	<b>CFU/gfish SD</b>	<b>Media</b>
K12	-24	2399151	210180	NA
K12	-24	0	0	XLD44
K12	0	91409	26863	NA
K12	0	0	0	XLD44
K12	8	14705882	0	NA
K12	8	1715686	712051	XLD44
K12	24	3993808	43784	NA
K12	24	20650	8012	XLD44
K12	48	29444444	28625224	NA
K12	48	0	0	XLD44
K12	72	120359281	0	NA
K12	72	0	0	XLD44
K12	144	16181818	4885465	NA
K12	144	0	0	XLD44
K12	240	5162659	2220335	NA
K12	240	0	0	XLD44

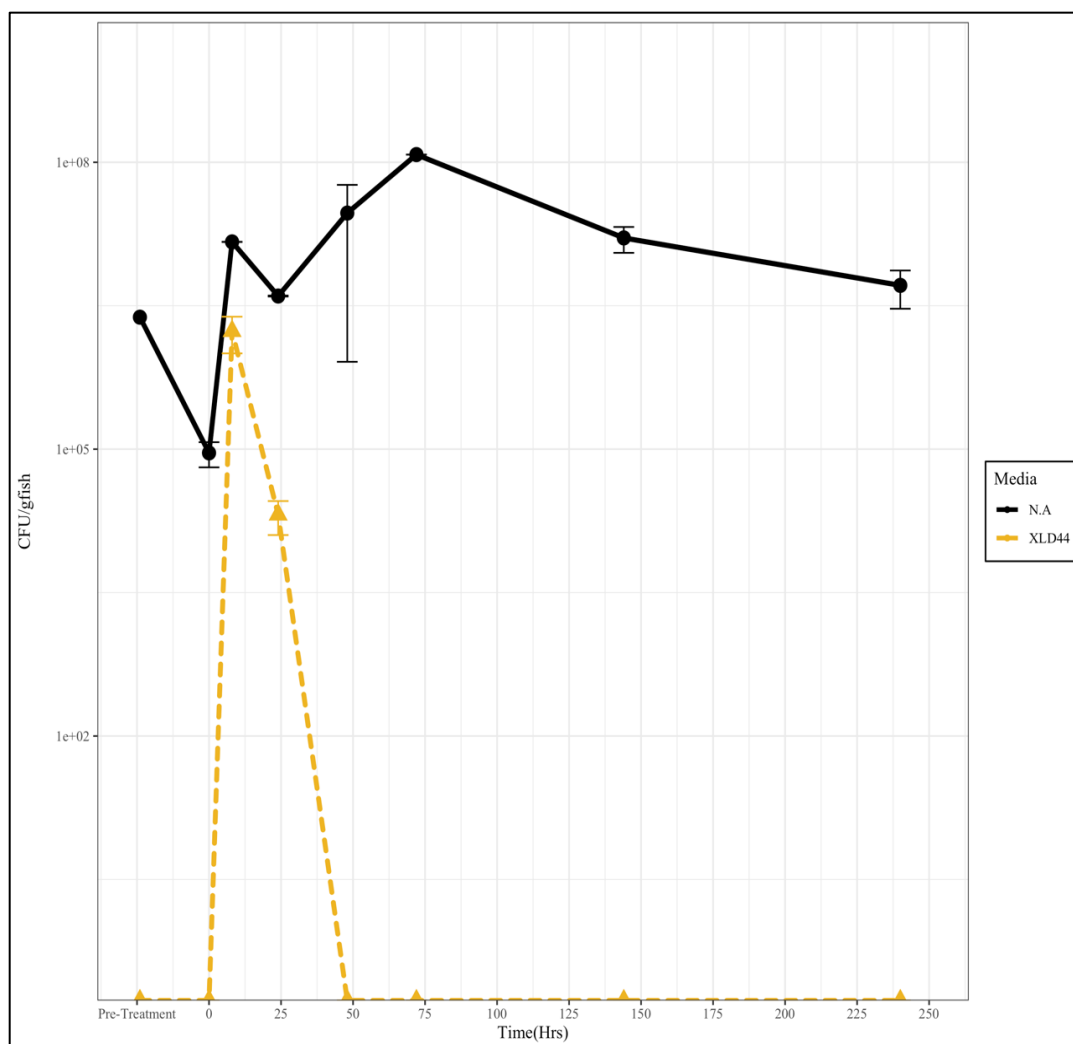
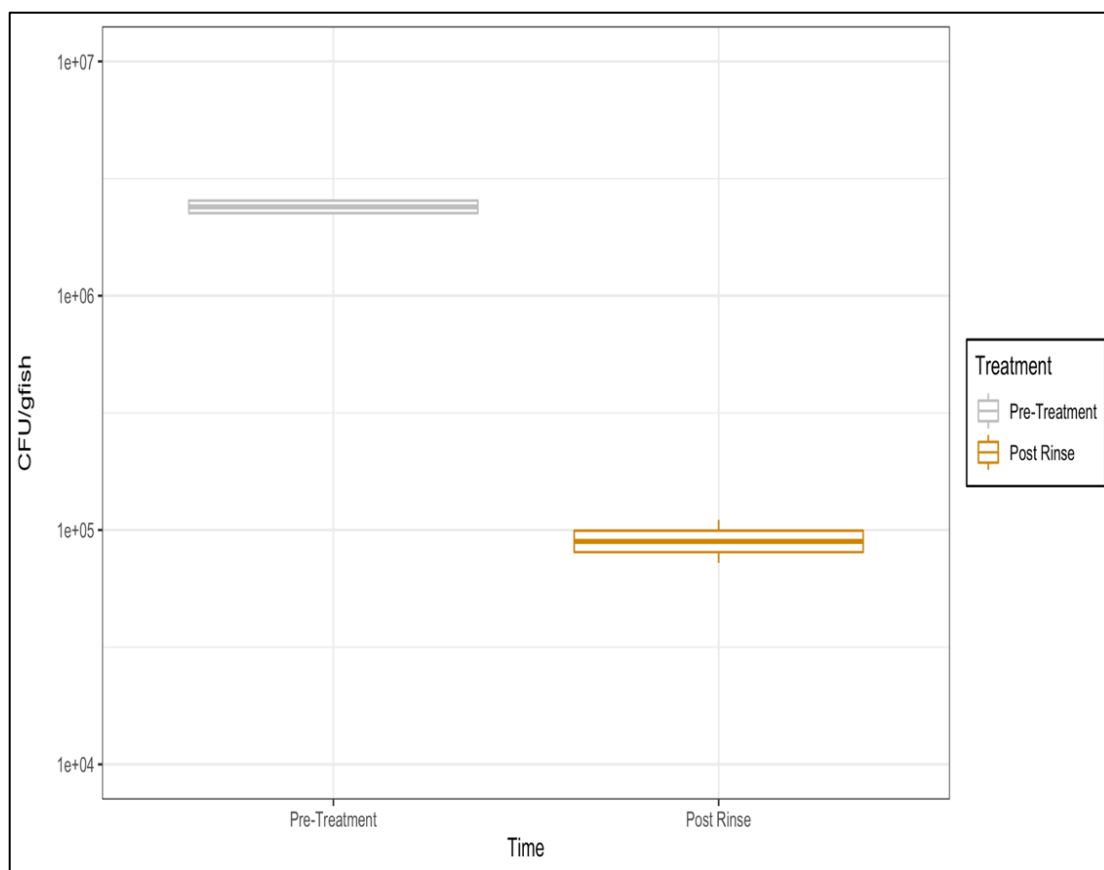


Figure 4 CFU comparison of total counts on NA and XLD44 selective for *E. coli* K12. Symbols represent mean and error bars represent standard deviation.



*Figure 5 Boxplot of CFU normalized by fish weight showing Pre-treatment and Post-Rinse treatments.*

Data are not normal (Shapiro test;  $p = 0.00086$ ). Difference between Pre-Treatment and Post-Rinse groups was near the significance cut off (Wilcox;  $p = 0.054$ ). Boxplots show values for median, upper and lower quartile, and whiskers represent interquartile range of 1.5 outside of the upper and lower quartile.



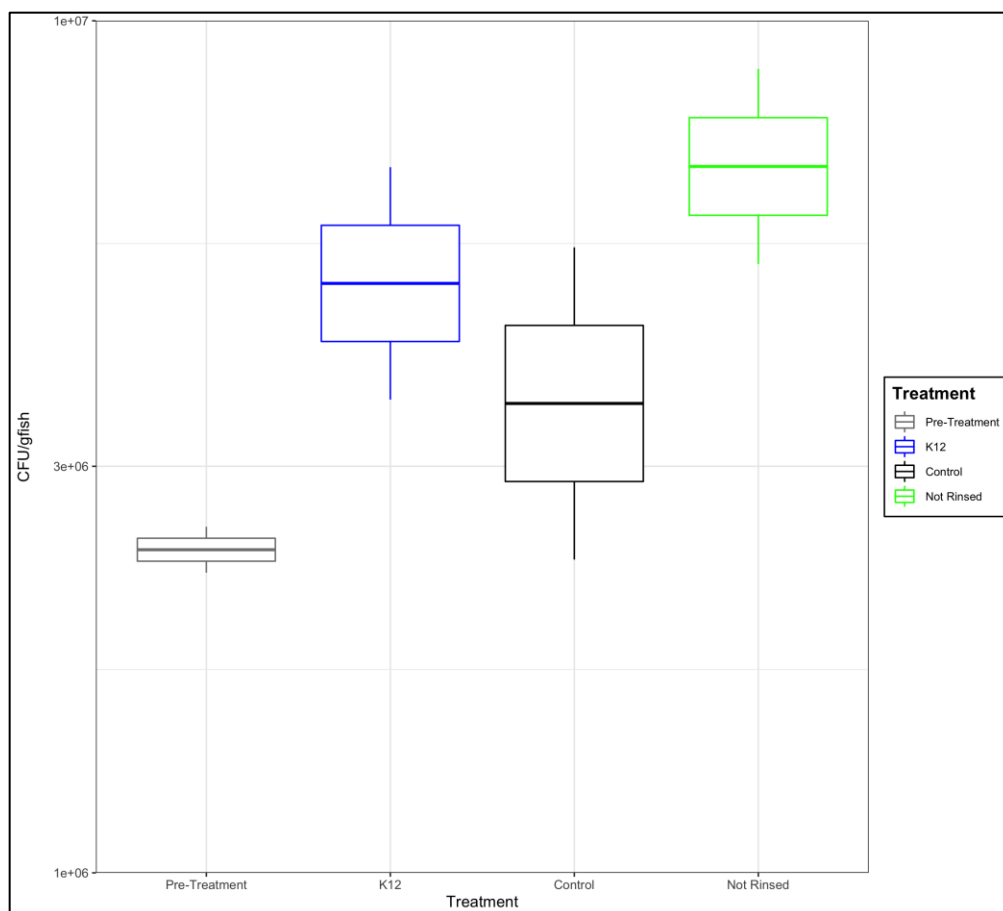


*Figure 6 Boxplot comparing pre-treatment samples and 240-hour samples of normalized CFU counts per fish weight.*

Data are normal (Shapiro's test;  $p = 0.392$ ). Community counts (total bacterial load) among the groups are not significantly different (One-Way ANOVA;  $p = 0.22$ ;  $N = 2$  per group).

### ***Fish Skin Microbiome 16S rRNA Coverage and Alpha Diversity***

The V3-V4 region of the 16S rRNA was sequenced to gain an insight into the bacterial communities at time points: pre-treatment, 8-hours into recovery, 48-hours in recovery, and 240-hours into recovery, and the DADA2 pipeline was used to gain insight into community composition. Sampling completeness was visualized by rarefaction curves that seem to plateau indicating sufficient sampling (Figure 7). Good's coverage was measured for every sample with an average Good's coverage of  $99.854 \pm 0.215$  (Table 2). There was an average of  $52,824 \pm 27,827$  sequences per sample and a total

of 529 ESVs identified in all 28 samples (total gamma diversity). Shannon's diversity index (SDI) quantifies a combination of community diversity and evenness (distribution of species). SDI was calculated for each sample (Table 3) and within groups (Table 4) at the ESV level. Analysis was done by focusing on genus level identifications (the most accurate taxonomic level available with short 16S fragments) obtained by comparison to the RDP database. A total of 169 classified genera were obtained across all 28 samples. SDI at the genus level is shown for each of the 28 samples (Table 5) and SDI average at the genus level for each group (Table 6).

As shown in Figure 8, the observed number of genera at 240 hours is not significantly different among the Experimental, Control, and Not Rinsed treatments. Addition of *E.coli* as a pioneer species after disruption did not significantly change the alpha diversity (Kruskal-Wallis;  $p = 0.13$ ). By comparing SDI at 240 hours of the different treatments, the Experimental treatment has a significantly higher SDI in comparison to Control and Not Rinsed treatment (ANOVA;  $p = 0.0187$ ; Tukey's honest test;  $p = 0.049$ ;  $p = 0.021$ , respectively).

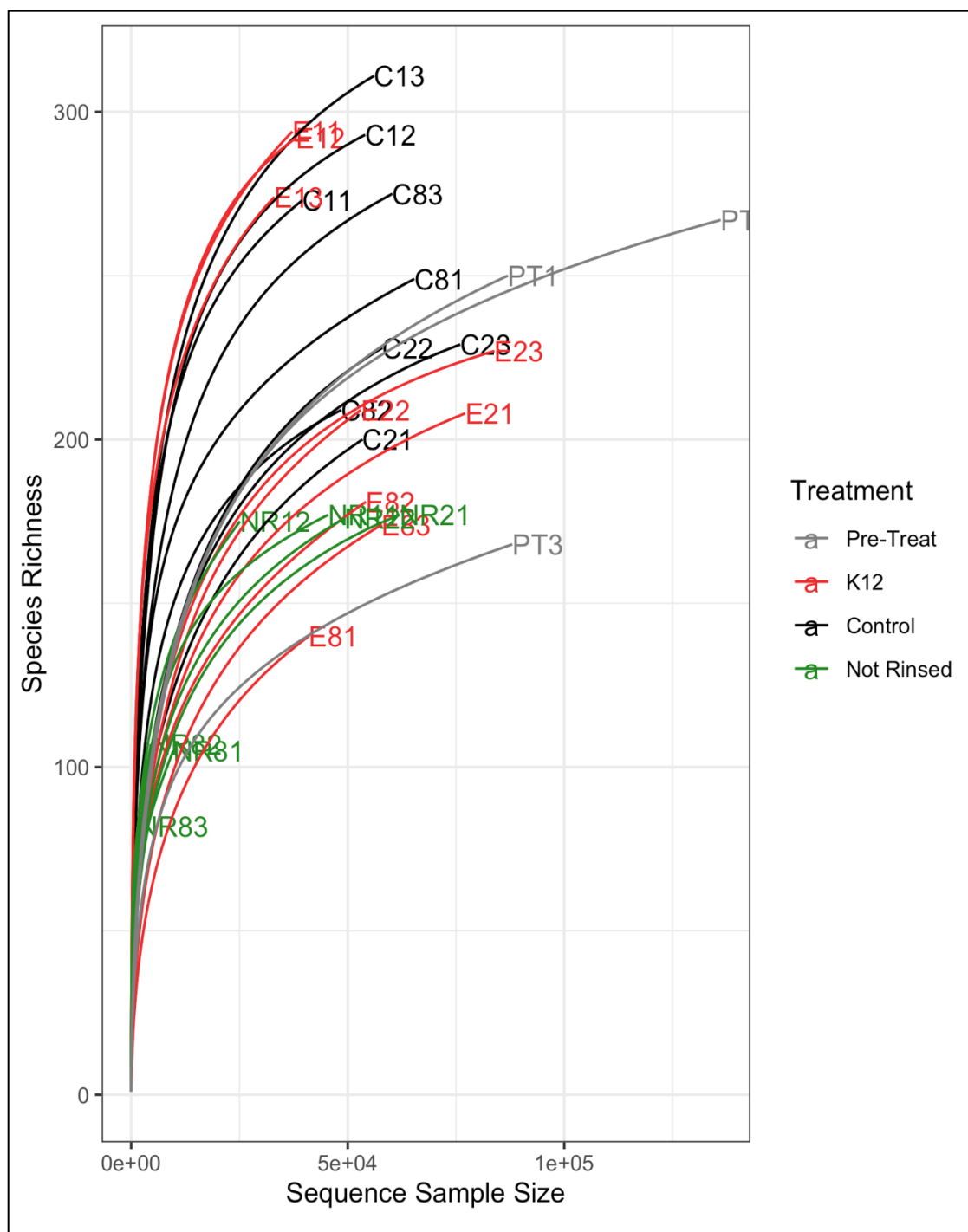


Figure 7 Rarefaction curve of samples showing sampling depth.

*Table 2 Good's coverage of the sequenced 16S V3-V4 for each sample.*

<b>Sample</b>	<b>Treatment</b>	<b>Time (Hrs)</b>	<b>Number of Singletons</b>	<b>Number of sequences</b>	<b>Good's coverage</b>
PT1	Pre-Treatment	-1	50	88725	99.944
PT2	Pre-Treatment	-1	52	138830	99.963
PT3	Pre-Treatment	-1	41	89482	99.954
C81	Control	8	43	64841	99.934
C82	Control	8	33	48465	99.932
C83	Control	8	46	60042	99.923
E81	K12	8	43	40999	99.895
E82	K12	8	51	52559	99.903
E83	K12	8	47	57888	99.919
NR81	Not Rinsed	8	33	9498	99.652
NR82	Not Rinsed	8	28	5534	99.494
NR83	Not Rinsed	8	19	1690	98.876
C21	Control	48	53	51569	99.897
C22	Control	48	50	55450	99.910
C23	Control	48	39	72040	99.946
E21	K12	48	43	75599	99.943
E22	K12	48	51	52794	99.903
E23	K12	48	32	82570	99.961
NR21	Not Rinsed	48	34	58561	99.942
NR22	Not Rinsed	48	35	38504	99.909
C11	Control	240	42	39367	99.893
C12	Control	240	42	54282	99.922
C13	Control	240	45	56727	99.921
E11	K12	240	55	37433	99.853
E12	K12	240	40	39323	99.898
E13	K12	240	46	33974	99.865
NR11	Not Rinsed	240	33	46653	99.929
NR12	Not Rinsed	240	45	25667	99.825

*Table 3 Shannon's Index of each sample at ESV level.*

<b>Groups</b>	<b>Time (Hrs)</b>	<b>Treatment</b>	<b>Shannon</b>
PT	-1	Pre-Treat	0.354
PT	-1	Pre-Treat	0.298
PT	-1	Pre-Treat	0.339
C8	8	Control	0.694
C8	8	Control	0.624
C8	8	Control	0.703
E8	8	K12	0.253
E8	8	K12	0.565
E8	8	K12	0.331
NR8	8	Not Rinsed	0.879
NR8	8	Not Rinsed	0.925
NR8	8	Not Rinsed	0.929
C48	48	Control	0.504
C48	48	Control	0.575
C48	48	Control	0.541
E48	48	K12	0.479
E48	48	K12	0.431
E48	48	K12	0.452
NR48	48	Not Rinsed	0.497
NR48	48	Not Rinsed	0.608
C240	240	Control	0.862
C240	240	Control	0.762
C240	240	Control	0.793
E240	240	K12	0.971
E240	240	K12	0.974
E240	240	K12	1.000
NR240	240	Not Rinsed	0.559
NR240	240	Not Rinsed	0.824

*Table 4 Mean and standard deviation of Shannon's Index of groups at the ESV level.*

<b>Treatment</b>	<b>Time (Hrs)</b>	<b>Shannon Mean</b>	<b>Shannon SD</b>
Pre-Treatment	-1	0.330	0.029
Control	8	0.673	0.043
K12	8	0.383	0.163
Not Rinsed	8	0.911	0.028
Control	48	0.540	0.036
K12	48	0.454	0.024
Not Rinsed	48	0.552	0.078
Control	240	0.806	0.051
K12	240	0.982	0.016
Not Rinsed	240	0.692	0.187

*Table 5 Shannon's Index of each sample at genus level.*

<b>Sample</b>	<b>Time (hrs)</b>	<b>Treatment</b>	<b>Shannon</b>
PT1	-1	Pre-Treat	0.324
PT2	-1	Pre-Treat	0.279
PT3	-1	Pre-Treat	0.273
C81	8	Control	0.708
C82	8	Control	0.638
C83	8	Control	0.707
E81	8	K12	0.275
E82	8	K12	0.514
E83	8	K12	0.356
NR81	8	Not Rinsed	0.877
NR82	8	Not Rinsed	0.942
NR83	8	Not Rinsed	0.954
C21	48	Control	0.472
C22	48	Control	0.555
C23	48	Control	0.533
E21	48	K12	0.473
E22	48	K12	0.436
E23	48	K12	0.456
NR21	48	Not Rinsed	0.480
NR22	48	Not Rinsed	0.599
C11	240	Control	0.801
C12	240	Control	0.730
C13	240	Control	0.753
E11	240	K12	0.949
E12	240	K12	0.975
E13	240	K12	1.000
NR11	240	Not Rinsed	0.554
NR12	240	Not Rinsed	0.791

*Table 6 Average Shannon's Diversity Index at genus level by time (hours).*

<b>Treatment</b>	<b>Time (Hrs)</b>	<b>Average Shannon Index</b>	<b>SD Shannon Index</b>
Pre-Treatment	-1	0.292	0.028
Control	8	0.684	0.040
K12	8	0.382	0.121
Not Rinsed	8	0.925	0.041
Control	48	0.520	0.043
K12	48	0.455	0.019
Not Rinsed	48	0.539	0.084
Control	240	0.761	0.036
K12	240	0.974	0.026
Not Rinsed	240	0.673	0.167



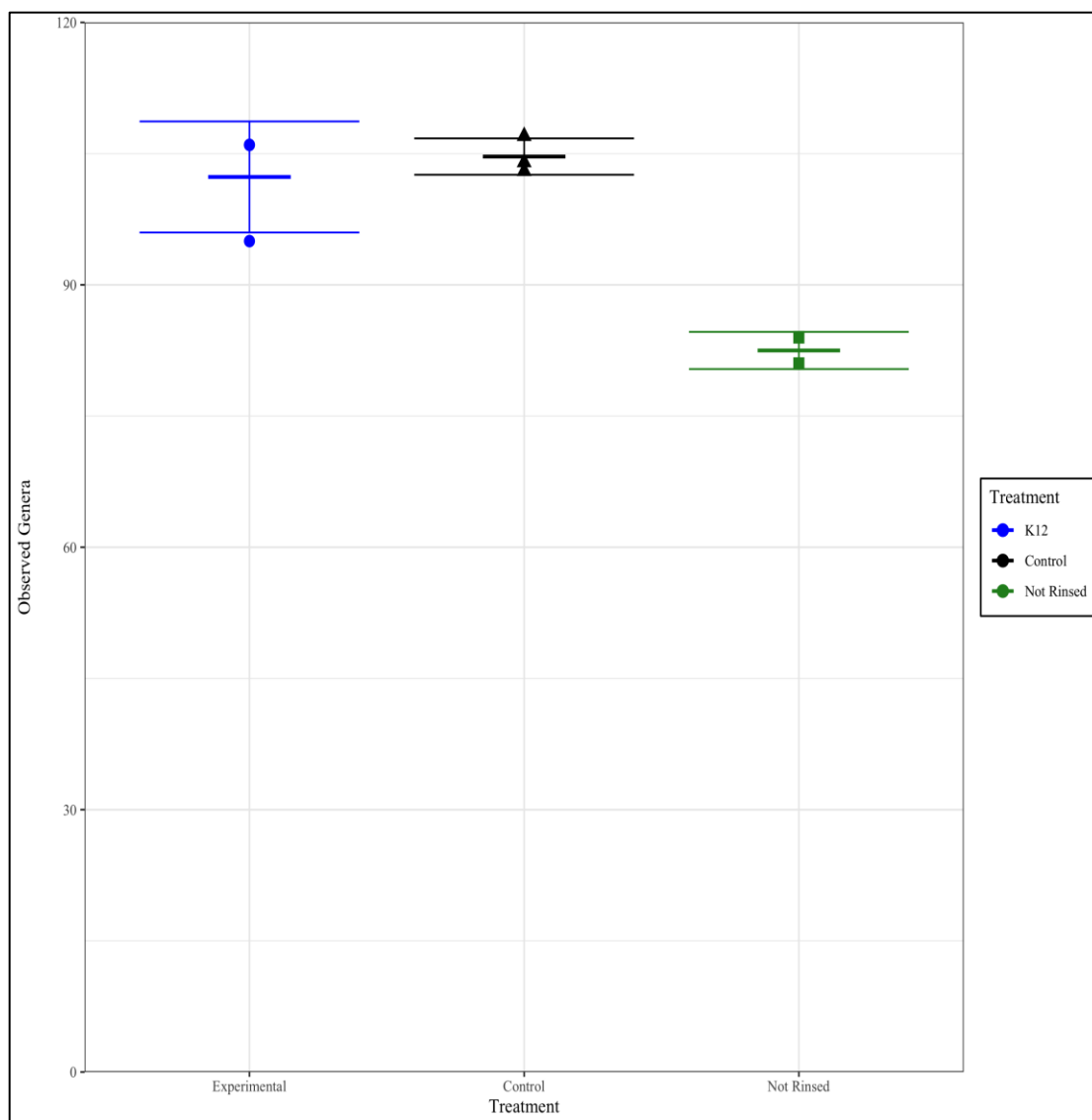


*Figure 8 Strip chart of alpha diversity (# of genera) at 240 hours per treatment.*  
 Data are not normal (Shapiro test;  $p = 0.027$ ). Total number of genera is not significantly different at 240 hours among groups (Kruskal-Wallis;  $p = 0.13$ ).

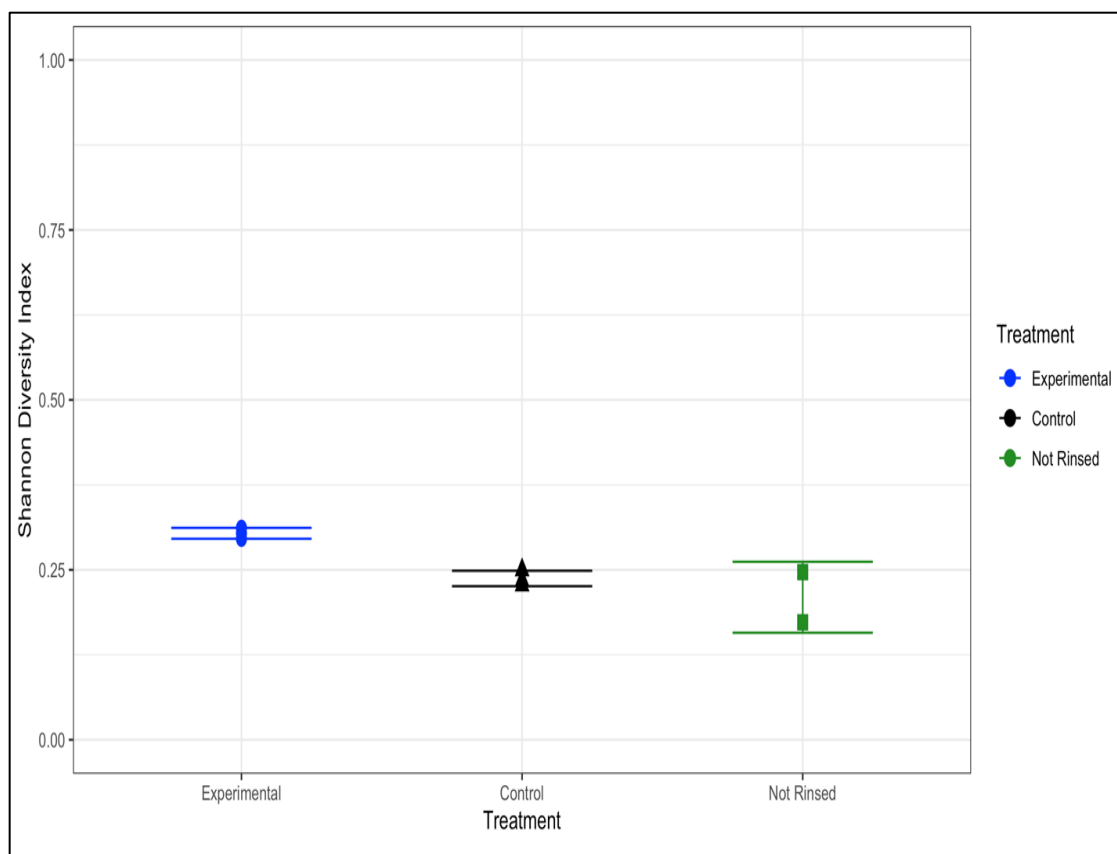


*Figure 9 Strip chart of Shannon diversity index at 240 hours per group.*

Data are normal (Shapiro's test;  $p = 0.495$ ). Shannon diversity is significantly higher in the experimental group compared to control or not rinsed groups at 240 hours (ANOVA;  $p = 0.0187$ ; Tukey's honest test;  $p = 0.049$ ;  $p = 0.021$ ).

### ***Fish Skin Microbiome Predicted Biochemical Profile***

Fish skin community biochemical profile was measured using 25 different tests in the Microgen Biochemical Identification Kit A + B strips. Predicted biochemical function was measured after 24 hours of incubation and results are shown in Table 7. To visualize community differences in biochemical profiles, a PCoA was calculated using the results of each individual test (Figure 10). Microbiome predicted function is similar among treatments within the same timepoint, and does not return to Pre-Treatment conditions during recovery.

*Table 7 Biochemical activity of fish skin microbiota at major sampling points.*

A total of 25 tests were recorded at each timepoint. The Not Rinsed group at 240-hours is missing due to fish mortality.

Groups	Time	Nitrate	Lysine	Orthinine	H <sub>2</sub> S	Glucose	Mannitol	Xylose	ONPG	Indole	Urease	V.P.	Citrate	TDA	Gelatine	Malonate	Inositol	Sorbitol	Rhamnose	Sucrose	Lactose	Arabinose	Adonitol	Raffinose	Salicin	Arginine
Pre-Treatment																										
	-1	+	+	-	+	-	+	-	+	+	+	-	+	+	-	-	-	-	-	+	-	-	-	+	-	+
Experiment																										
	8	+	+	+	-	+	+	-	+	+	-	+	+	-	-	-	-	-	-	+	-	-	-	+	-	-
Control																										
	8	+	+	-	+	+	+	-	+	+	-	+	+	-	-	-	-	-	-	+	-	-	-	+	+	+
Not Rinsed																										
	8	+	+	-	-	-	-	-	-	+	-	-	+	-	-	-	-	-	-	-	-	-	-	-	-	-
Experiment																										
	48	+	+	-	+	+	-	-	+	+	-	-	-	-	-	-	-	-	-	+	-	-	-	-	-	+
Control																										
	48	+	+	-	+	+	-	-	+	+	-	-	+	-	-	-	-	-	-	+	-	-	-	-	-	+
Not Rinsed																										
	48	+	-	-	+	+	+	-	+	+	-	-	-	-	-	-	-	-	-	-	-	-	-	-	-	-
Experiment																										
	240	+	+	+	+	+	+	-	+	+	-	-	-	-	-	-	-	-	-	+	-	+	-	-	-	+
Control																										
	240	+	+	-	+	+	+	-	+	+	-	-	+	+	+	-	-	-	-	+	-	+	-	-	-	+

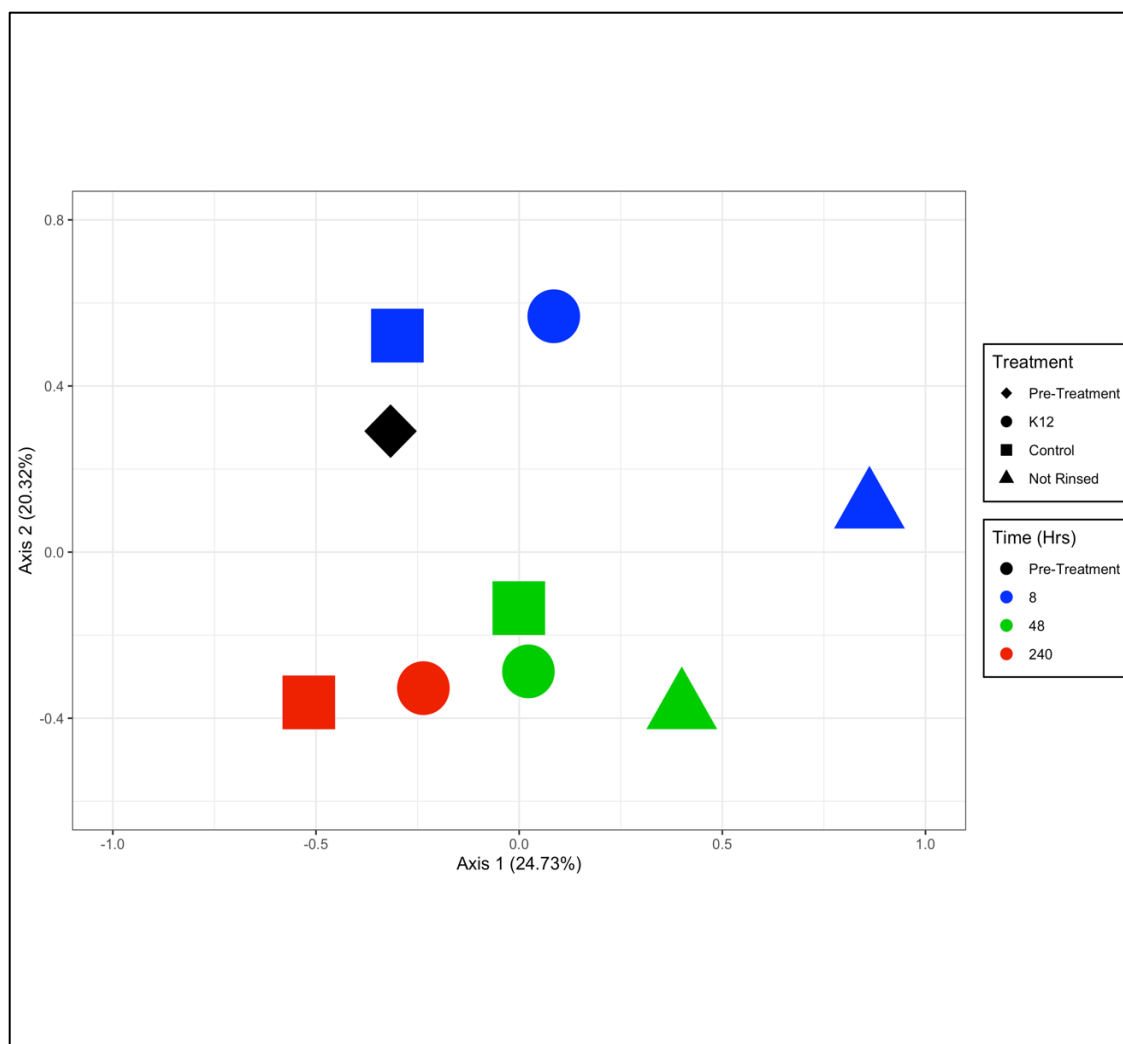


*Figure 10 Principal components analysis of biochemical profiles across the major sampling points.*

Each symbol represents the biochemical pattern from one fish.

### ***Fish Skin Microbiome 16S Gene Analysis***

The ten most abundant genera from each sample were identified and their relative abundance is shown in Figure 11. At 8-hours in recovery, only the Experimental treatment is heavily dominated by *E.coli* (shown in red, Fig 11), which is the pioneer species. The genus *Chryseobacterium* is present in the pretreatment community, dominates all treatments at 48-hours in recovery. It is a major community member at 240-hours in recovery in all treatments and was identified as a major contributor to driving diversity in all treatments, but was not statistically significant (SIMPER,  $p > 0.05$ ), indicating it could be a foundation species. The relative abundance in each sample of the five most abundant genera across the experiment is shown in Figure 12. Core taxa are defined as taxa present in every sample. Table 8 shows the core genera across all samples. The relative abundance of each genus has a high variation across samples and the experiment. Community beta diversity is shown in Figure 13. Bray-Curtis distance was used instead of weighted Unifac distance because samples are phylogenetically closely related and better community separation can be achieved. At the 240-hour time-point, all three treatments are close to each other, but the confidence intervals do not overlap. Experimental and Control treatments are not statistically significantly different from each other at 240-hours (Figure 12; PERMANOVA;  $R^2 = 1, p = 0.1$ ). Lack of significance may be due to not enough power of analysis (too few samples in each group) given the visualization. The next experiment employed more samples per group to address this issue (and significant differences were observed between the 240-hour groups [Table 21]).

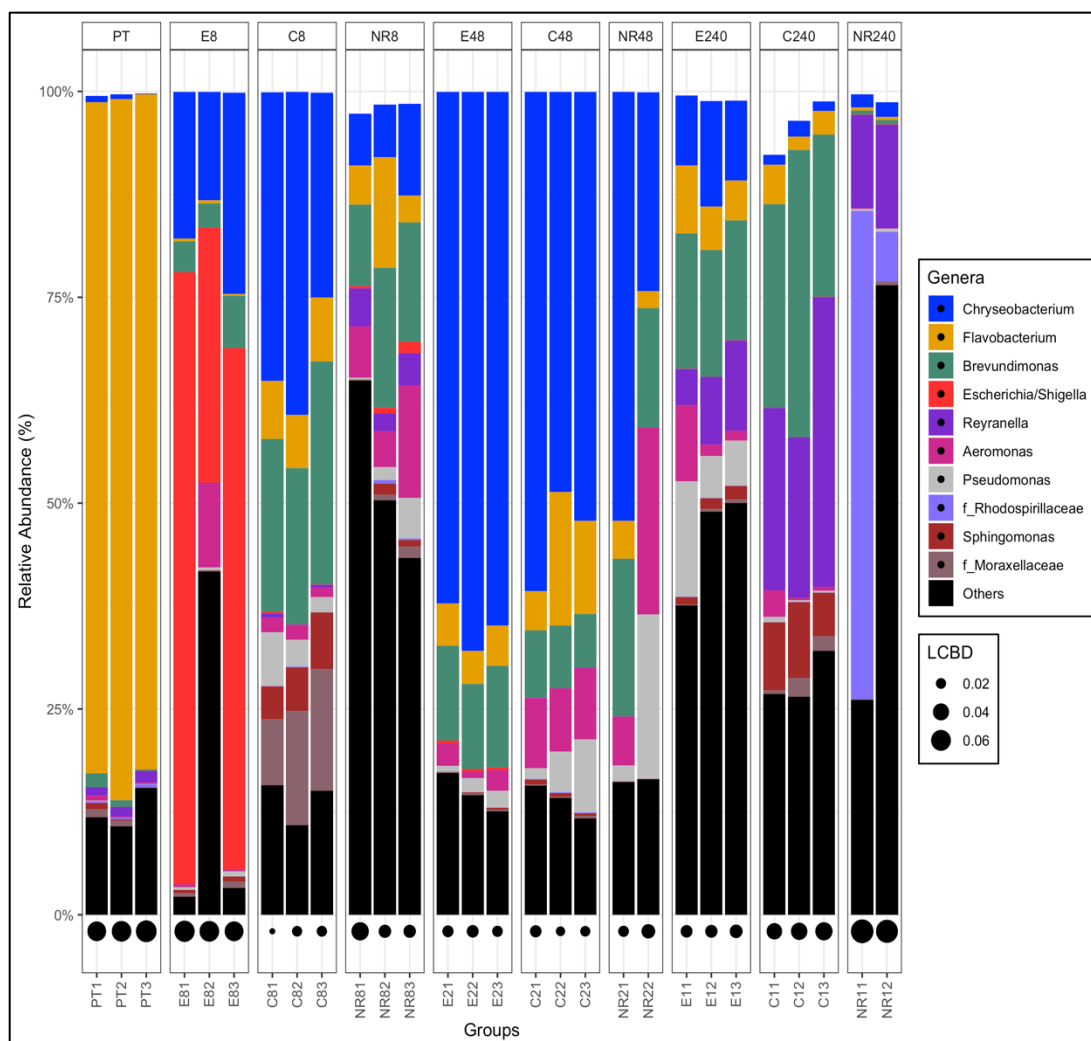


Figure 11 Bar graphs of relative abundance of ten most abundant genera across all samples gathered by groups.

For three taxa, the identification is accurate to the family level. LCBD (local contribution to beta diversity) scores represent the degree of uniqueness of the composition of each sample compared to the rest of the dataset. At the top of the graph are group names (i.e. E8 is the pioneer *E.coli* K12 added, 8 hrs timepoint; and NR48 is non-rinsed at 48 hrs), while at the bottom of the graph are individual sample names.

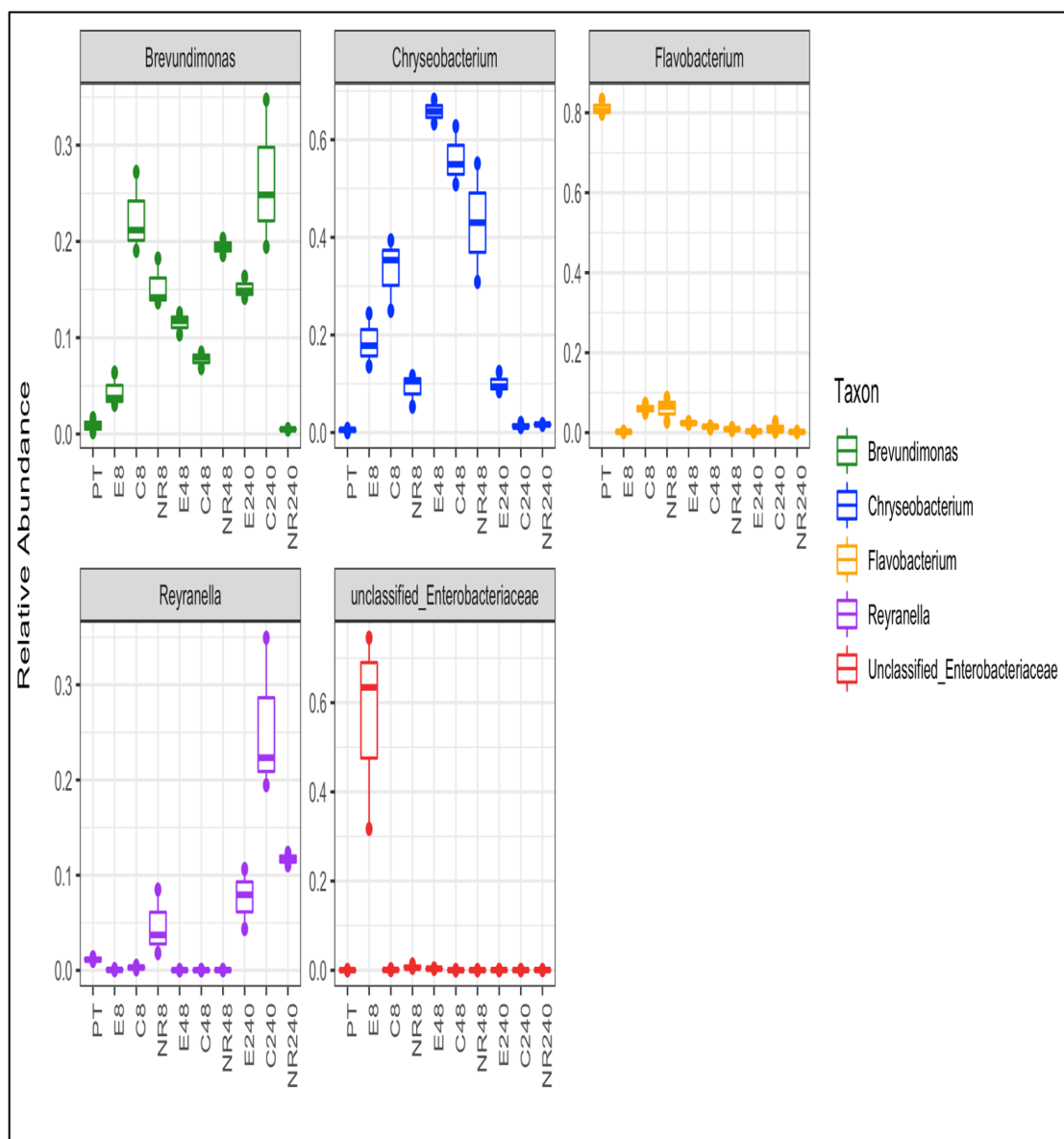


Figure 12 Boxplots showing relative abundance of the five most abundant genera across samples.

Table 8 Averages of core taxa at the genus level in every sample.  
Seven taxa are accurately classified at the family level.

<b>Genus</b>	<b>Relative Abundance Average</b>	<b>Relative Abundance SD</b>
<i>Aeromonas</i>	0.0063	0.0095
<i>Ancylobacter</i>	0.0132	0.0188
<i>Bosea</i>	0.0014	0.0021
<i>Brevundimonas</i>	0.0586	0.0828
<i>Chryseobacterium</i>	0.2390	0.2370
<i>Enhydrobacter</i>	0.0171	0.0387
<i>Flavobacterium</i>	0.0956	0.2440
<i>Niveispirillum</i>	0.0235	0.1090
<i>Pseudoxanthomonas</i>	0.0031	0.0044
<i>Reyranella</i>	0.0232	0.0465
<i>Shinella</i>	0.0017	0.0027
<i>Sphingobium</i>	0.0035	0.0047
<i>Stenotrophomonas</i>	0.0045	0.0056
<i>f_Aeromonadaceae</i>	0.0012	0.0020
<i>f_Burkholderiaceae</i>	0.0043	0.0073
<i>f_Enterobacteriaceae</i>	0.0620	0.1870
<i>f_Flavobacteriaceae</i>	0.0178	0.0241
<i>f_Pseudomonadaceae</i>	0.0321	0.0536
<i>f_Rhizobiaceae</i>	0.0065	0.0090
<i>f_Sphingomonadaceae</i>	0.0120	0.0191



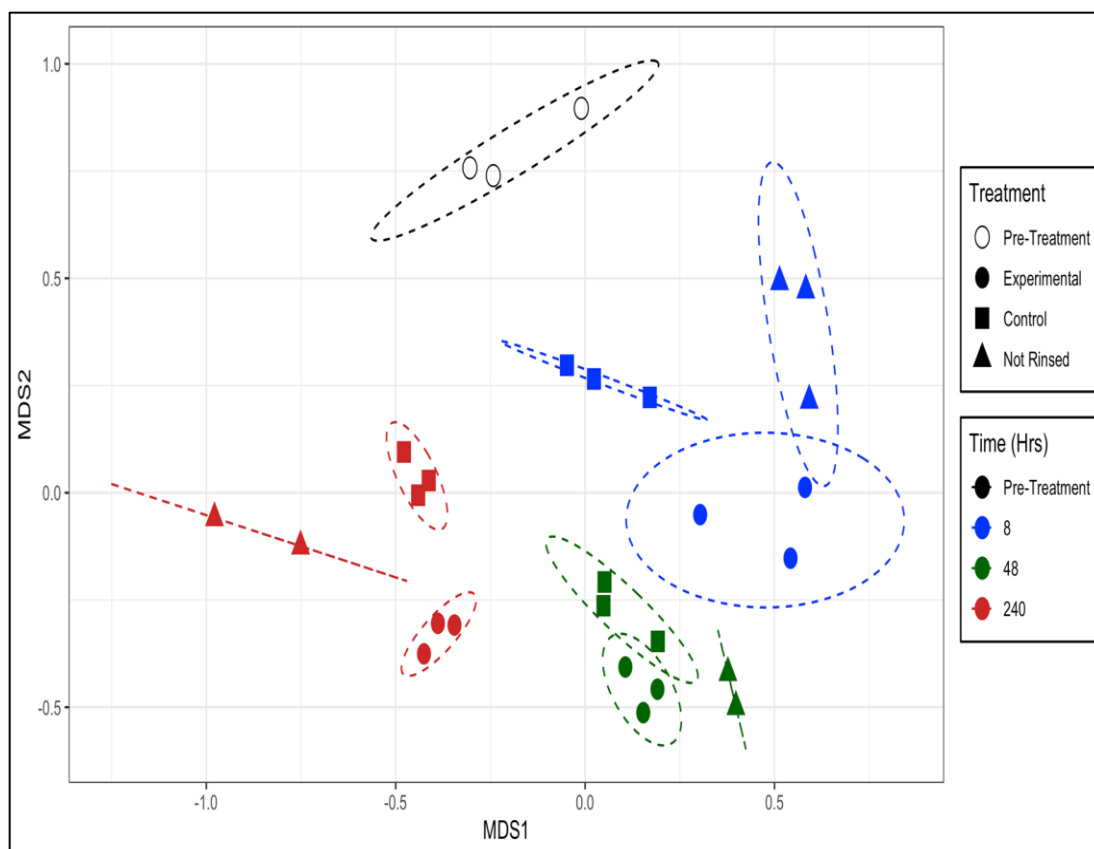


Figure 13 NMDS of all genera comparing composition of communities across major sampling times.

Each symbol represents the skin microbiome of one fish. Dashed lines indicate standard error of the community composition.

### ***Microbiome Composition and Water Chemistry***

API Freshwater Master Test Kit and Tetra EasyStrips 6-in-1 Aquarium Test Strips were used to measure the water quality for major sampling timepoints (Table 8). Nitrate is at its highest in Pre-Treatment and it becomes undetectable after disruption. Increases in ammonia, pH, and alkalinity are positively correlated with community composition changes during recovery after disruption over time, and Nitrite and Hardness are not significantly different (Figure 13 and Table 9).

*Table 9 Environmental characteristics collected at major sampling points using API Freshwater Master Test Kit and Tetra EasyStrips 6-in-1 Aquarium Test Strips.*

<b>Treatment</b>	<b>Time (Hrs)</b>	<b>pH</b>	<b>Ammonia</b>	<b>Nitrate</b>	<b>Nitrite</b>	<b>Hardness</b>	<b>Alkalinity</b>
Pre-Treatment	-1	7.4	0.5	10	0	250	3.5
Control	8	7.0	2	0	0	120	3.5
Experimental	8	7.0	2	0	0	120	2.5
Not Rinsed	8	7.0	1	0	0	120	2.5
Control	48	7.0	4	0	0	180	7.2
Experimental	48	7.6	8	0	0	180	7.2
Not Rinsed	48	7.0	1	0	0	180	7.2
Control	240	7.6	8	0	0	180	7.2
Experimental	240	7.6	8	0	0	180	7.2
Not Rinsed	240	7.4	4	0	0	120	4.8

*Table 10 Correlation of water chemistry with community changes over time by regression.*

$R^2$  refers to how much of the data variation is explained by the variable, and the  $p$ -value is obtained from permutations (<999). Changes Ammonia, pH, nitrate, and alkalinity are significantly correlated with community changes over time.

<b>Environment Variable</b>	<b>R<sup>2</sup></b>	<b>p-value</b>
pH	0.477	0.0002
Ammonia	0.578	0.0001
Nitrate	0.519	0.0004
Nitrite	0	1
Hardness	0.1	0.272
Alkalinity	0.644	0.0001

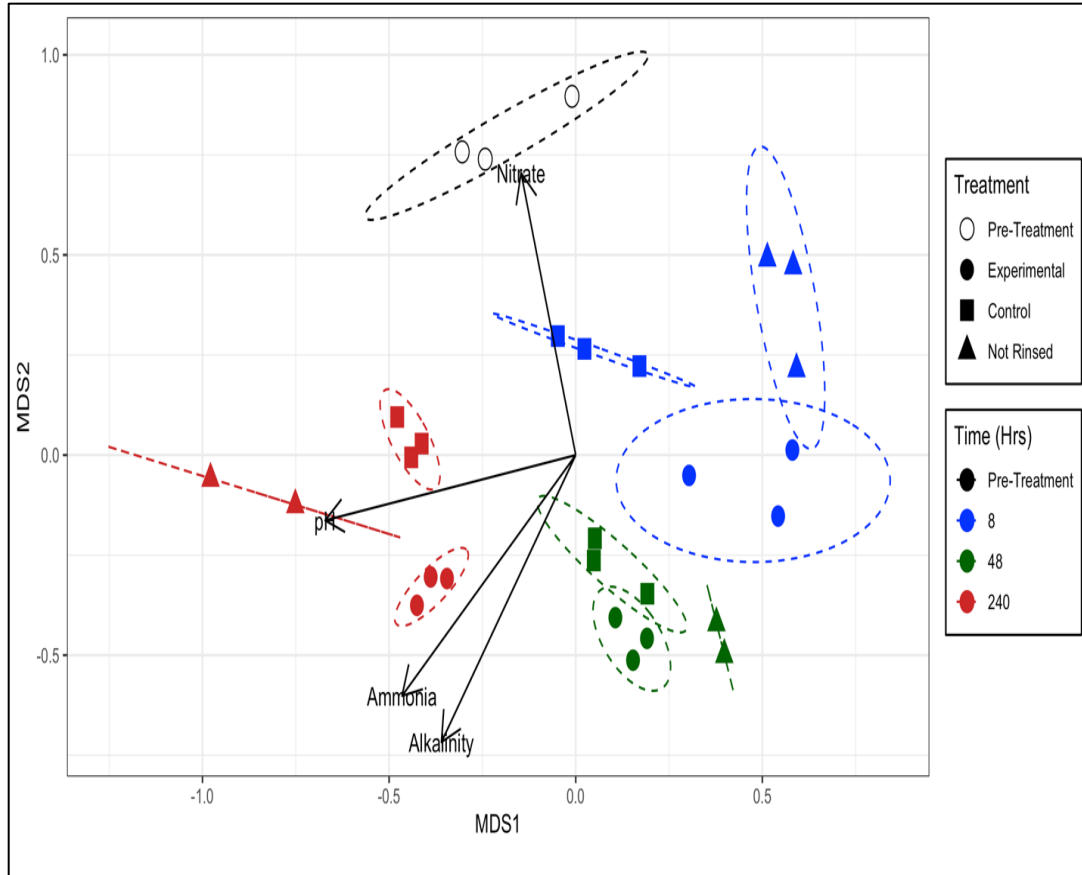


*Figure 14 NMDS of all genera showing the correlation of fish skin community composition and water chemistry across major sampling times.*

Water chemistry that correlate significantly with community composition are shown by arrows.

## Discussion

### *Fish Skin Carrying Capacity*

Fish skin microbiota can be impacted or disrupted in a relatively easy manner. The rinse effect is a strong pulse disruption that affects community stability because fish skin microbiota lose ~97% of their total CFU. After severely affecting fish skin microbiota, secondary succession takes place until a stable climax community is reached. In ecology, climax communities are the last stage of succession, and are balanced and stable; however, bacterial climax communities are not defined or accurately known because bacteria are highly dynamic compared to plants or animals (Luzopone et al., 2012).

Pre-treatment fish skin bacterial load (CFU) was used as a basal level to assess community carrying capacity. Carrying capacity is the population size that an ecosystem can sustain (Hui 2006). Experimental and Control treatments were sampled right after disruption to assess fish skin bacterial load. Experimental and Control fish had an average of 97% loss of bacterial CFU compared to Pre-Treatment levels. The Not Rinsed treatment was transferred to APW and not did not go through the rinse protocol, yet water transfer caused a slight loss of bacterial skin CFU. The fish skin CFU overgrowth phenomenon at ~48 hours is common after disruption of fish skin microbiota and commonly when domination by one taxon occurs (Brumlow et al., 2019, Carlson et al., 2017). Bacterial CFU peak at around 48 hours in recovery suggest microbiota are still disrupted, and 16S data shows the community heavily dominated by one taxon (the pioneer in secondary succession), yet bacterial CFU steadily decrease with time until they reach Pre-Treatment CFU levels. Fish skin carrying capacity was determined by Pre-

Treatment bacterial CFU, and bacterial CFU are not different at 240-hours indicating the carrying capacity of the fish skin returned to normal conditions, suggesting the climax community has been reached because of their stability. Counts of *E. coli* from selective media correlated with abundance from 16S sequencing data, with K-12 only being highly abundant in the 8-24 hour timeframe, and after that, below detection limits for culture and very rare for sequence abundance.

### ***Fish Skin Microbiome Alpha Diversity***

Alpha diversity of each sample and in groups was determined by SDI. SDI was used because it measures alpha diversity and evenness of the community from 0 to 1. Values closer to 1 are more diverse and more evenly distributed, and values closer to 0 are less diverse and less evenly distributed. SDI for each sample and average SDI by treatment and time are shown in Table 3 and Table 4 at the ESV level. Taxonomic identification of genus level was used instead of ESV because genus level is the lowest taxonomic rank, and therefore, more accurate representation of the community. A total of 169 genera were identified by using the RDP database. At 8-hours in recovery, SDI of *E.coli* treatment is at its lowest, which is expected because it is heavily dominated by *E.coli*. Furthermore, all treatments at 48-hours exhibit a low SDI, which is consistent with the overgrowth effect (Brumlow et al., 2019). Experimental treatment at 240-hours has the highest SDI when compared to Control and Not Rinsed at 240-hours. Analysis of observed genera and SDI suggest introduction of *E.coli* as a pioneer species increased the distribution of the community composition. The bacterium *E.coli* could drive early metabolism to alter nutrient availability for later species to thrive.

### ***Fish Skin Microbiome Biochemical Profile***

Microbiome data are powerful, but HMP indicated the predicted pathway across samples is conserved (HMP, 2012). The 25 different tests were used to predict fish skin microbiome function and generate a profile for each sample. Nitrate, Indole, Malonate, Inositol, Sorbitol, Rhamnose, Lactose, Adonitol, and Xylose tests varied between positive or negative across samples. Interestingly, *E.coli* is known for lactose fermentation and, while it is abundant in the 8 hour treated microbiome by the 16S data and culture methods, the lactose biochemical results are negative. As complexity of the ecosystem increases, bacteria may interact with each other and provide nutrients and growth conditions that may affect metabolism and behavior of the community (Morin et al., 2018) and negative interactions can occur in high nutrient environments allowing bacteria to negatively affect other bacteria (Ratzke et al., 2020). Strain K12 is non-native and not found in *G.affinis*, and so may have been outcompeted by native fish skin bacteria.

### ***Fish Skin Microbiome Analysis***

Pre-Treatment fish are dominated by *Flavobacterium* and have a low SDI (Fig 11 and Table 6). At 8-hours in recovery, *E.coli* is dominant on the Experimental treatment only because it is an experimentally added non-native strain. At 8-hours in recovery, the Control treatment also has a low SDI, which is expected because the fish skin microbiome was severely disrupted by the rinse. At 48-hours in recovery, all treatments are dominated by the natural pioneer, the genus *Chryseobacterium*, which persists in the community strongly after 240 hours suggesting the genus *Chryseobacterium* as a foundation species. Also, *Chryseobacterium* was identified as driving differences among groups (Simpser) indicating *Chryseobacterium* had a strong effect in the composition of

the community, further supporting its role as a foundation species. Fish mucus is primarily made out of mucins, proteins that are highly glycosylated, and can be used as an energy source for microbes; the main source of nutrients in the fish skin microbiome is mucus (Chiarello et al., 2018). The natural pioneer on this experiment was isolated from the CFU plates and the full 16S rRNA gene was sequenced to obtain species ID. The bacterium *Chryseobacterium scophthalmum* (*C. scophthalmum*) was positive for mucin degradation *in vitro*. M9-minimal media was modified containing 5 mg/ml mucin as the only nitrogen and carbon source, therefore, only bacteria that are able to breakdown the mucin will grow. Native pioneer species must be able to take advantage of the available niches opened by the decreased competition, and *C. scophthalmum* can use mucin as a sole carbon and nitrogen source. It outcompeted the rest of the microbes to dominate the community at 48-hours in recovery, possibly by consuming host mucin on the skin.

At 240-hours, fish skin carrying capacity returns to normal conditions and 16S rRNA data shows the community is diverse for each treatment. Since community composition is not significantly different between groups, this suggests that introduction of the K-12 pioneer did not affect recovery of the disrupted microbiome community. However, the non-significant statistical result could be due to a lower of number samples and low power for the PERMANOVA test to discriminate between treatments. Furthermore, given that the K-12 strain did not persist in the community, this may be the reason why it had little effect on the climax composition.

## Conclusion

Pioneer species may help shape the environment after disruption by occupying available niches, but are transient and then replaced by foundation species in the community that will drive ecological interactions in the community. According to ecological succession theories, pioneer species should drive specific pathways that drive specific species succession (Connell & Slatyer, 1977). In this series of experiments, addition of *E.coli* as a pioneer species was transiently dominant in the experimental treatment community at 8-hours in recovery, but then became a rare member, showing a clear pioneer species behavior according to Connell and Slatyer (1977). Community composition of Experimental and Control treatments at 240-hours were not different from each other and *C. scophthalmum* dominated the community in all treatments indicating the initial community composition may influence taxon bloom after disruption. Since *E.coli* is a non-native species in the fish skin microbiome, it might have not been able to utilize many of the nutrients found in the fish skin microbiome. An understanding of initial community composition could help researchers understand *Enterobacteriaceae* blooms and CDI after antibiotic treatment. Using native pioneer species that persist longer in the fish skin microbiome could have a stronger foundation species effect and therefore, change climax community composition.



## CHAPTER III

### Pioneer Species Tested as Foundation

#### Fish Skin Pioneers

After the experimental approach had been validated, allowing addition of selected pioneers after disruption and observing community effects, and testing if introduced pioneer species act as foundation was done by choosing three native fish skin species isolated from the fish skin microbiome, since these bacteria have the capacity to use resources from their natural environment. Three different strains were isolated using different selective media from previous experiments. Based on the water chemistry measured in the previous chapter, chemistry related to nitrogen recycling may be important. It is well known that fish secrete nitrogen in the water in the form of ammonia, which can be transformed to nitrite or nitrate by bacteria (Eck et al., 2019; Graber & Junge, 2007). Both ammonia and nitrate can be toxic to fish at high levels in the water (Jensen, 1996; Van Kessel et al., 2016), therefore, species that recycle nitrogen are important for fish health.

The mucus secreted by the skin of the fish plays an important role for protection against the external environment and it is the first line of protection against possible pathogens in the water column (Legrand et al., 2018), but it is also a source of nutrients for bacteria (Marcobal et al., 2013). Mucin sialidases are a group of enzymes that catalyze the breakdown of carbohydrate chains on mucin and they are part of the first step of mucin breakdown (Juge et al., 2016). Porcine mucin has been used to grow and isolate mucin-utilizing bacteria *in vitro* (Marcobal et al., 2013), and the fish skin mucus could be a main carbon source, therefore minimal media containing mucin was used to

identity mucin-associated bacteria. The bacteria used as introduced pioneer species were chosen based on nitrate and mucin utilization because they should be able to thrive and/or compete in the fish skin microbiome.

***Stenotrophomonas* spp.**

Using M9-mucin agar plates, an FMI1B isolate was recovered from the fish skin microbiome from untreated aquarium fish. The biochemical profile of a pure culture of this strain using Microgen A+B matches *Stenotrophomonas maltophilia* with 99.97% probability and 23.46% likelihood. (Table 11), and the full 16S rRNA gene sequence matches *Stenotrophomonas rhizophilia* strain e-p10 (best match: score 2566; 1401 bp identical over 1407 total, with 2 gaps), the next closest match was much lower (*Stenotrophomonas bentonitica*, score 2507; 1391/1407 with 5 gaps). To differentiate FMI1B from the native fish skin bacteria in culture, a nalidixic acid-resistant strain was generated. The minimum inhibitory concentration (MIC) of FMI1B for nalidixic acid was 32 µg/mL and for the generated resistant strain was >512 µg/mL. The selective media for FMI1B was modified pseudomonas isolation agar with 30 µg/ml Ampicillin and 50 µg/ml nalidixic acid (PAIN), which grows only FMI1B with no background bacteria when the fish skin suspension is plated. FMI1B is a Gram-negative rod that grows white, round, mucoid colonies on PAIN agar plates as shown in Figure 15.

*Table 11 FMI1B biochemical profile.*

*Profile obtained from Microgen A+B system. Positive results equal plus symbol and negative results equal minus symbol.*

<b>FMI1B</b>	<b>Test</b>	<b>Test</b>
	Nitrate	+
	Lysine	+
	Orthinine	-
	H <sub>2</sub> S	-
	Glucose	-
	Mannitol	-
	Xylose	-
	ONPG	-
	Indole	-
	Urease	-
	V.P.	-
	Citrate	+
	TDA	-
	Gelatine	+
	Malonate	-
	Inositol	-
	Sorbitol	-
	Rhamnose	-
	Sucrose	-
	Lactose	-
	Arabinose	-
	Adonitol	-
	Raffinose	-
	Salicin	-
	Arginine	-



*Figure 15 FMI1B morphology.*

Triple-streak of FMI1B on PAIN agar plate.

***Aeromonas* spp.**

FBI408 was isolated from the normal aquarium fish skin microbiome by students in the laboratory portion of the BIOL 2420 course during the spring 2015 semester. The biochemical profile of FBI408 matches *Aeromonas caviae* at 93.6% (Table 12) and the full 16S rRNA gene sequence matches *Aeromonas hydrophila* strain DSM 30187 (best match: score 2595; 1410 bp identical over 1412 with a one gap). The second-best match was *A. dhakensis* with a 2591 score from 1409 identical across 1412 bp with two gaps. Thus, while it is highly confident that FBI408 is within genus *Aeromonas*, it is less confident to be species *hydrophila*, yet that is the most likely species. The genus *Aeromonas* is ubiquitous in aquatic environments and known to be present in fish (Sugita et al., 1995), and was the natural pioneer in previous experiments in our system (Brumlow et al., 2019). To differentiate FBI408 from native *Aeromonas* spp. present in the fish microbiome, a nalidixic acid resistant strain was generated. The MIC of FBI408 with nalidixic acid is 4 µg/ml while the resistant derived strains is >512 µg/ml. Selective media used for FBI408 was modified thiosulfate-citrate-bile salts-sucrose agar (TCBS) with 30 µg/ml ampicillin and 50 µg/ml nalidixic acid (TCBSAN), which only grows FBI408 with no background bacteria when fish skin suspension is plated. FBI408 is a Gram-negative rod that grows as small, yellow, round, mucoid colonies on TCBSAN agar (media starts as green and as FBI408 ferments the sucrose and generates various organic acids; the pH drops and turns the media yellow due to the indicator bromothymol blue) plates as shown in Figure 16. From the biochemical tests, it was noted that FBI408 can convert nitrate into nitrite.

*Table 12 FBI408 biochemical profile.*

*Profile obtained from Microgen A+B system. Positive results equal plus symbol and negative results equal minus symbol.*

<b>FBI408</b>	<b>Test</b>		<b>Test</b>	
	Nitrate	+	Gelatine	-
	Lysine	-	Malonate	-
	Orthinine	-	Inositol	-
	H <sub>2</sub> S	-	Sorbitol	-
	Glucose	+	Rhamnose	-
	Mannitol	+	Sucrose	+
	Xylose	-	Lactose	-
	ONPG	+	Arabinose	+
	Indole	+	Adonitol	-
	Urease	-	Raffinose	-
	V.P.	-	Salicin	+
	Citrate	-	Arginine	+
	TDA	+		

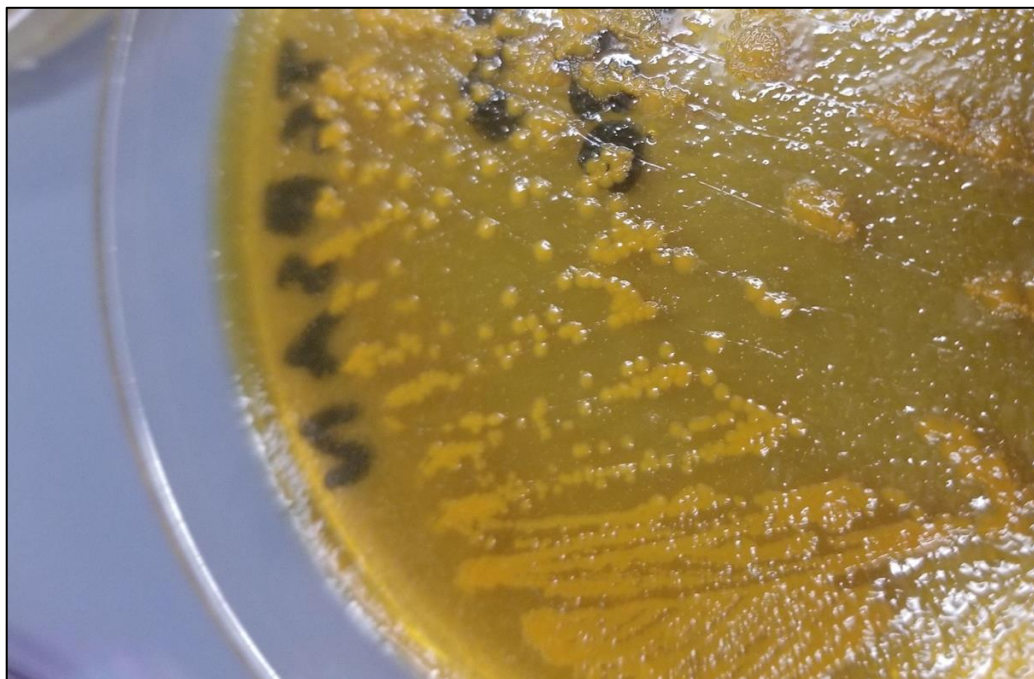


*Figure 16 FBI408 morphology.*

Triple-streak of FBI408 on TCBSAN agar plates.

***Brevibacterium* spp.**

FSI38B was isolated from aquarium fish using PIA media. The Microgen database for species identification only includes members of the *Enterobacteriaceae*, thus *Brevibacterium* is not included. The best match to the biochemical profile of FSI38B within ABIS (Advanced Bacterial Identification System software, Stoica and Sorescu, 2012) online was *Brevibacterium massiliense* at 85.9% (Table 13). The full 16S rRNA gene sequence matches *Brevibacterium casei* strain NCDO 2048 (best match: score 752, 407/407, no gaps). While it is fully identical across that 407 bp sequence, this sequence is not long enough to be discriminatory between other species within the *Brevibacterium* genus. It was noted that FSI38B has the capacity to reduce nitrate to nitrogen gas (poorly soluble in water and evaporates), and thus could reduce the amount of available nitrogen in an aqueous environment. Thus, strain FSI38B at this time can most accurately be described as *Brevibacterium* sp. (unknown species). FSI38B is a Gram-positive bacillus, and we confirmed this by both Gram staining from pure overnight cultures and by a negative, non-stringy result on the KOH test (data not shown). To differentiate FSI38B from the native fish skin microbiome in culture, a nalidixic acid resistant strain was generated. Selective media for FSI38B was modified pseudomonas isolation agar with 30 µg/ml ampicillin and 50 µg/ml nalidixic acid (PAIN), which only grows FSI38B and with no background bacteria when fish skin suspension is plated. FSI38B grows as white, round, mucoid colonies on PAIN agar plates as shown in Figure 17.

*Table 13 FSI38B biochemical profile.*

*Profile obtained from Microgen A+B system. Positive results equal plus symbol and negative results equal minus symbol.*

<b>FSI38B</b>	<b>Test</b>		<b>Test</b>	
	Nitrate	+	Gelatine	-
	Lysine	+	Malonate	-
	Ornithine	-	Inositol	-
	H <sub>2</sub> S	-	Sorbitol	-
	Glucose	-	Rhamnose	-
	Mannitol	-	Sucrose	-
	Xylose	-	Lactose	-
	ONPG	-	Arabinose	-
	Indole	-	Adonitol	-
	Urease	-	Raffinose	-
	V.P.	-	Salicin	-
	Citrate	+	Arginine	-
	TDA	+		



*Figure 17 FSI38B morphology.*

Triple-streak of FSI38B on PAIN agar plates.

## Materials and Methods

### *Pioneer Inoculation*

The bacteria *A. hydrophilia* (FBI408), *S. rhizophilia* (FMI1B), and *Brevibacterium* (FSI38B) were grown in nutrient broth (NB) at 25°C overnight. Bacterial cultures grown overnight were quantified by measuring the optical density at 650 nm. Then, a 2.5-qt. Polyethylene tub (HDX Model # 05M3HDX) containing 2 L of APW was inoculated with each pioneer at a calculated OD<sub>650</sub> of 0.05. After rinsing, the fish were exposed to one pioneer per group in the water column for 8 hours to allow the pioneer species to invade the skin microbiome. Afterwards, the fish were transferred to fresh APW for recovery where they were sampled at later time points. Mortality is low, as expected, during this procedure because the pioneer species are native to the fish microbiome.

### *Experimental Design*

All fish were collected from the same aquarium to ensure minimal starting community variance (homogeneity). A total of ~110 fish were used for this study, where 20 fish were required per group. Experimental and control groups were rinsed and transferred to the appropriate APW bucket (with bacteria and with no bacteria) as groups. The experimental groups were incubated for 8-hours with pioneer species and then transferred to a clean APW bucket for recovery. The control group was incubated for the same amount of time in sterile APW, then transferred into a clean APW bucket for recovery. As a further comparison, one group of fish was not rinsed (Not Rinsed), but these fish went through the same transfers as the experimental and control groups. After treatment (Rinsed or Not Rinsed), fish were sampled for 240-hours in recovery. Major samples were collected pre-treatment (PT), post-rinse (PR), after an 8-hour incubation



(which confirms levels of pioneer introduction), 48-hours in recovery (to represent mid-recovery), and 240-hours in recovery (to represent final recovery).

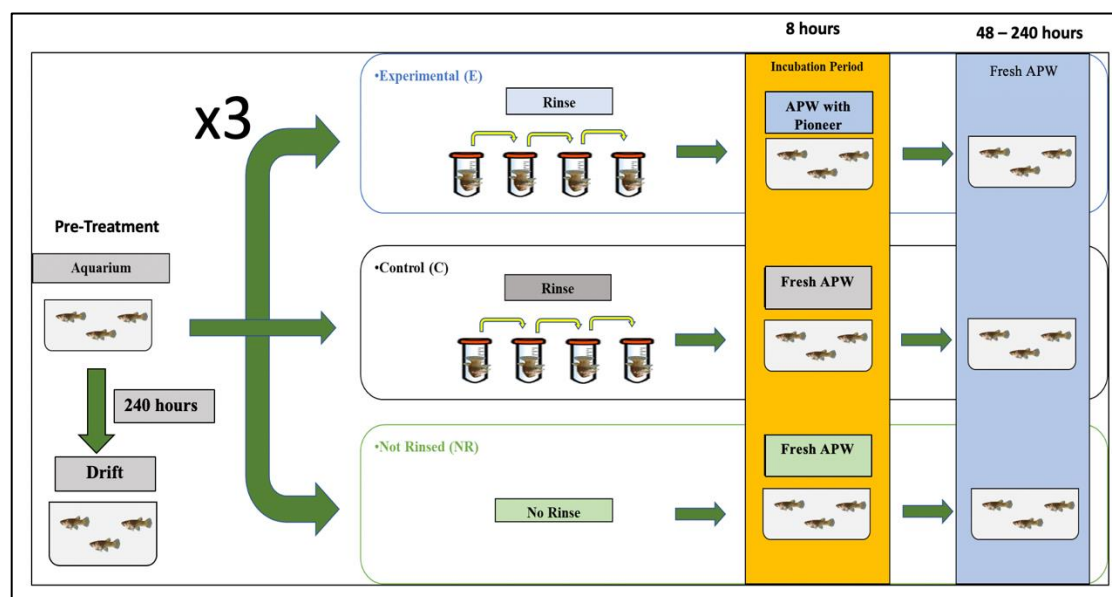


Figure 18 Experimental design of BCE experiments.

### Microbiome 16S rRNA Extraction and Amplification

For 16S rRNA gene profile analysis, the microbiome was extracted from the fish using the protocol above, then bacteria were pelleted by a 2-minute spin in a centrifuge at room temperature at top speed (14,000 rpm). The pellet was frozen and stored at  $-80^{\circ}\text{C}$  until all were ready for DNA extraction. Total DNA was extracted using the PowerSoil DNA isolation kit (MO BIO Laboratories) following manufacturer's instructions. The 16S gene sequencing used PCR primers 515F/806R (5'-GTGCCAGCMGCCGCGGTAA-3'/5'-GGACTACHVHHHTWTCTAAT-3'), covering the V3-V4 regions, on the sequencing platform MiSeq v3 with 300-bp paired-end reads following manufacturer's protocol.

### Biochemical Analysis

To determine the microbiome function profile, using a VWR® Standard Heavy-Duty Vortex Mixer (catalog#: 97043-562), skin microbiome communities were extracted by placing a one fish per time point in a 15 mL conical tube with 5 mL of sterile saline water (0.85% NaCl). Each fish was vortexed at maximum speed (3200 rpm) for 1-minute pausing shortly for 1 second every 10 seconds, then the fish was removed aseptically from the tube and placed in a recovery aquarium where the fish was not resampled. Fish skin extract was inoculated into the Microgen A+B system. A total of 100µL were placed into each well, and wells 1, 2, 3, 9, and 24 were overlaid with 100µL of sterile immersion oil. Wells were read according to manufacturer's instructions. A limitation of this method is that while a positive result in this test indicates that the community has a certain biochemical capability, it does not prove that this function is active while the community is actually on the fish skin. So, it demonstrates possibility, not *in situ* results.

### **Data Analysis**

R version 3.6.3 (2020-02-29) was used with R Studio version 1.2.5033. Exact Sequence Variants (ESV) were generated using the dada2 package version 1.14.0 (Callahan et al., 2016) for a total of 2896 of ESVs. Taxonomic classifications were assigned by *IdTaxa* using the Ribosomal Database Project (Cole et al., 2014) release version 16 released March 2018 by the DECIPHER package version 2.14.0 (Wright, 2016). Rarefaction curves were generated using *ggrare* from ranacapa package version 0.1.0 (Gaurasv, 2019). Before analysis was performed, ESVs that matched Archaea, Eukarya, or unidentified at the level of domain (no database match) were filtered out, for a total of 773 ESVs for analysis.

The phyloseq package version 1.30.0 (McMudie & Holmes, 2013) and the microbiome package version 1.9.95 (Lahti et al., 2017) were used to generate multiple measures. Observed and Shannon Diversity Indices (SDI) for all samples and all groups at the ESV level and genus level were generated through the *estimate\_richness* function in the microbiome package. NMDS using Bray-Curtis dissimilarity was generated using *ordinate* function in the phyloseq package to visualize differences between the composition (beta diversity) of skin communities at different times points. Statistical analysis of Bray-Curtis diversity among groups was analyzed by the *adonis* function in the vegan package version 2.5-6 (Oksanen et al., 2019). Furthermore, SIMPER analysis via *simper* function from vegan package was used to assess taxon driving community differences. Normality was measured by *shapiro.test* function; a significant p-value indicates a non-normal distribution and variables were tested based on normality. All figures were generated using ggplot2 package version 3.2.1 (Whickman, 2016).

## **Results**

### ***Bacterial Load on the Fish Skin***

Fish skin bacterial load was measured by counting CFU on NA plates. As shown in Figures 18 and 19, the trend is consistent with the previous experiment (Fig 3), where rinsing heavily reduces the bacterial load of the fish skin (Brumlow et al., 2019) and bacterial load returns to pre-treatment levels after 240 hours in recovery.

### ***Artificial introduction of the pioneer species after rinsing.***

The rinsing procedure removed 89% of the total skin CFU. In all three treated 8-hour samples, the total CFU is much higher (~3-log higher) than 8-hour control or non-rinsed groups, suggesting the introduced pioneers are gathering onto the fish skin from

the water column (Wilcoxon;  $p = 4e-04$ ). Consistent with overgrowth seen in previous experiments (Brumlow et al., 2019) and the previous chapter, all groups had elevated counts at the 48-hour time point.

The four rinsed groups at 48 hours on average had 190-fold higher counts than the pre-treatment samples (Wilcoxon;  $p = 1.7e-4$ ). The not-rinsed group counts were higher than pre-treatment as well (Wilcoxon,  $p = 4.9e-3$ ), but not as high as all of the rinsed groups (Wilcoxon,  $p = 1.7e-4$ ). The counts of all of the groups at 10 days are all statistically similar (Kruskal-Wallis,  $p=0.388$ ). Consistent with the previous experiment, the 10-day samples are also not significantly different from the pre-treatment (Kruskal-Wallis;  $p\text{-value} = 0.1423$ ).

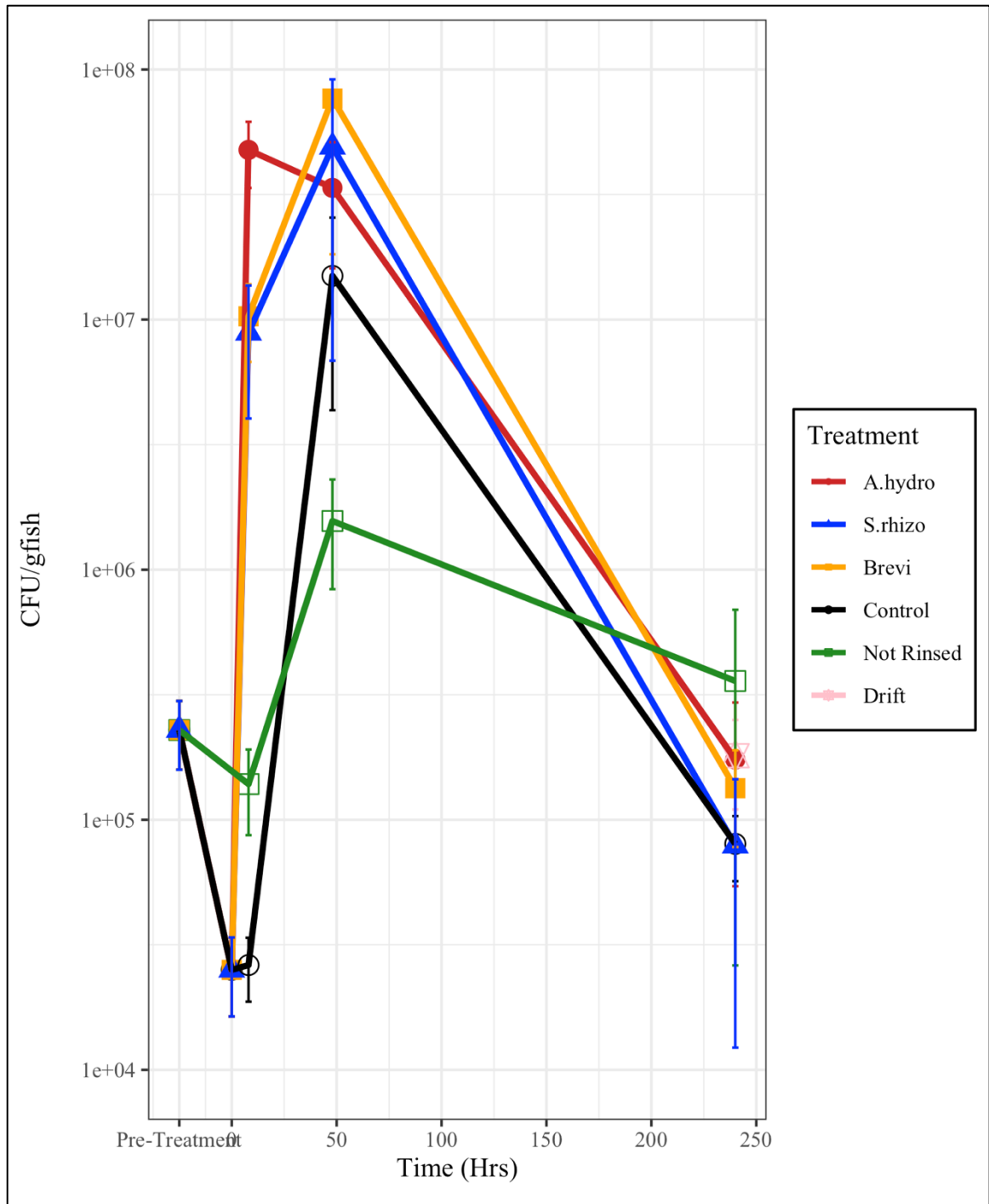


Figure 19 Line plot of CFU by group across time (hours).

Fish were sampled from the undisturbed aquarium (Pre-Treatment), Post-Rinse (0 hours), 8-hour, 48-hour, and 240-hour timepoints. Each dot represents a different group and the error bars represent SD.

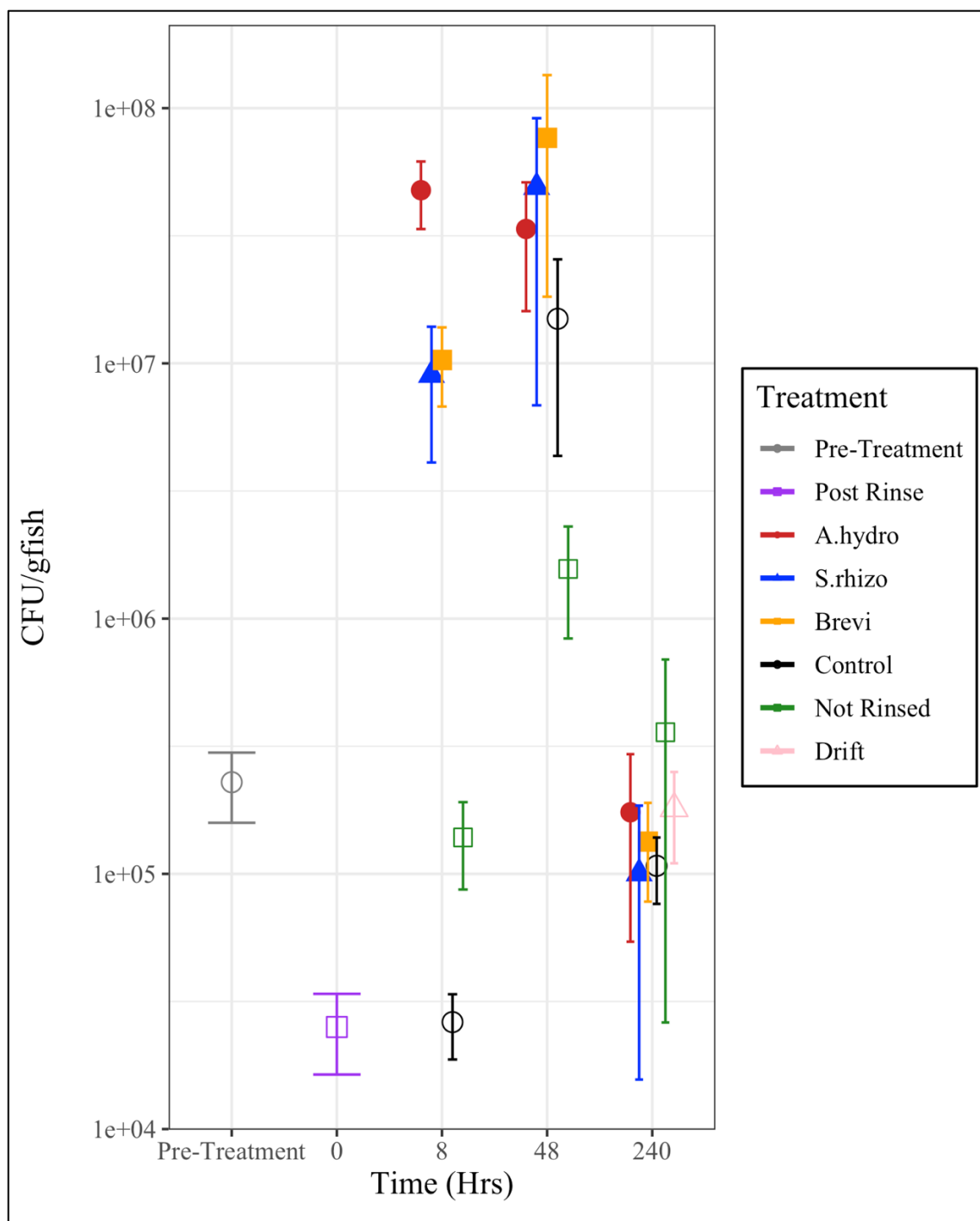


Figure 20 Scatterplot of CFU across the major sampling times.

Fish were sampled from the undisturbed aquarium (Pre-Treatment), Post-Rinse (0 hours), 8-hour, 48-hour, and 240-hour timepoints. Each dot represents a different group and the line represents SD. N = 20 per treatment, and each data point is the mean with standard deviation of a group of 5 fish.

Table 14 Tracking of introduced pioneer *S.rhizophilia* by plating CFU.

Treatment	Time	Mean_Counts	SD_Counts	Media
S.rhizo	Pre-Treatment	228551.8	70024.4	NA
S.rhizo	Pre-Treatment	0	NA	PAIN
S.rhizo	0	25114.7	8754.7	NA
S.rhizo	0	0	NA	PAIN
S.rhizo	8	8854549.9	4833191.9	NA
S.rhizo	8	3138337	992518.6	PAIN
S.rhizo	48	49077328.6	42227016	NA
S.rhizo	48	6795547.7	2734040.8	PAIN
S.rhizo	240	78796.6	66522.6	NA
S.rhizo	240	2871	2122.2	PAIN

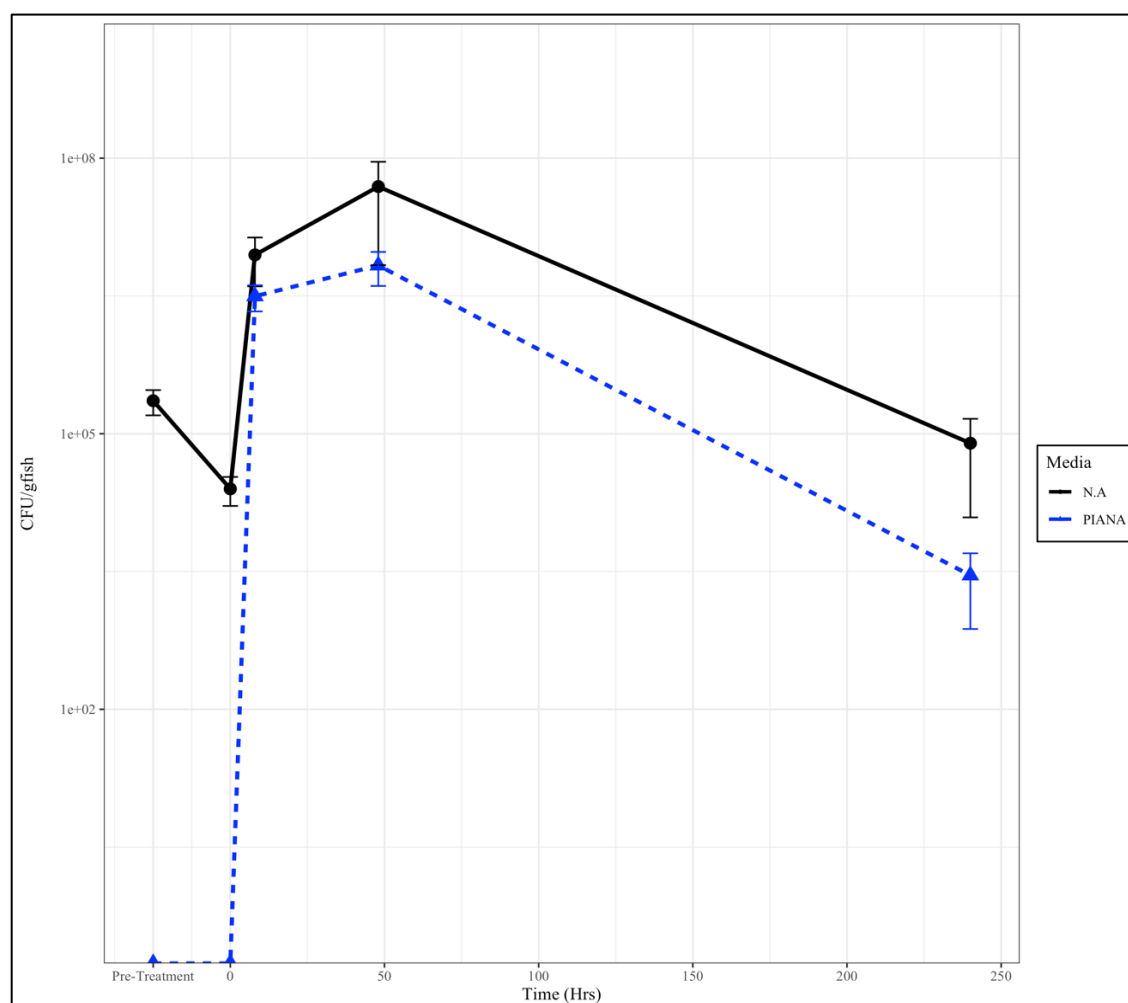


Figure 21 Line plot of CFU of PAIN and NA plates tracking *S.rhizophilia*.

Symbols represent average CFU normalized by fish weight and error bars represent standard deviation.

Table 15 Tracking of introduced pioneer *A.hydrophilia* by plating CFU.

Treatment	Time	Mean_Counts	SD_Counts	Media
A.hydro	Pre-Treatment	228551.8	70024.4	NA
A.hydro	Pre-Treatment	0	0	TCBSAN
A.hydro	0	25114.7	8754.7	NA
A.hydro	0	0	0	TCBSAN
A.hydro	8	47702813.4	14098523.8	NA
A.hydro	8	23641969.4	11352541	TCBSAN
A.hydro	48	33622355.7	17599360.8	NA
A.hydro	48	9722730	2664101.3	TCBSAN
A.hydro	240	174300.1	120070.3	NA
A.hydro	240	9439.8	2557.6	TCBSAN

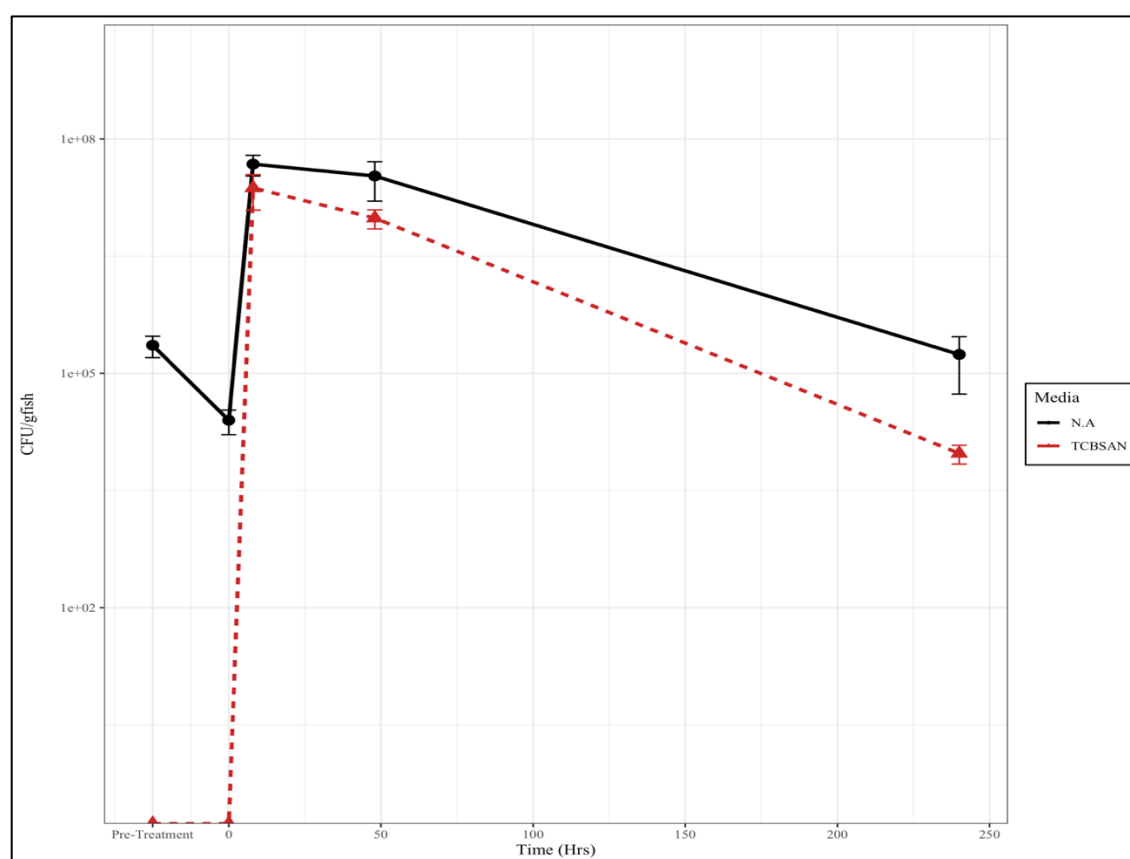


Figure 22 Line plot of CFU of TCBSAN and NA plates tracking *A.hydrophilia*. Symbols represent average CFU normalized by fish weight and error bars represent standard deviation.



Table 16 Tracking of introduced pioneer *Brevibacterium* by plating CFU.

Treatment	Time	Mean_Counts	SD_Counts	Media
Brevi	Pre-Treatment	228551.8	70024.4	NA
Brevi	Pre-Treatment	0	NA	PAIN
Brevi	0	25114.7	8754.7	NA
Brevi	0	0	NA	PAIN
Brevi	8	10307835.8	3531248.7	NA
Brevi	8	676306	298653.2	PAIN
Brevi	48	76501650.2	58252790.3	NA
Brevi	48	0	NA	PAIN
Brevi	240	133768.4	55942.7	NA
Brevi	240	0	NA	PAIN

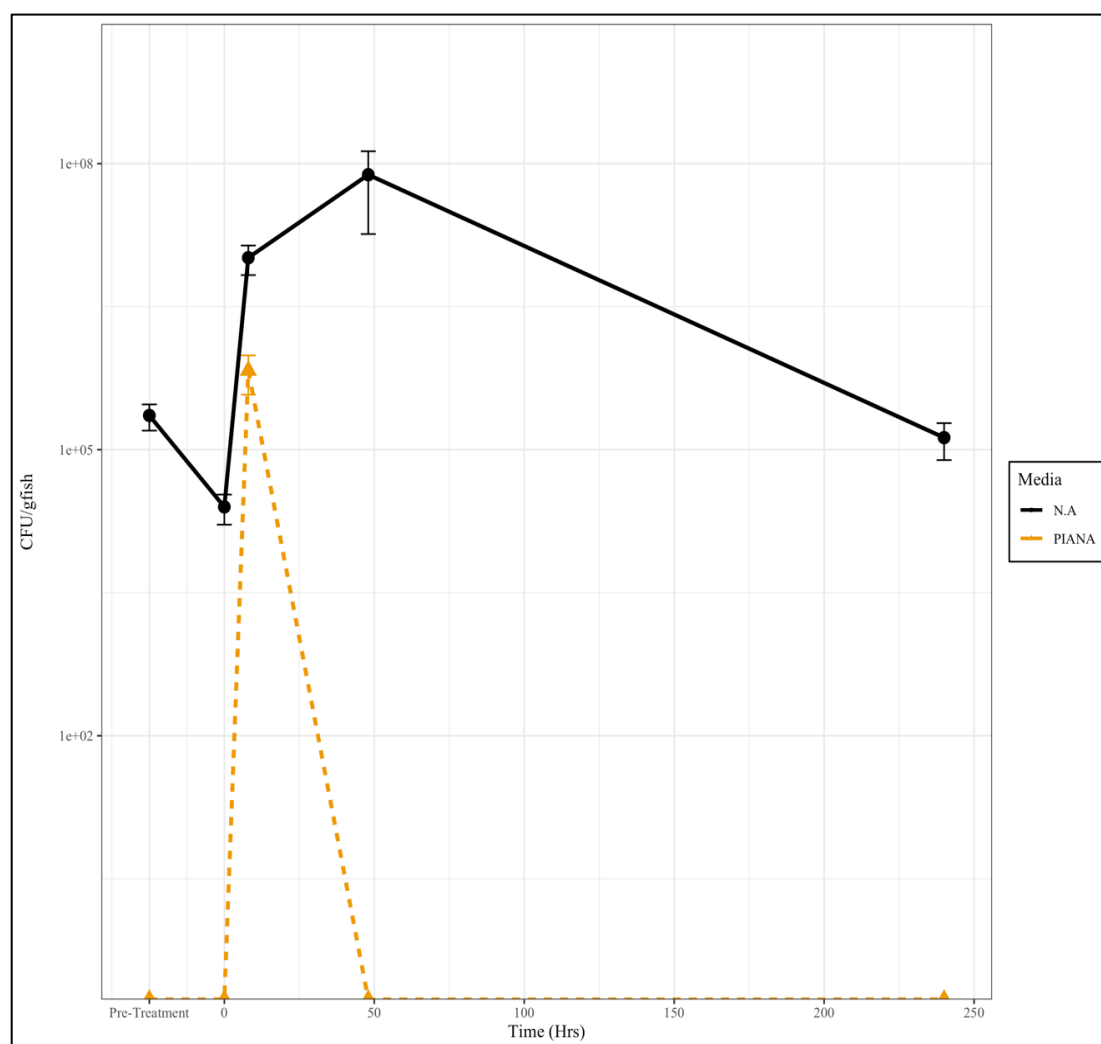


Figure 23 Line plot of CFU of PAIN and NA plates tracking *Brevibacterium*. Symbols represent average CFU normalized by fish weight and error bars represent standard deviation.

### ***Fish Skin Microbiome Biochemical Profile***

The biochemical profile of the fish skin microbiome was measured across 25 tests using Microgen A+B strips (Table 17). Some activities are not observed in any of the communities, including xylose, sorbitol, adonitol, and lactose fermentation. This is not surprising since the activities in the Microgen system were selected to identify taxa within the *Enterobacteriaceae* family, of which not many are native to fish skin (most are members of mammalian gut communities). Other activities are rare, occurring in only one sample, namely urease and malonate utilization and inositol fermentation, or in two samples only: rhamnose fermentation. Since fish excrete nitrogen waste as ammonia (not urea like mammals), a lack of urease in the skin microbiome is not surprising. Conversely, some activities are universal, found in every sample. This includes nitrate reduction, hydrogen sulfide production from thiosulfate, glucose fermentation, production of beta-galactosidase enzyme (ONPG hydrolysis, the first step in lactose utilization), sucrose and arabinose fermentation, and production of acetoin by glucose fermentation (VP reaction). Thus, one would predict that the strips are not a very comprehensive measure of our community (fish skin microbiome) functions, since out of the 25 activities measured, eleven have no discriminating capability, being always lacking or always present. Thus, only fourteen activities can detect any community differences. Of those, three are only seen in one community and three (production of indole from tryptophan, presence of tryptophan deaminase, and arginine dihydrolase activity) were present in all but one community. Principal coordinate analysis shows that indeed the strips do not discriminate well between the communities (Fig 23).

*Table 17 Biochemical activity of fish skin microbiota at major sampling times. A total of 25 tests were recorded at each timepoint. Positive results and negative results are represented by “+” and “-”, respectively.*

ONPG	Xylose	Mannitol	Glucose	H2S	Ornithine	Lysine	Nitrate	Time (Hrs)	Treatment
+	-	-	+	+	-	+	+	-1	Pre-Treatment
+	-	+	+	+	-	-	+	8	A.hydro
+	-	+	+	+	+	+	+	8	S.rhizo
+	-	-	+	+	+	+	+	8	Brevi
+	-	+	+	+	+	+	+	8	Control
+	-	+	+	+	-	+	+	8	Not Rinsed
+	-	+	+	+	-	+	+	48	A.hydro
+	-	+	+	+	+	+	+	48	S.rhizo
+	-	+	+	+	+	+	+	48	Brevi
+	-	+	+	+	+	+	+	48	Control
+	-	+	+	+	-	+	+	48	Not Rinsed
+	-	+	+	+	-	+	+	240	A.hydro
+	-	+	+	+	-	+	+	240	S.rhizo
+	-	+	+	+	-	+	+	240	Brevi
+	-	+	+	+	-	+	+	240	Control
+	-	+	+	+	-	+	+	240	Not Rinsed
+	-	+	+	+	-	-	+	240	Drift





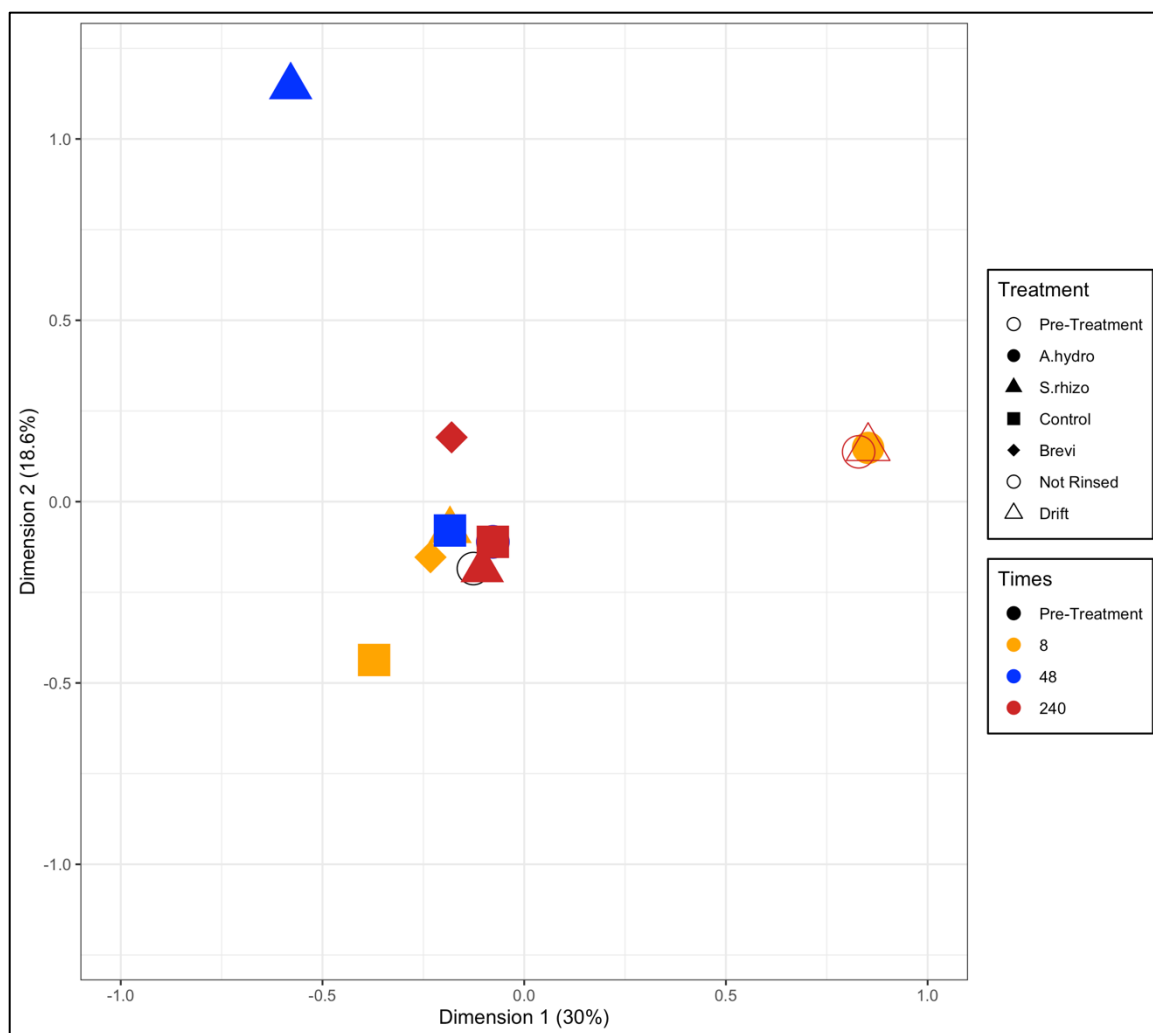


*Figure 24 Fish skin microbiome biochemical profile.*  
Each symbol represents the biochemical pattern from one fish.

### ***Fish Skin Microbiome Coverage***

The total number of sequences after quality filtering from all 75 samples was 7,002,622. Sampling is representative, as the average Good's coverage for all samples was 99.97% and the average Chao1 was only 11.5% higher than the average number of observed ESVs, which complement the rarefaction curves (Figure 24). Also, the coverage is not slanted to any one particular experimental group (Table 18) and groups have a Good's coverage average of 99.9 (Table 19). The total gamma diversity (total number of ESVs identified in all 75 samples was 773.

Figure 25 Rarefaction curves showing sampling depth of all samples. Each treatment is represented by a different color.



Table 18 Sequence coverage for all samples.

Sample	Treatment	Time	Singletons	Sequences	Good's Coverage	Observed ESV	Chao1
BCEPT1	Pre-Treatment	-1	30	40430	99.93	248	275.19
BCEPT1-2	Pre-Treatment	-1	20	99460	99.98	290	304.62
BCEPT2	Pre-Treatment	-1	19	46617	99.96	204	214.69
BCEPT2-2	Pre-Treatment	-1	22	113610	99.98	238	251.59
BCEPT3	Pre-Treatment	-1	17	51012	99.97	234	243.07
BCEPT3-2	Pre-Treatment	-1	12	116560	99.99	265	270.5
BCEA81	A.hydro	8	18	149375	99.99	71	101.6
BCEA82	A.hydro	8	22	126719	99.98	85	106
BCEA83	A.hydro	8	12	96863	99.99	62	78.5
BCES81	S.rhizo	8	24	144726	99.98	90	113
BCES82	S.rhizo	8	15	120498	99.99	79	90.67
BCES83	S.rhizo	8	23	135320	99.98	100	125.3
BCEP81	Brevi	8	15	76193	99.98	57	78
BCEP82	Brevi	8	21	58410	99.96	72	95.33
BCEP83	Brevi	8	16	68827	99.98	90	99.23
BCEC81	Control	8	10	45358	99.98	84	89.63
BCEC82	Control	8	9	99627	99.99	80	84
BCEC83	Control	8	28	88756	99.97	80	155.6
BCEN81	Not Rinsed	8	13	51432	99.97	117	156
BCEN82	Not Rinsed	8	15	113428	99.99	116	129.13
BCEA41	A.hydro	48	8	53975	99.99	72	75.11
BCEA42	A.hydro	48	25	272801	99.99	103	140.5
BCEA42-2	A.hydro	48	15	104713	99.99	87	97.5
BCEA43	A.hydro	48	17	298721	99.99	117	128.33
BCEA43-2	A.hydro	48	18	113118	99.98	100	117
BCES41	S.rhizo	48	18	177415	99.99	109	120.77
BCES41-2	S.rhizo	48	29	94061	99.97	105	134
BCES42	S.rhizo	48	29	171757	99.98	175	196.37
BCES43	S.rhizo	48	23	121900	99.98	118	133.81
BCES43-2	S.rhizo	48	31	101705	99.97	121	163.27
BCEP41	Brevi	48	21	114257	99.98	97	127
BCEP41-2	Brevi	48	20	294711	99.99	108	139.67
BCEP42	Brevi	48	14	90898	99.98	97	115.2
BCEP42-2	Brevi	48	13	189186	99.99	106	117.14
BCEP43	Brevi	48	3	49970	99.99	55	55.43
BCEC41	Control	48	11	170173	99.99	136	139.67
BCEC41-2	Control	48	20	254986	99.99	309	319.56
BCEC42	Control	48	17	114729	99.99	91	103.36

BCEC43	Control	48	25	106624	99.98	143	173
BCEC43-2	Control	48	19	136489	99.99	150	171.38
BCEN41	Not Rinsed	48	20	132632	99.98	115	142.14
BCEN41-2	Not Rinsed	48	12	110420	99.99	103	112.43
BCEN42	Not Rinsed	48	13	7804	99.83	68	76.67
BCEN42-2	Not Rinsed	48	15	88062	99.98	91	108.5
BCEA21	A.hydro	240	13	70383	99.98	135	143.67
BCEA22	A.hydro	240	22	33791	99.93	160	170.04
BCEA23	A.hydro	240	19	39645	99.95	150	163.15
BCEA24	A.hydro	240	23	67013	99.97	167	186.46
BCEA25	A.hydro	240	24	99049	99.98	172	197.09
BCES21	S.rhizo	240	11	67146	99.98	125	131.11
BCES22	S.rhizo	240	18	39045	99.95	152	165.91
BCES23	S.rhizo	240	26	33213	99.92	149	168.12
BCES24	S.rhizo	240	15	11117	99.87	117	122.25
BCES25	S.rhizo	240	25	43535	99.94	168	183
BCEP21	Brevi	240	15	62831	99.98	142	153.67
BCEP22	Brevi	240	6	50034	99.99	132	134.5
BCEP23	Brevi	240	16	45406	99.96	158	167.23
BCEP24	Brevi	240	19	51668	99.96	156	168.21
BCEP25	Brevi	240	20	54459	99.96	152	167.83
BCEC21	Control	240	19	52514	99.96	166	183.1
BCEC22	Control	240	13	52378	99.98	171	175.59
BCEC23	Control	240	20	41004	99.95	166	183.27
BCEC24	Control	240	10	49756	99.98	155	159.5
BCEC25	Control	240	7	57420	99.99	140	143
BCEN21	Not Rinsed	240	16	84969	99.98	137	150.33
BCEN22	Not Rinsed	240	18	79601	99.98	145	155.93
BCEN23	Not Rinsed	240	14	61620	99.98	146	161.17
BCEN23-2	Not Rinsed	240	14	94608	99.99	155	168
BCEN24	Not Rinsed	240	15	129535	99.99	143	156.13
BCED21	Drift	240	12	43124	99.97	179	195.5
BCED21-2	Drift	240	16	104297	99.98	205	217
BCED22	Drift	240	15	22051	99.93	207	218.67
BCED22-2	Drift	240	15	65365	99.98	238	243.25
BCED23	Drift	240	9	23901	99.96	195	201
BCED23-2	Drift	240	9	57816	99.98	214	218.5

*Number of singletons (ESVs with only one sequence detected) is Singletons. Total number of sequences per sample is Sequences. Goods is the Good's percent coverage estimate. Observed ESV is the number of ESVs for each sample. Chao1 is an estimate of the total number of ESVs that would be present if sequencing was fully representative.*

*Table 19 Sequence coverage per group.*

<b>Treatment</b>	<b>Time</b>	<b>Goods Mean</b>	<b>Goods SD</b>	<b>Chao1 Mean</b>	<b>Chao1 SD</b>	<b>Observed Mean</b>	<b>Observed SD</b>
Pre-Treatment	-1	99.97	0.02	259.94	30.8	246.5	29.23
A.hydro	8	99.99	0	95.37	14.77	72.67	11.59
S.rhizo	8	99.98	0	109.66	17.56	89.67	10.5
Brevi	8	99.97	0.01	90.85	11.3	73	16.52
Control	8	99.98	0.01	109.74	39.81	81.33	2.31
Not Rinsed	8	99.98	0.01	142.56	19	116.5	0.71
A.hydro	48	99.99	0	111.69	25.86	95.8	17.05
S.rhizo	48	99.98	0.01	149.64	30.41	125.6	28.37
Brevi	48	99.99	0.01	110.89	32.49	92.6	21.62
Control	48	99.99	0.01	181.39	82.29	165.8	83.3
Not Rinsed	48	99.95	0.08	109.93	26.79	94.25	20.06
A.hydro	240	99.96	0.02	172.08	20.76	156.8	14.72
S.rhizo	240	99.93	0.04	154.08	26.05	142.2	20.85
Brevi	240	99.97	0.01	158.29	14.64	148	10.86
Control	240	99.97	0.01	168.89	17.41	159.6	12.42
Not Rinsed	240	99.98	0	158.31	6.64	145.2	6.5
Drift	240	99.97	0.02	215.65	16.74	206.33	19.69

*Goods is the Good's percent coverage estimate. Observed is the number of ESVs for each sample. Chao1 is an estimate of the total number of ESVs that would be present if sequencing was fully representative.*

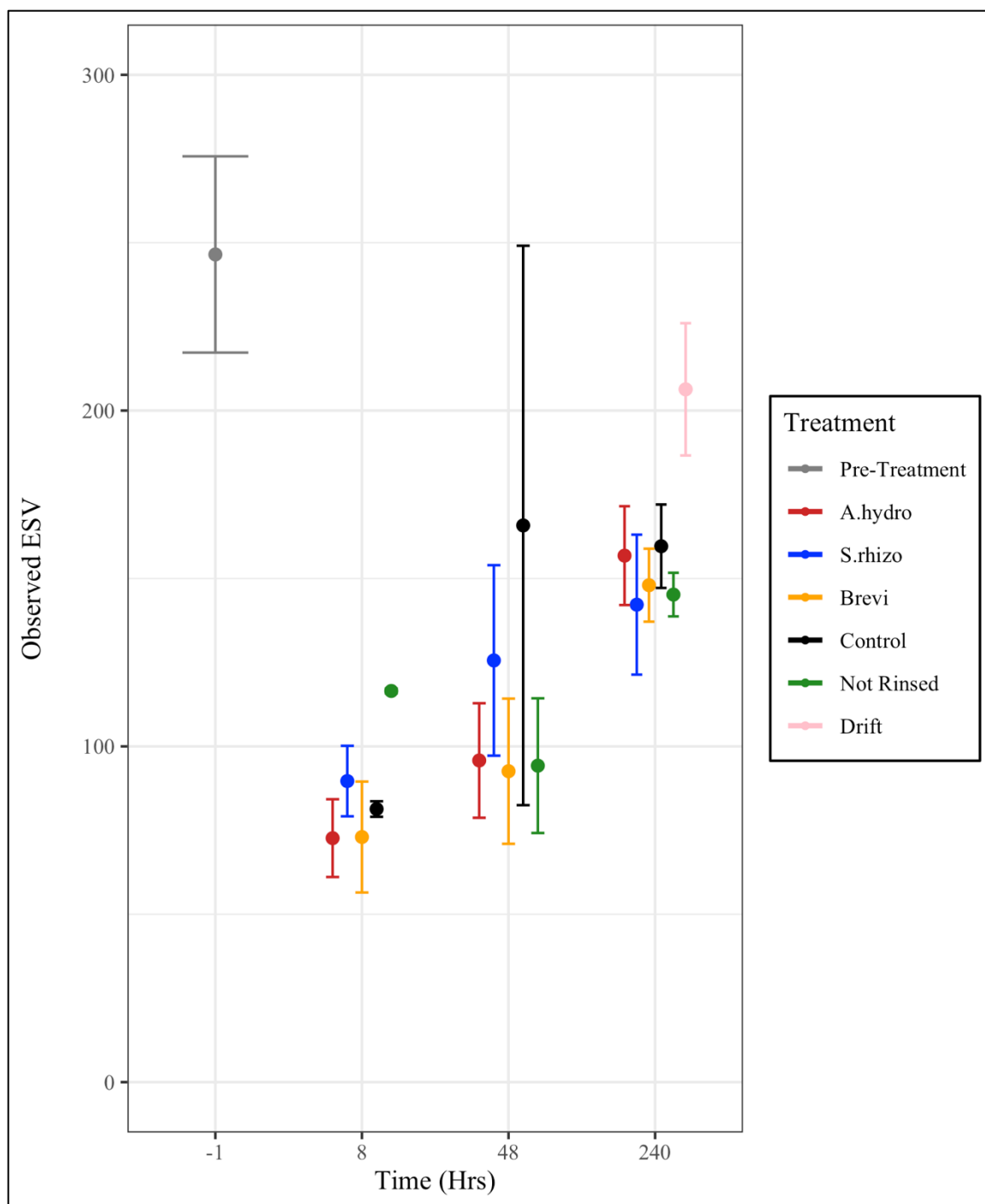


*Figure 26 Mean observed number of ESVs across groups.*

The average of each treatment is represented by a different color and the standard deviation is represented by the error bars.

Rinsing is a strong disruption which lowers the richness (247 mean ESVs in pre-treatment samples compared to 79 in the 8-hour rinsed groups). Transfer is also a disruption, but not as strong (117 ESVs in 8-hour group). At 48 hours, the diversity has risen but not returned to the pre-treatment level (control at 48-hrs has 166 ESVs). As expected, groups with added introduced pioneer strains have lower diversity compared to the control group at 48 hours (126 vs 96 vs 93 for the pioneers *S. rhizo*, *A. hydro*, and *Brevibacterium*, respectively). After 240-hours, all five groups have similar diversity, with  $150 \pm 7.5$  ESVs (ANOVA,  $p = 0.252$ ), but did not return to the pre-treatment level of 247 ESVs (Wilcoxon;  $p=0.00033$ ). Drift is also significantly different from pre-treatment (T-test;  $p=0.021$ ).

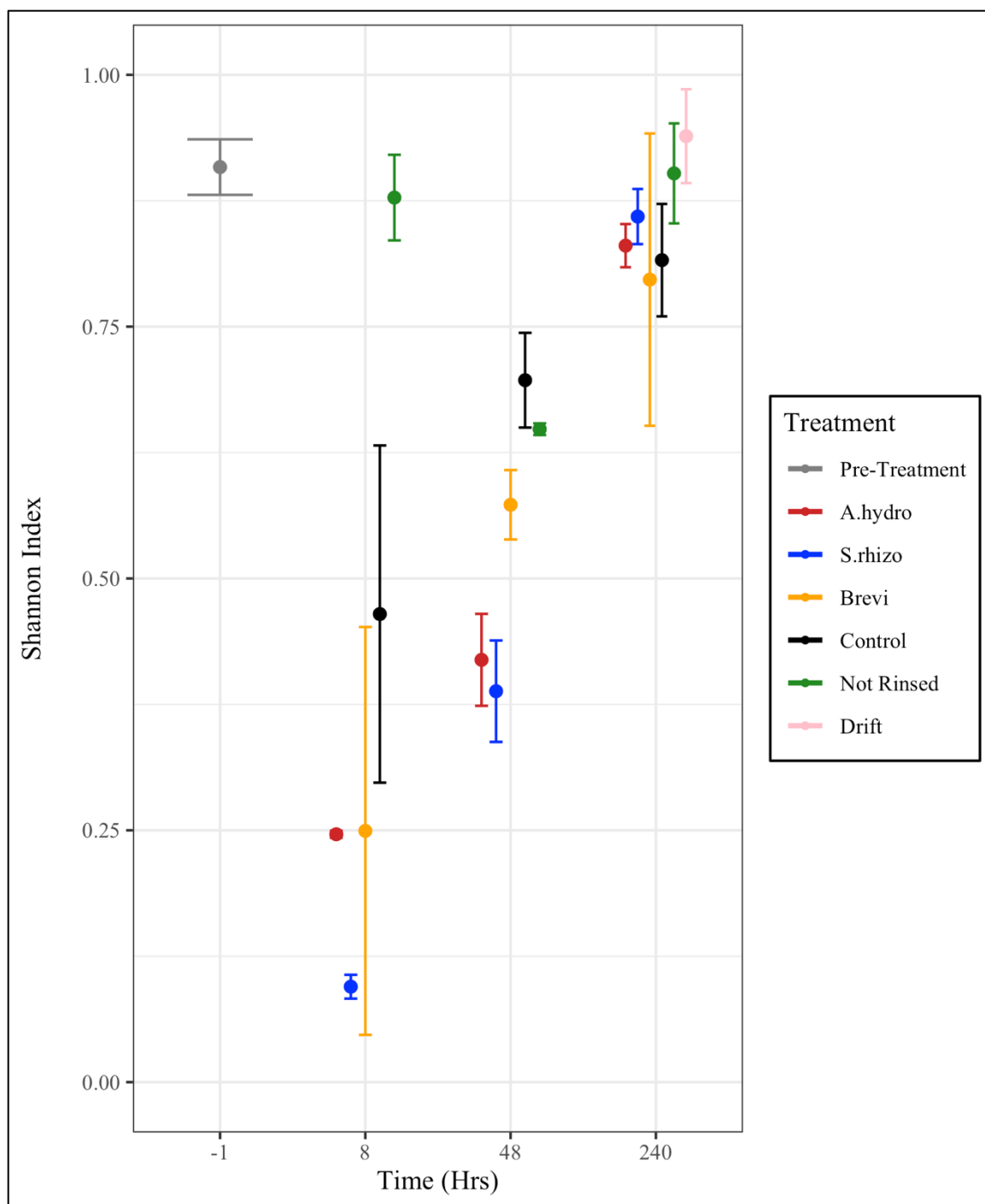


Figure 27 Shannon Diversity Index of groups, calculated at the ESV level. The average of each treatment is represented by a different color and the standard deviation is represented by the error bars.

The values of Shannon's Diversity Index are from 0 to 1, and the index includes both richness and evenness (Magurran, 1988). Using this measure, all of the treatment groups at 240-hours days are similar compared to each other (Kruskal-Wallis;  $p$ -value = 0.1759) and to the pre-treatment group (Dunn's test;  $p > 0.05$ ). The drift group is only different from the 240-hour A.hydro group and control group (Dunn's test;  $p = 0.021$ ,  $p = 0.021$ , respectively).

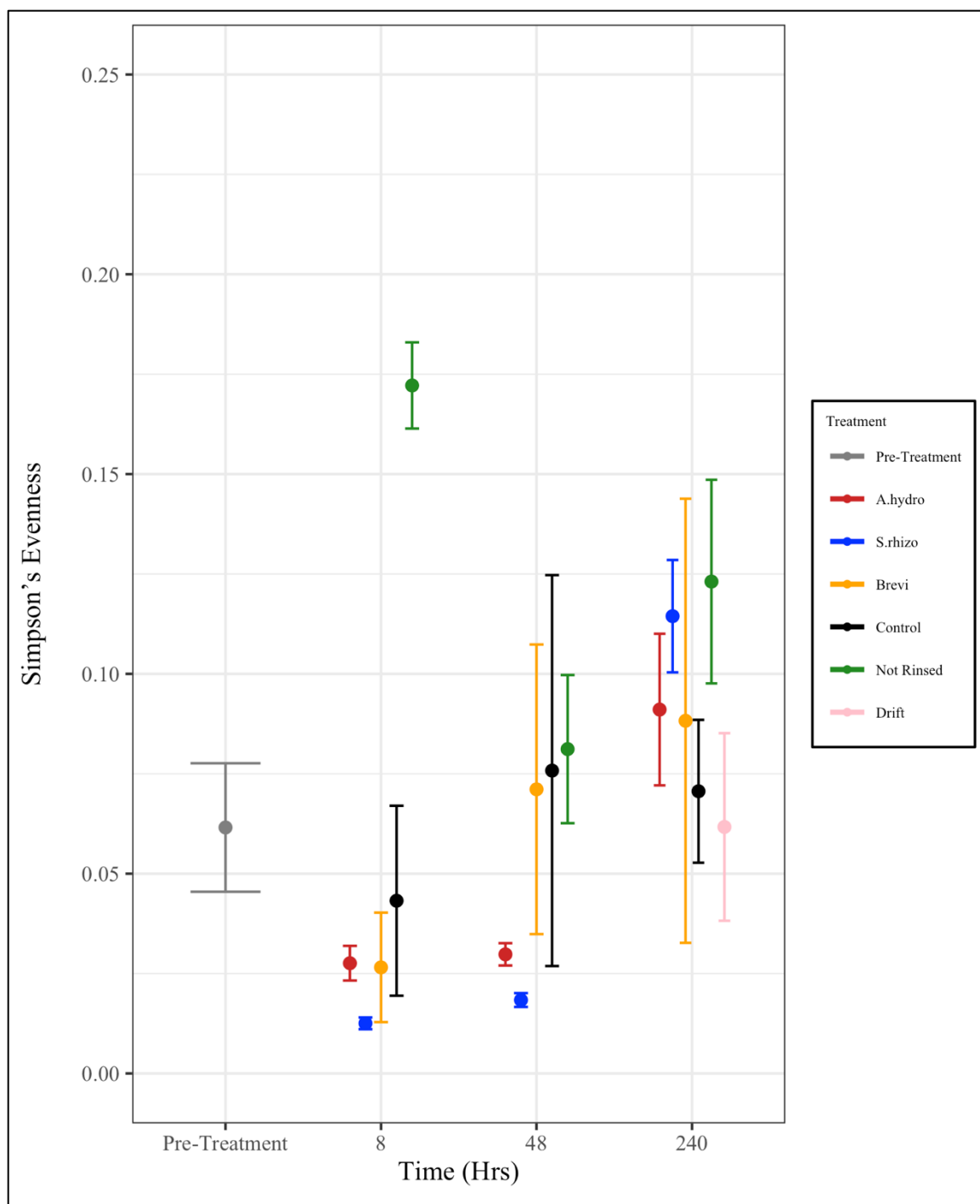


Figure 28 Average evenness index including all ESVs.

The average of each treatment is represented by a different color and the standard deviation are represented by the error bars. The data is normally distributed. Pairwise Tukey's Honest Test shows that not rinsed and pre-treatment ( $p=0.013$ ) as well as *S. rhizo*-exposed and pre-treatment ( $p=0.046$ ) are significantly different.



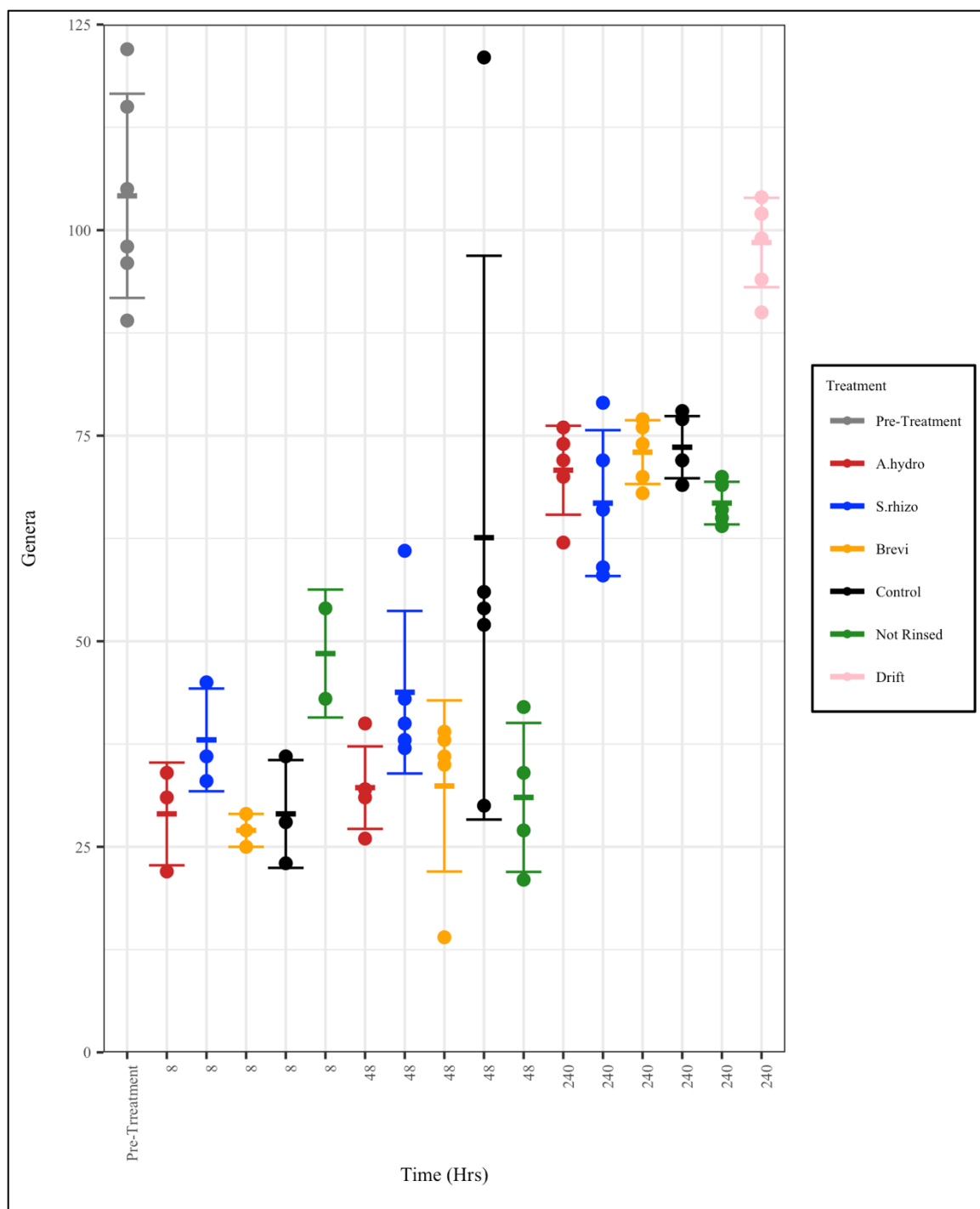


Figure 29 Richness of groups at the level of genus.

The observed number of genera of each group and each treatment is represented by a different color and the standard deviation are represented by the error bars.

Looking at richness (alpha diversity) at the lowest accurate taxonomic level of genus gives the same pattern as with ESVs and as expected, rinsing disruption lowers the evenness temporarily, which returns to pre-treatment levels after recovery. Rinsing lowers the richness by two-thirds of all groups ( $104 \pm 12$  genera in the pretreatment group compared to  $31 \pm 4.9$  for all the rinsed groups at 8 hours). Transfer lowers richness by half (8 hour “Not-rinsed” group has  $49 \pm 7.8$ ). At 48 hours, the mean richness of the rinsed groups rose somewhat to  $43 \pm 14$  genera while the variability between fish rose even more (the relative SD within the six pre-treatment fish was 12% while the 48-hour groups ranged from 16% to 55%, with an average of 31%). In contrast to ESV data, the drift group was not significantly different from pre-treatment richness (T-test; p-value = 0.341). Again, the 240-hour treated groups are not different from each other (ANOVA; p = 0.157) and pre-treatment group and drift group have higher richness than all treated groups at 240 hours (Wilcoxon, p-value = 0.001; p-value = 0.0114, respectively). While some genera (about 25) are lacking in the 10d treated groups compared to the pre-treatment, none of those genera are abundant in the pre-treatment community (highest individual abundance of genus *Cetobacterium*, only 0.0092 relative abundance in pre-treatment group, and total abundance in pre-treatment group of all 25 was 0.36%, therefore, only rare genera are lost).

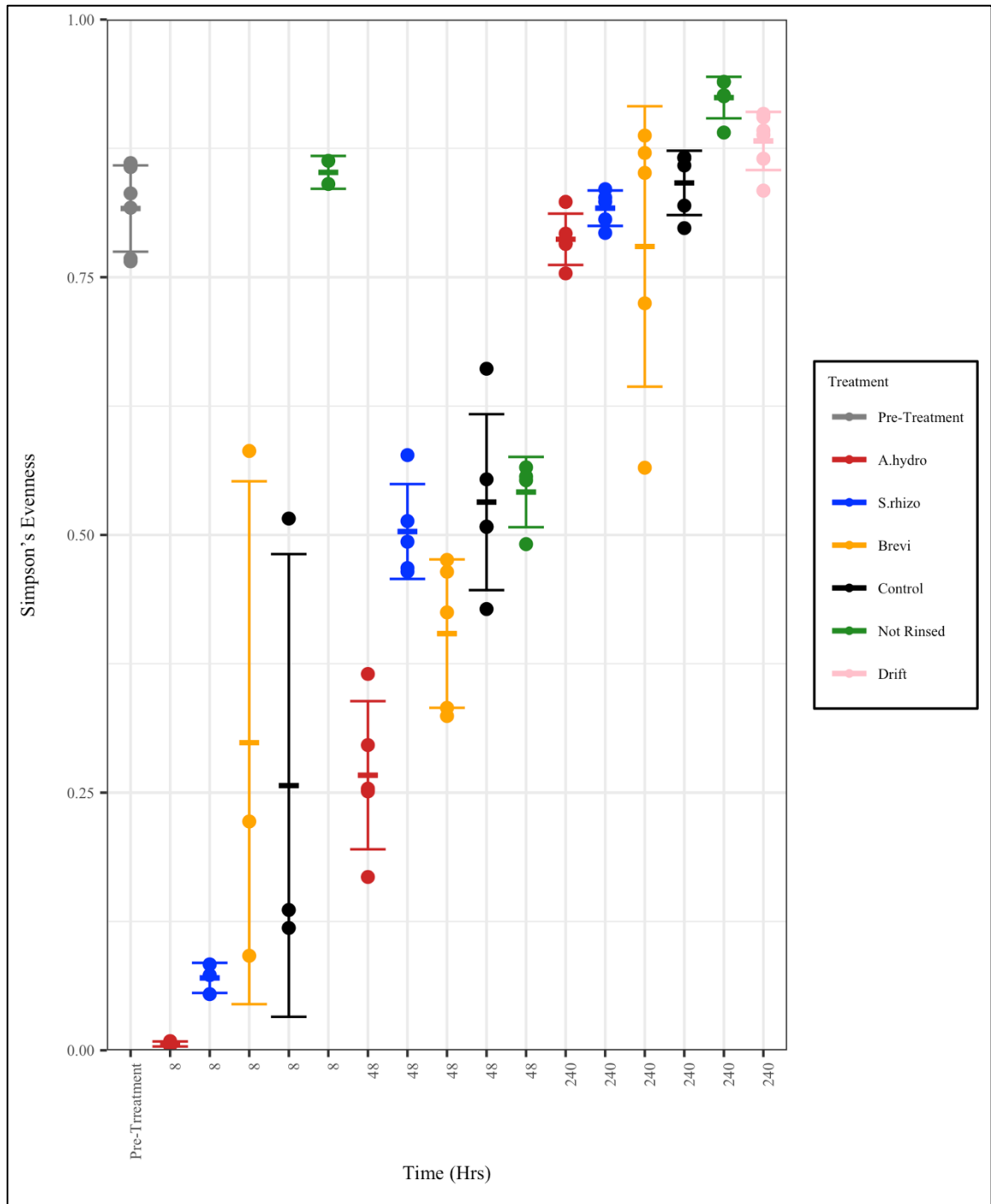


Figure 30 Simpson's evenness of groups at the level of genus.

The observed number of genera of each group and each treatment is represented by a different color and the standard deviation are represented by the error bars.

**Figure 31** Abundance of dominant ESVs across major sampling times for all samples. Column graph of the ten most abundant ESVs in the entire dataset, with all other ESVs grouped into “other,” shown across all 75 samples, which are grouped. LCBD (local contribution to beta diversity) scores represent the degree of uniqueness of the composition of each sample compared to the rest of the dataset. At the top of the graph are group names (i.e. A8 is the pioneer *A. hydrophila* added, 8 hrs timepoint; and N48 is non-rinsed at 48 hrs), while at the bottom of the graph are individual sample names. Note D240 is the drift group.

*Table 20 Identification of dominant ESVs.*

*Counts is the combined number of sequences for that ESV in all 75 samples (total number of sequences in dataset of 7,002,622). Overall abundance is the percent abundance of that ESV in the entire dataset. Presence is the number of samples in which that ESV was found (75 samples total in dataset).*

<b>ESV</b>	<b>Identification</b>	<b>Counts</b>	<b>Overall Abundance</b>	<b>Presence</b>
ESV1	<i>Aeromonas</i>	877,980	12.5%	65
ESV2	<i>Stenotrophomonas</i>	833,895	11.9%	63
ESV3	<i>Aeromonas</i>	537,325	7.67%	75
ESV4	<i>Aeromonas</i>	374,787	5.35%	73
ESV5	<i>Flavobacterium</i>	312,519	4.46%	75
ESV8	<i>Aeromonas</i>	238,766	3.41%	73
ESV11	<i>Flavobacterium</i>	175,454	2.51%	75
ESV12	<i>Runella</i>	171,650	2.45%	53
ESV13	<i>Flavobacterium</i>	163,172	2.33%	67
ESV14	<i>Brevibacterium</i>	152,360	2.18%	37

The genus *Aeromonas* includes 56 ESVs, including the most abundant ESV1.

ESVs are numbered in order of total abundance in the dataset before filtering. ESVs 3, 4, 7, 8, and 10 are also identified as *Aeromonas*. It is the most common genus in the entire dataset, not a surprise since it is the natural pioneer that appears after disruption, and it is also present in the pre-treatment and drift samples. Most of the ESVs (40 of the 56) are present in the pre-treatment samples. The introduced pioneer strain of *Aeromonas* and the natural pioneer strain(s) cannot be distinguished in the sequencing data.

*Brevibacterium* includes three ESVs, namely ESV14, 982, and 2519, with only 14 being dominant in abundance. *Stenotrophomonas* includes 17 ESVs, but only ESV2 is abundant, as the next are ESV108 and 128. Of those 17 ESVs, 98% of all sequences identified as *Stenotrophomonas* are ESV2. While not an introduced pioneer,

*Flavobacterium* was the most abundant genus in the pre-treatment samples, and returns to

prominence in the 240-hour samples. *Flavobacterium* included 35 ESVs, including ESV5, 11, 13, 16, and 25.

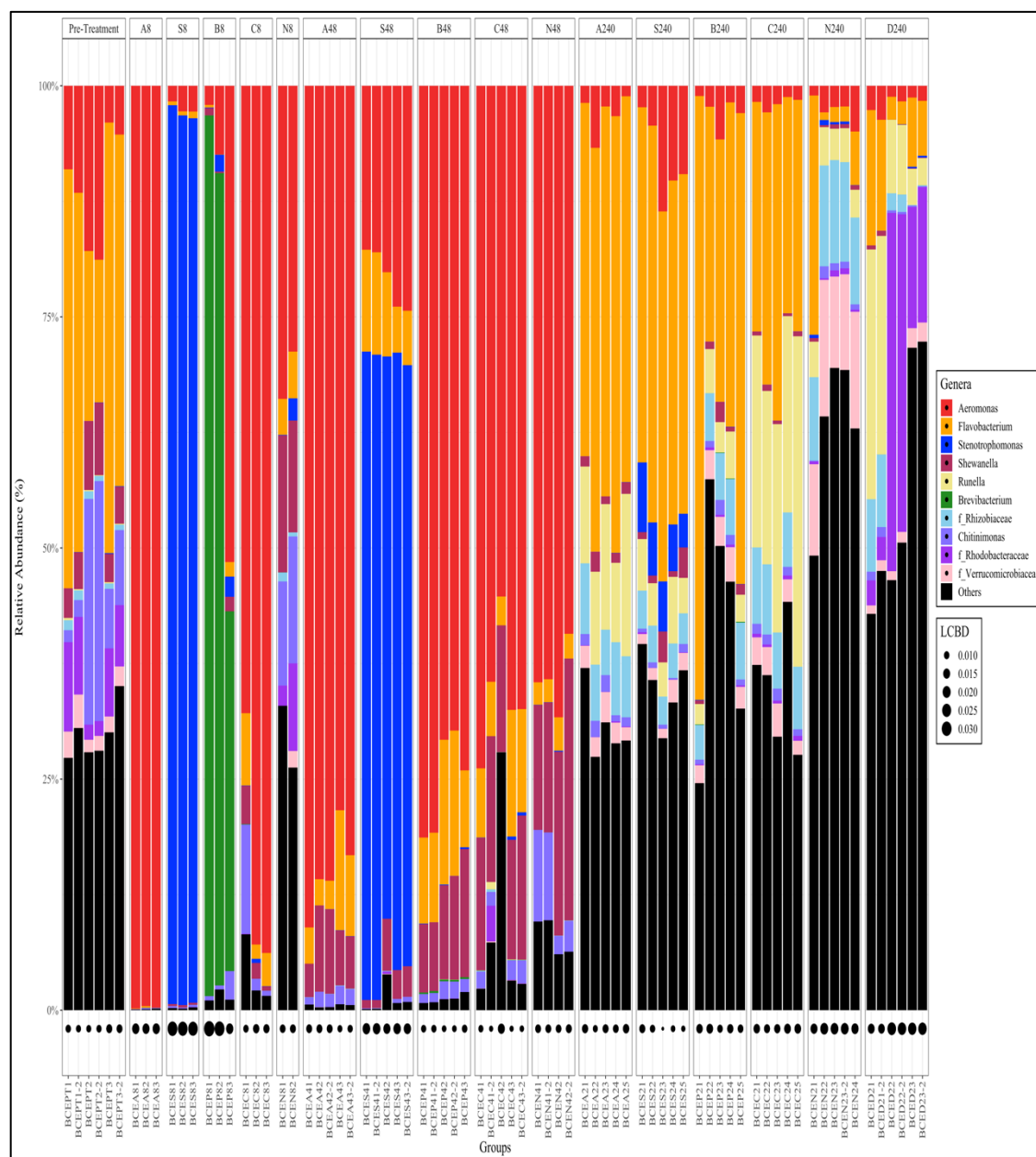


Figure 32 Abundance of dominant genera across major sampling times across all samples.

Pre-treatment, the fish skin microbiome is dominated by *Flavobacterium* ( $33.7 \pm 13.5\%$ ), *Chitinimonas* ( $11.3 \pm 11.1\%$ ), *Aeromonas* ( $11.1 \pm 6.2\%$ ), family

*Rhodobacteraceae* ( $5.9 \pm 3.5\%$ ), and family *Comamonadaceae* ( $5.7 \pm 2.8\%$ ). Eight hours after rinsing, the control fish are dominated by the natural pioneer *Aeromonas* ( $84.9 \pm 14.7\%$ ). Other dominant genera are *Chitinimonas* ( $4.6 \pm 6.3\%$ ), *Flavobacterium* ( $4.3 \pm 3.2\%$ ), and *Shewanella* ( $2.1 \pm 1.9\%$ ), which was 4.9% in the pre-treatment group. So, some of the same genera are dominant, just the relative abundance has changed.

However, most genera have been lost. There were 92 genera in the pre-treatment, with a cumulative 12.7% abundance, that are not present in the control 8-hour group (taxa lost after rinse). Eight genera (total 0.23% abundance) were present in the control and absent in the pre-treatment fish (taxa gained). For fish exposed to *A. hydrophila* after the rinse, 99.7% of the microbiome is the genus *Aeromonas*, a combination of the added pioneer strain and pre-existing indigenous strains. Genera lost (present in pre-treat but not in the A8 group) were again 92, totaling 9.46% of the pre-treat abundance. So, the *A. hydrophila*-exposed group is not less diverse than the C8 group at the genus level, but is less even. Forty-one of those 92 genera lost in the A8 group return in the 240-hour group (A240), and those 41 comprise 10.7% of the 240-hour community. While distinguishing the introduced pioneer versus native strains of *Aeromonas* is not possible in the sequencing data, the selective plating requires double antibiotic resistance (ampicillin and nalidixic acid). Consistent with this, no colonies grew on the selective media from pre-treatment fish (Table 15 and Figure 21). Looking at the counts from the selective media compared to the total counts on NA, selective counts were 49.6% of total at 8 hours, 28.9% at 48 hours, and 5.4% at 240 hours. By comparison, the relative abundance of the genus in the sequencing was 99.7% at 8 hours, 84.9% at 48 hours, and 3.05% at 240 hours. However, it cannot be assumed that NA captures all bacteria, in fact, it likely does

not. Just like the PCR primers used in amplification before sequencing are biased against certain sequences (Kennedy et al, 2014), so too the media are biased against certain bacteria.

By comparison, the B8 group is  $74.0 \pm 30.6\%$  *Brevibacterium*, along with *Aeromonas* ( $20.3 \pm 27.1\%$ ), with other genera at much lower levels, such as *Stenotrophomonas* ( $1.4 \pm 1.1\%$ ). Two fish in the B8 group have similar composition, with the third being rather divergent. For example, for *Brevibacterium*, fish B81 has 95.3%, fish B82 had 87.9%, but fish B83 had 38.9% abundance, and for *Aeromonas*, B81 had 2.1%, B82 had 7.4%, but B83 had 51.5%. In the S8 group, the fish skin microbiome was dominated by *Stenotrophomonas* ( $96.4 \pm 0.77\%$ ), followed by *Aeromonas* ( $2.4 \pm 0.63\%$ ), and *Flavobacterium* ( $0.52 \pm 0.17\%$ ). Comparing culture and sequencing abundance in the *Brevibacterium*-exposed groups, the selective media gives 6.6% of the counts of NA at 8 hours and no counts are recovered at 48 and 240 hours. Again, no colonies were seen from the pre-treatment samples. While the numbers do not match, the pattern does (abundant only at 8 hours). For the *Stenotrophomonas*-exposed groups, selective plating revealed 35.4% of total counts at 8 hours, 13.8% at 48 hours, and 3.6% at 240 hours. This compares to sequencing abundances of 96.4%, 66.5%, and 5.5%, respectively. Again, numbers are different, but patterns match.

Comparing the three introduced pioneers, we can notice some differences. The genus including all three pioneers strongly dominates in their respective 8-hour group; with A8 having  $99.7 \pm 0.12\%$  *Aeromonas*, S8 having  $96.4 \pm 0.77\%$  *Stenotrophomonas*, and B8 having  $74.0 \pm 30.6\%$  *Brevibacterium*. Note that the natural pioneer is also *Aeromonas*, at  $84.9 \pm 14.7\%$  abundance in the C8 group. At 48 hours, both A48 (*Aeromonas* at



84.9±4.6%) and S48 (*Stenotrophomonas* at 66.5±3.8%) are still dominated by the pioneers, while in B48 *Brevibacterium* has declined to 0.20±0.01% abundance. So, similar to *E. coli* K-12, this organism is transient. Again, the rinsed control is still dominated by *Aeromonas* at 48 hours, with 65.7±6.8% abundance. After 240 hours, *Aeromonas* has declined (1.87±0.63%) in the control and *Flavobacterium* has returned to 27.4±4.5% abundance (it dominated pre-treatment). The three groups with introduced pioneers mirror this, with A240 containing 3.05±2.2% *Aeromonas* and 42.6±3.3% *Flavobacterium*, S240 containing 5.5±1.4% *Stenotrophomonas* along with 8.0±4.6% *Aeromonas* and 39.1±2.5% *Flavobacterium*, and B240 containing 0.05±0.02% *Brevibacterium* along with 2.8±1.8% *Aeromonas* and 16.8±27.3% *Flavobacterium*. While *Stenotrophomonas* persists in the S240 group, it does not appear to suppress, but indeed may enhance the levels of *Aeromonas* and *Flavobacterium*, compared to the control group, C240.

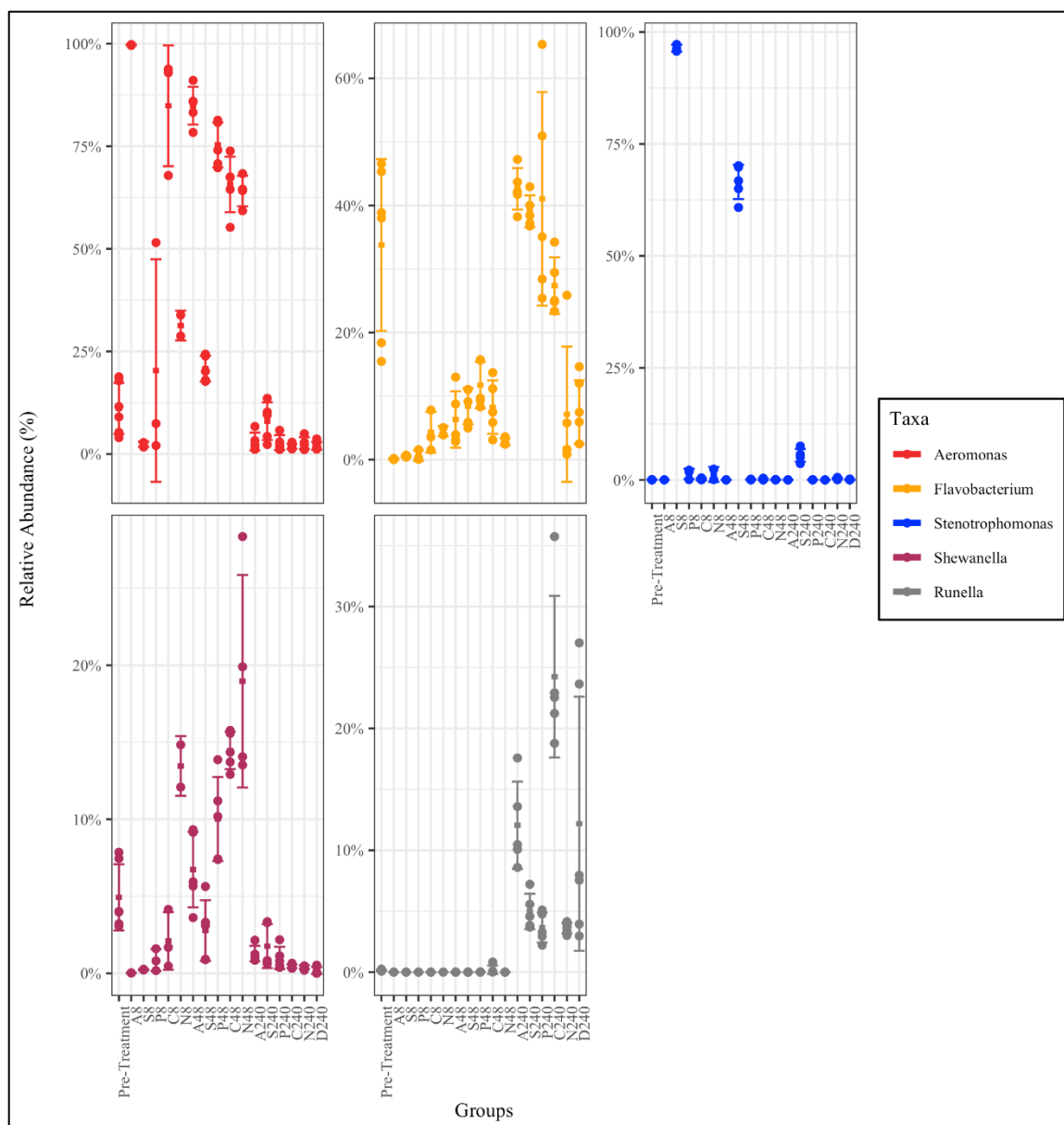


Figure 33 Strip plot of the five most abundant genera across all groups. Each symbol represents a sample and the line represents SD.

Looking at the abundance of genera across the groups, there are a few patterns. *Aeromonas* is more dominant in the pre-treatment and 8-hour and 48-hour samples, but less in the 240-hour samples, so it has a pattern of losing abundance over time. Interestingly, it is also lost in the drift ( $2.0 \pm 0.97$ ) compared to pre-treat ( $11.1 \pm 6.2$ ), even

though drift fish are in the same aquarium for 240 hours that pre-treatment fish were drawn from. In contrast, *Flavobacterium* is abundant in the pre-treat, is lower abundance in 8 hr and 2 d samples, but then is higher again in the 10 d samples, thus having a returning pattern. Yet again, *Flavobacterium* is reduced in drift ( $7.5 \pm 5.0$ ) relative abundance compared to pre-treat ( $33.8 \pm 13.5$ ), likely because of a bloom in the family *Rhodobacteraceae* in the drift ( $17.7 \pm 15.5$  as opposed to  $5.9 \pm 3.5$  in pre-treat). *Stenotrophomonas* is abundant after addition as an introduced pioneer in the S8 and S48 samples, but otherwise, while present, is rare ( $\leq 0.2\%$ ) in other groups. *Shewanella* has the same losing pattern as *Aeromonas*, being mostly abundant in 2 d samples and pre-treat, and lower elsewhere. However, *Runella* has a gaining pattern, being most dominant in the 10 d and drift samples. This genus is  $0.14 \pm 0.06\%$  abundance in pre-treat, while  $12.2 \pm 10.4$  in drift,  $24.2 \pm 6.6$  in control 10 d, and  $12.1 \pm 3.6$  in *A. hydrophila*-treated at 10d.

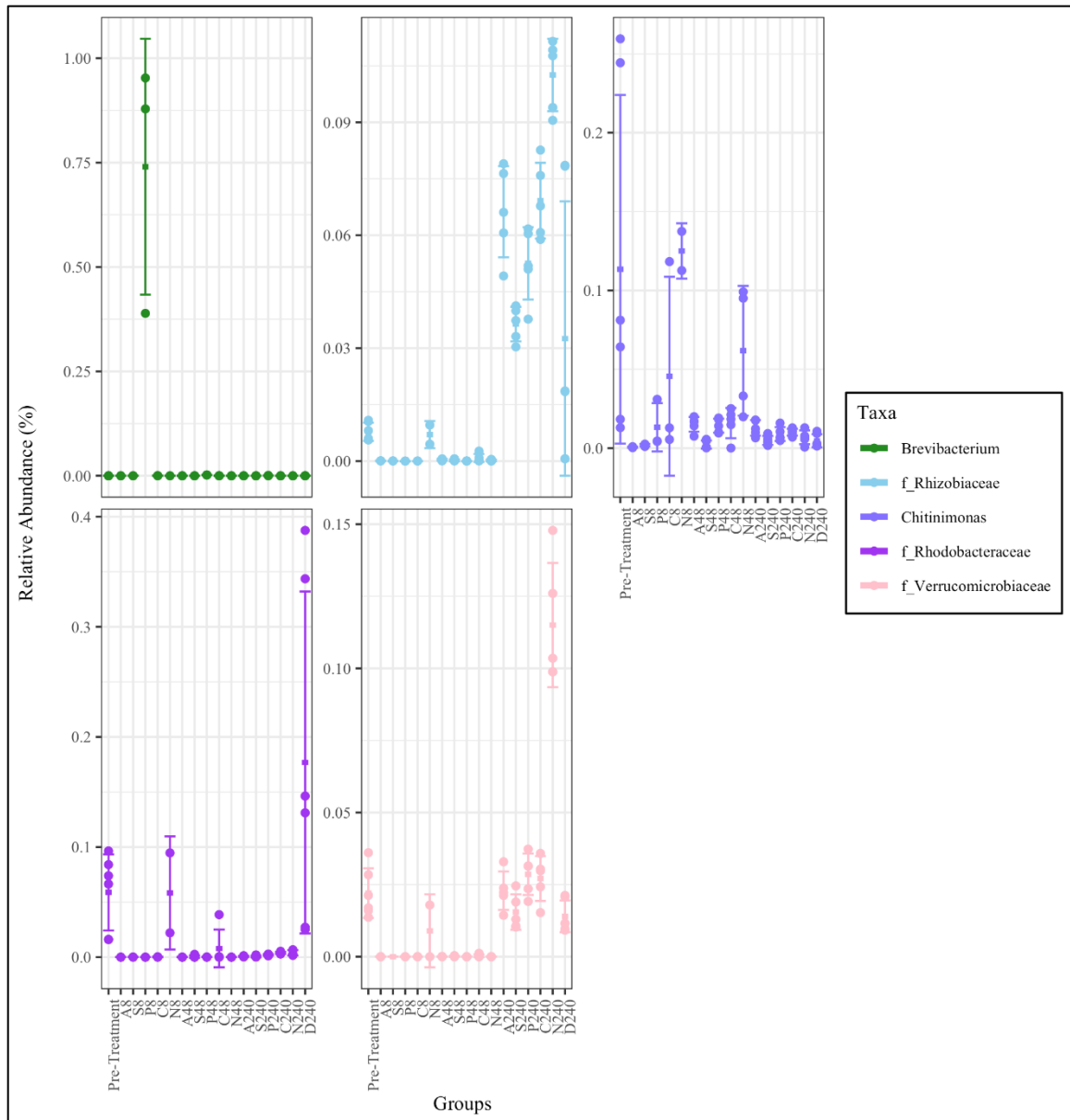


Figure 34 Strip plot of the next five most abundant genera (6 through 10-most) across all groups.

Each symbol represents a sample and the line represents SD.

The introduced pioneer *Brevibacterium*, as seen before, is transient, and only dominant in the 8 hr sample just after introduction. It is rare in other groups and even lacking in samples in the 10 d groups of A240, S240, C240, and non-rinsed 240. There is

some natural indigenous *Brevibacterium*, but at very low abundance ( $0.001 \pm 0.001$  in the pre-treatment group). The family *Rhizobiaceae* has a gaining pattern, as does *Runella*. *Chitinimonas* is generally lost, as is *Aeromonas*. In addition to blooming in the drift, family *Rhodobacteraceae* is rare in other groups, and only noticeably abundant in the non-rinsed at 8 hours ( $5.8 \pm 5.1\%$ ). Family *Verrucomicrobiaceae* has a returning pattern, and blooms in the non-rinsed 10 d group.

Six of the 773 observed ESVs are defined as core taxa, i.e. present in every one of the 75 samples. There are also some ESVs that are not core by the strict definition (present in every single sample), but are present in at least one fish in every sampled group. These include ESV18 (f\_*Rhodobacteraceae*), ESV28 (f\_*Comamonadaceae*), and ESV8 (*Aeromonas*).

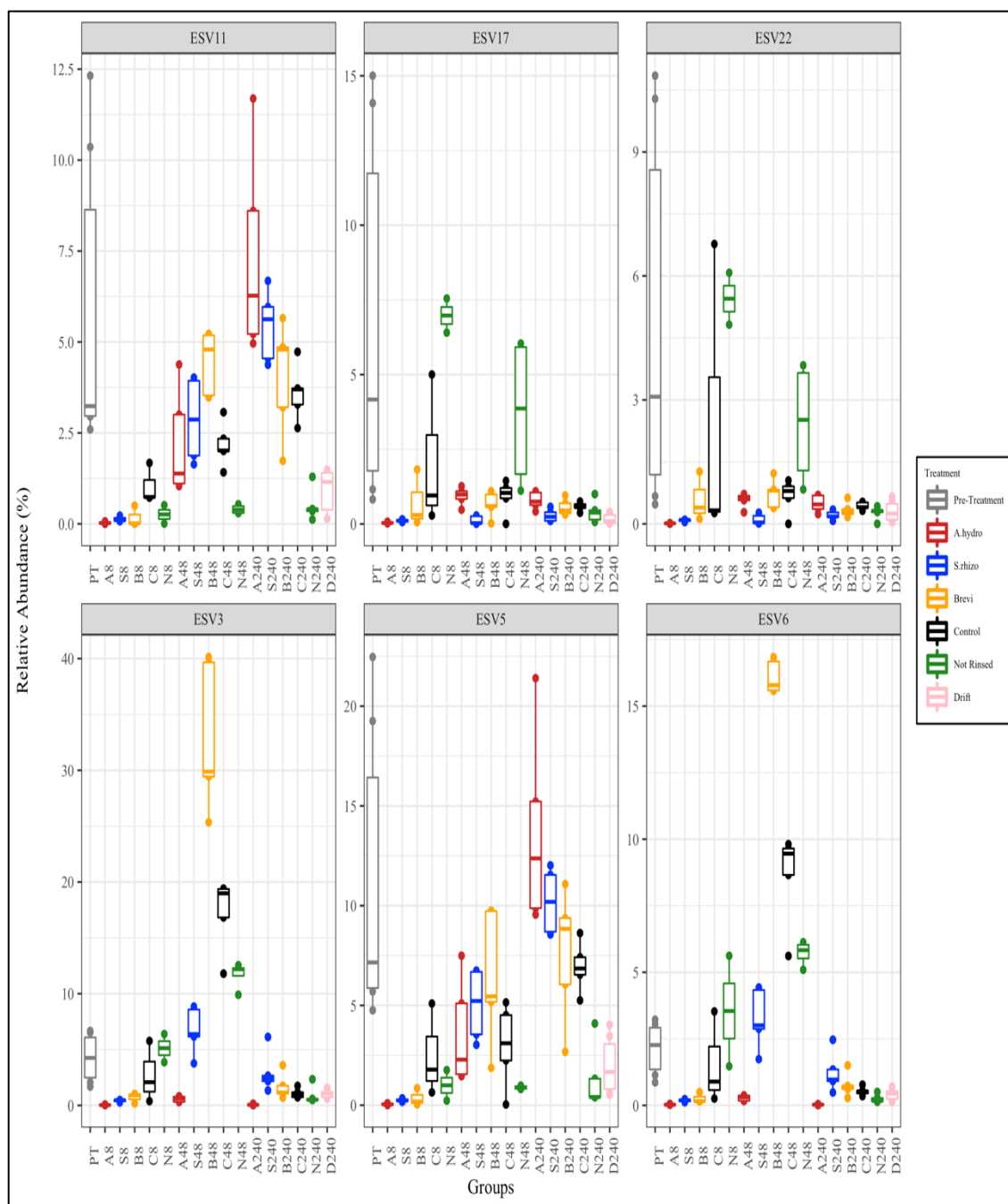
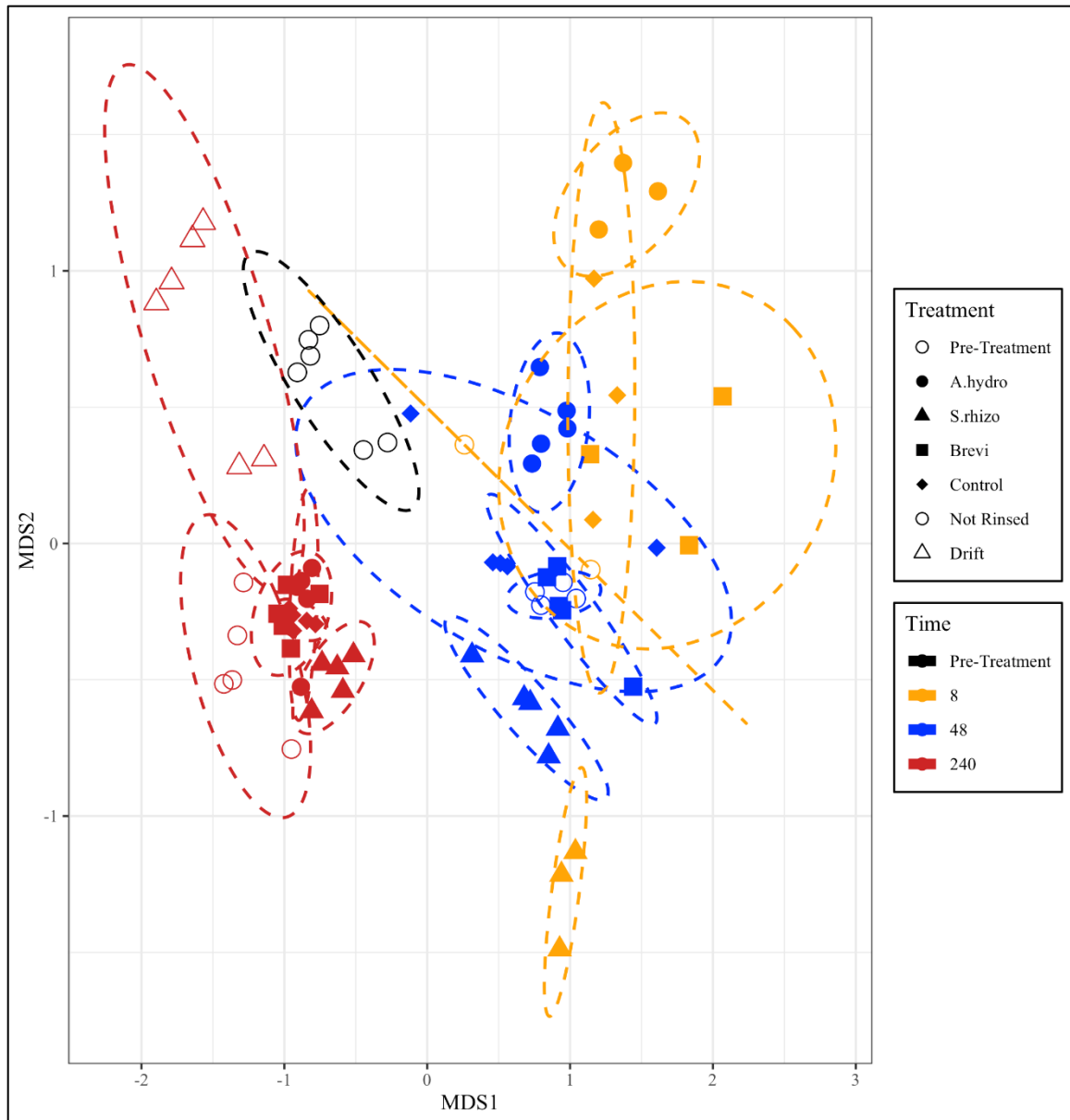


Figure 35 Relative abundance of core ESVs in all groups.

The identity of ESVs 3, 5, and 11 are given in Table 12. ESV6 is genus *Aeromonas*, ESV17 is *Chitinimonas*, and ESV22 is also *Chitinimonas*.



*Figure 36 NMDS of all ESVs. Non-metric multidimensional scaling visualization of the similarity (Bray-Curtis dissimilarity matrix calculated from all ESVs) between the communities, with each symbol representing one fish community. Treatment is represented by different shapes, time is represented by different colors, and dashed circles represent standard error within each group.*

The drift communities are closely related to the pre-treatment. All three of the treated communities at 10 days are closely related, and also not far from the pre-treatment. The most divergent from the pre-treatment are the 8 hour communities, still

presumably strongly disrupted by the rinse. The most distant from the pre-treatment are the S8 communities, likely because they are dominated by ESV2 (which is *Stenotrophomonas*), which is rare in other communities (see Figures 35-37).

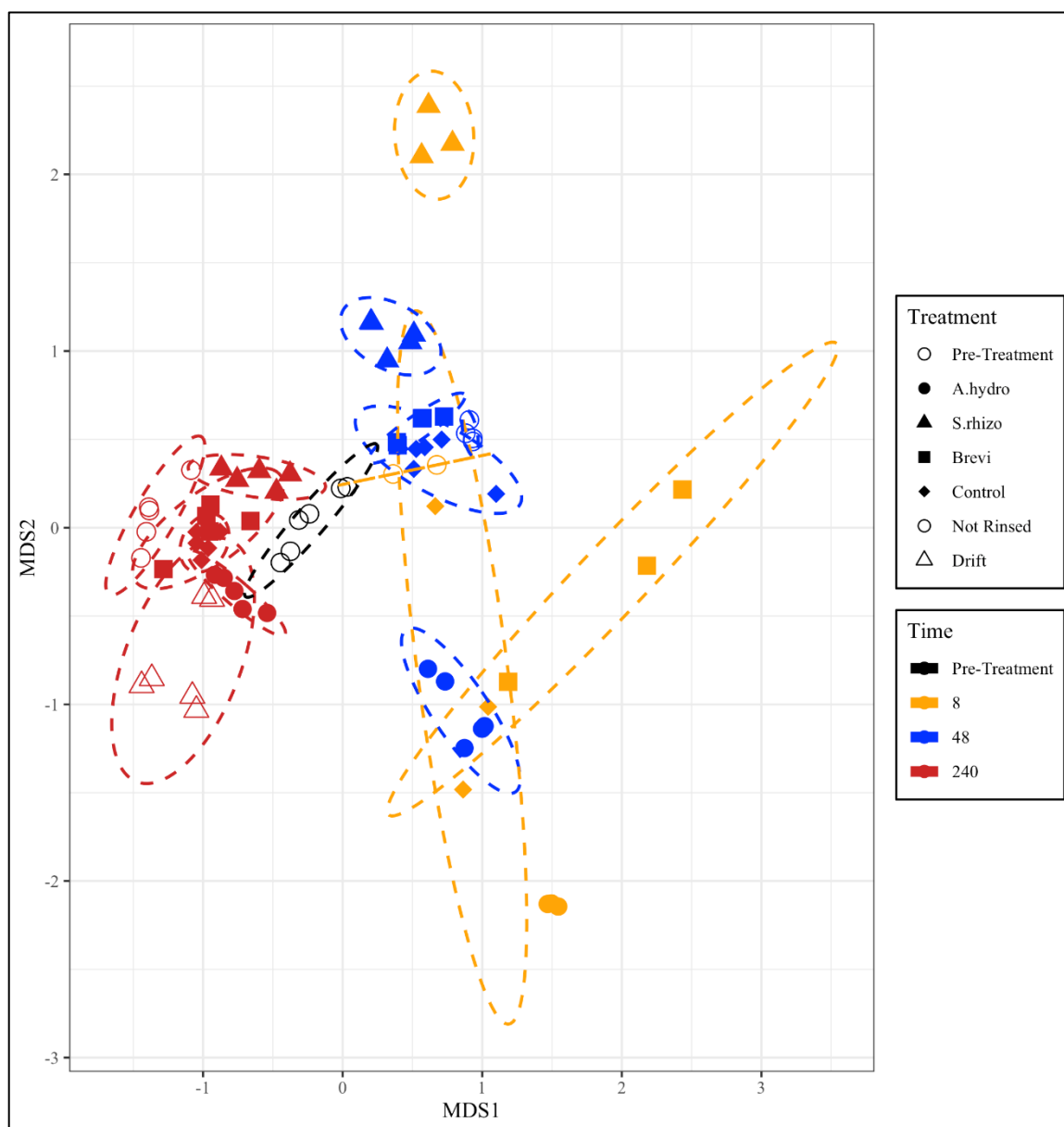


Figure 37 NMDS of abundant ESVs. Analysis includes only ESVs that are above 0.1% abundance in each sample using Bray-Curtis distance.

Treatment is represented by different shapes, time is represented by different colors, and dashed circles represent standard error within each group.



When the beta diversity visualization is restricted to ESVs that are at least 0.1% in abundance, the same pattern emerges. Visualization of groups using all genera also shows a similar pattern, yet more compressed, likely because this includes 213 total genera compared to 773 ESVs.

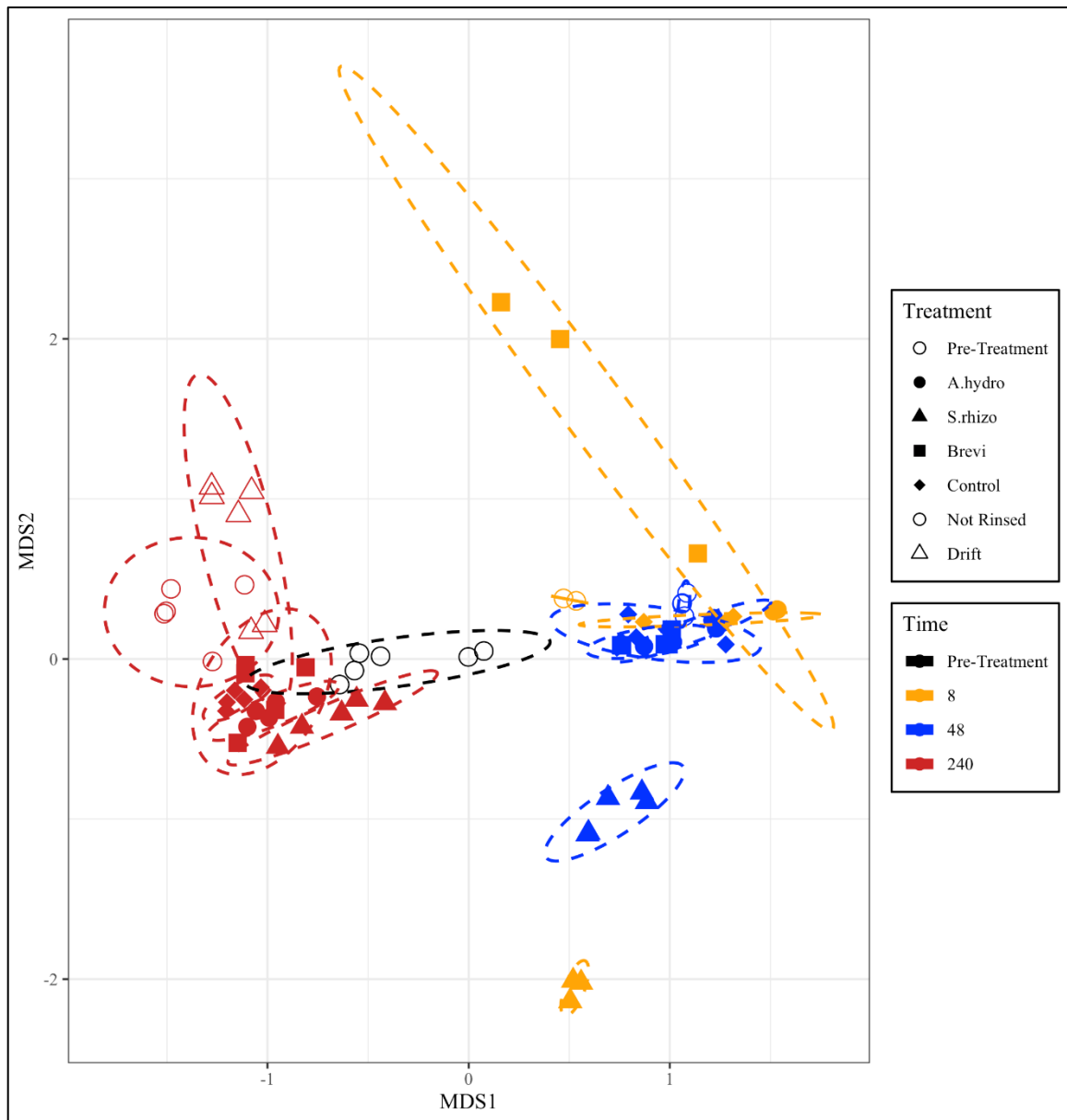


Figure 38 NMDS of all genera using Bray-Curtis distance.

Treatment is represented by different shapes, time is represented by different colors, and dashed circles represent standard error within each group.

### ***Water Chemistry Correlation with Community Composition***

Nitrate and nitrite were only present in the aquarium water, thus the arrows in the visualization (Fig 38) point upwards, as the pre-treatment and drift samples are in the upper section of the graph. Ammonia was the most variable parameter measured.

Ammonia is secreted by fish into the water, and is likely a major nitrogen source for bacteria, as almost all bacterial species can acquire and utilize it. Ammonia accumulates over time in the tubs, typically 2 ppm at 8 hrs, rising to 4 ppm at 48 hours and 8 ppm by 240 hours. Interestingly, the non-rinsed group has consistently lower values. This may be due to several reasons, and with the current dataset, the cause can't be determined. The bacterial load on the fish skin is consistently lower in the rinsed group compared to treatment groups (Fig 18). Not only that, the community composition also varies between the samples. This is further complicated as bacteria can be both producers and consumers of ammonia. However, the initial density of fish (the ammonia source) in the tub was different as well, with 20 fish initially in each treatment group and 14 in the non-rinsed group.

Alkalinity and hardness also generally accumulate over time in the tubs, and pH is mostly trending up. Thus all of the arrows have a similar direction in Figure 33.

Alkalinity is a measure of buffering capacity of the water which comes from calcium, magnesium, carbonates and bicarbonates, and chlorides. These would be coming from the fish food that is added daily, either diffusing into the water, or more likely being excreted by the fish, as they rapidly consume the food flakes after addition. Similarly, water hardness is a measure of the calcium and magnesium in the water. An increase in pH could be explained by the increase in ammonia, as ammonia is a weak base, and the APW

is of low buffering capacity. To confirm this, the pH of a sample of APW was measured at 7.6. While adding 1 ppm of ammonia (from a stock solution of ammonia hydroxide) did not change the pH reading, 2 ppm raised the pH to 7.8, 4 ppm raised it to 8.0, and 8 ppm resulted in a reading of 8.4. While *Brevibacterium* can reduce nitrate to nitrogen gas, and thus potentially lower the available nitrogen in the water, the treatment group with *Brevibacterium* added as an introduced pioneer does not display lower levels of ammonia.

*Table 21 Environmental characteristics collected at major sampling points using API Freshwater Master Test Kit and Tetra EasyStrips 6-in-1 Aquarium Test Strips.*

Treatment	Time (Hrs)	pH	Ammonia	Nitrate	Nitrite	Hardness	Alkalinity
Pre-Treatment	-1	7.0	0.1	120	0.3	300	1.5
A.hydro	8	7.8	2.0	0	0	300	4
S.rhizo	8	7.0	0.5	0	0	300	2.5
Brevi	8	7.0	2.0	0	0	300	2.5
Control	8	7.0	2.0	0	0	250	2.5
Not Rinsed	8	7.0	0.5	0	0	100	1
A.hydro	48	6.8	4.0	0	0	425	2.5
S.rhizo	48	7.2	4.0	0	0	425	3.5
Brevi	48	7.0	4.0	0	0	425	2.5
Control	48	7.2	4.0	0	0	425	3.5
Not Rinsed	48	7.2	2.0	0	0	300	2.5
A.hydro	240	8.2	8.0	0	0	425	4.8
S.rhizo	240	8.0	8.0	0	0	425	4.8
Brevi	240	8.0	8.0	0	0	425	4.8
Control	240	8.0	8.0	0	0	425	4.8
Not Rinsed	240	7.4	4.0	0	0	425	2.5
Drift	240	7.2	0	160	0	425	1.0

*Table 22 Correlation of water chemistry with community changes over time.  $R^2$  refers to how much of the data variation is explained by the characteristic, and  $p$ -value is obtained from permutations ( $<999$ ). All variables were significantly correlated with community changes over time.*

<b>Environmental Variable</b>	<b><math>R^2</math></b>	<b><math>p</math>-value</b>
pH	0.2756	0.001
Ammonia	0.2508	0.001
Nitrate	0.5043	0.001
Nitrite	0.1273	0.009
Hardness	0.2386	0.001
Alkalinity	0.1509	0.004

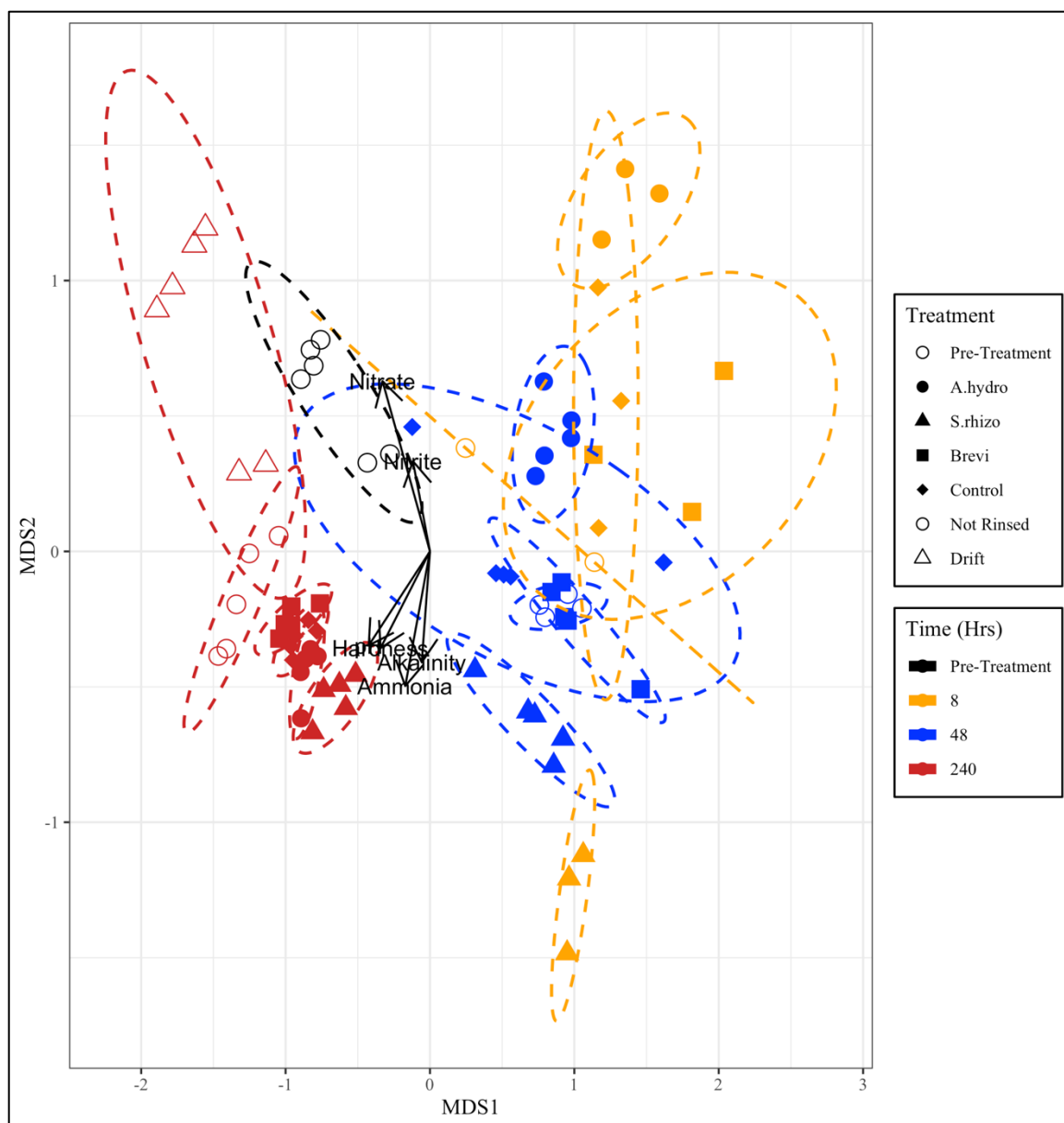
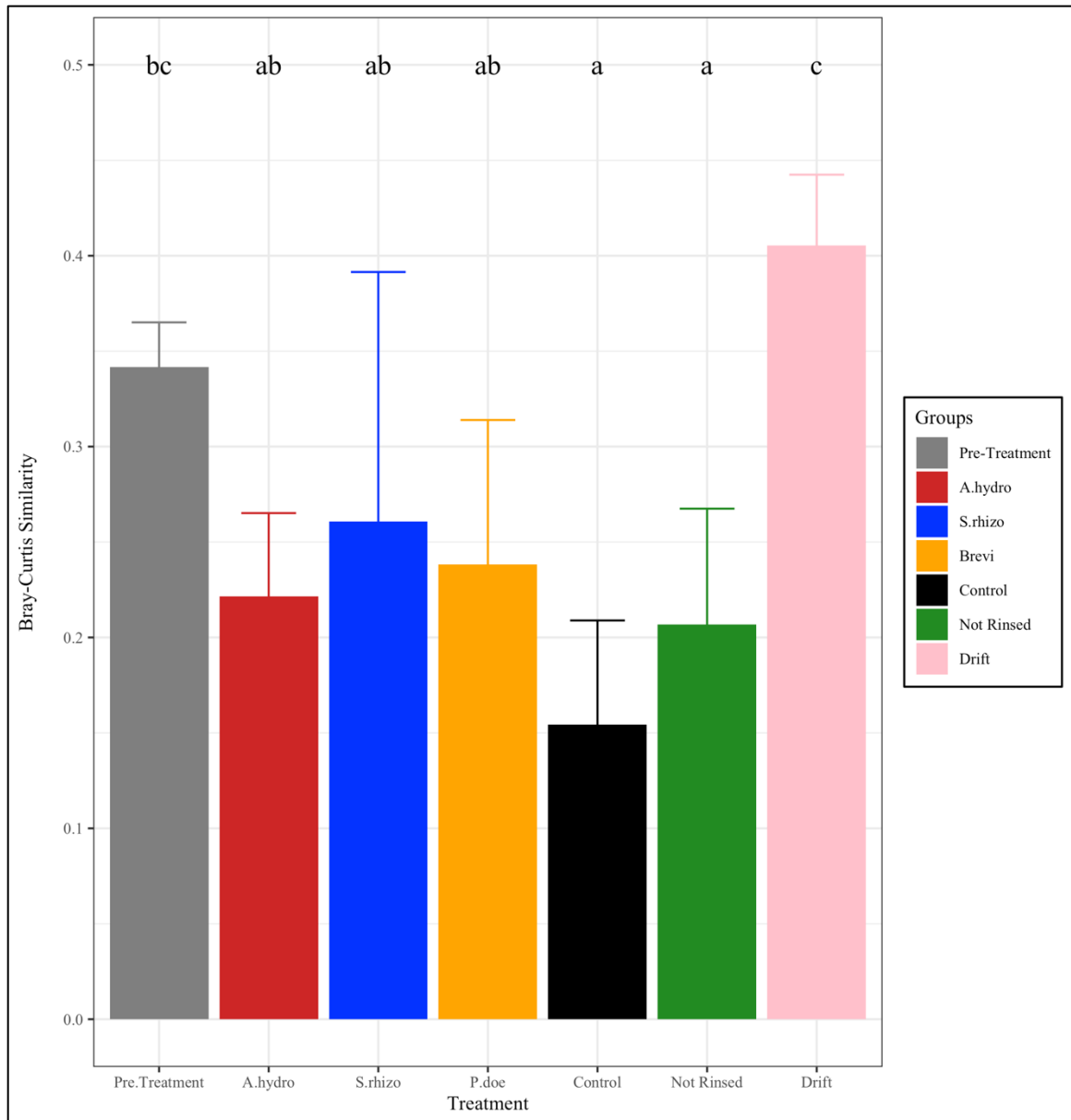


Figure 39 NMDS of all ESVs using Bray-Curtis distance, and the correlation of water chemistry and samples.

Treatment is represented by different shapes, time is represented by different colors, and dashed circles represent standard error within each group.



*Figure 40 Homogeneity of pre-treatment, drift and treatments at 240 hours.*

Groups are different at 240 hours (ANOVA;  $p = 1.12e-05$ ). Shown is within group mean and standard deviation of beta diversity measured by Bray-Curtis distance. Treatments are represented by different colors and lines represent standard deviation. Grouping letters were calculated by Tukey's honest test.

## Discussion

### *Skin Carrying Capacity*

Fish skin microbiome bacterial load is important to determine the stable number of microbes on the skin, which is the carrying capacity of the ecosystem. The same CFU trend is seen in as the previous chapter, where after 240-hrs, the carrying capacity of the fish skin returns to pre-treatment levels. The rinsing method shows to be a strong method of disruption by lowering CFUs about 90%. Exposure to the introduced pioneer species affected the carrying capacity of the fish skin by increasing the total CFUs almost 100-fold after 8 hours on treated groups, while the control group counts were still depressed from the rinse. This can be explained by invasion of the pioneers from the water column into the skin microbiome. Microbiomes exhibit competitive exclusion to prevent foreign microbes from invading and/or establishing into the community, and this has been observed across many model organisms, including mosquitofish (Bauer et al., 2018; Leonard et al., 2014; Wiles et al., 2016). Exclusion is likely lowered here by the rinse, since ~90% of the microbiome is removed. The Not Rinsed group had water transfer, which is less disruptive, and within 8 hours in recovery, counts are similar as pre-treatment levels. Even after being disrupted, fish skin CFU recovers quickly from disruption and seems to return to a stable carrying capacity at 240 hours, consistent with the *E.coli* chapter.

Consistent with Brumlow et al., 2019, there is a strong overgrowth effect seen at 48 hours in recovery. This was observed both in this experiment and in the previous one with *E. coli*. Overgrowth is not caused by the introduced pioneers. Overgrowth at 48 hours after water transfer (6.8-fold) is much less than after rinsing (65-fold), suggesting

greater disruptions may result in greater overgrowth. Overgrowth is not an artifact of rinsing, as other disruptions (multiple antibiotics, disinfectants, rapid temperature change) also cause overgrowth (Carlson et al., 2015; Carlson et al., 2017; Brumlow et al., 2019). Most published studies on the microbiome include 16S rRNA gene sequencing data, which is normalized, thus there is no measurement of total bacterial abundance. Of 21 published studies that include fish skin microbiome data, only four (three used plate counts and one used digital droplet PCR) included total abundance (Gomez and Primm, *review in progress*). With this lack of data across the microbiome field, the overgrowth effect cannot be generalized. We do know that specific groups of organisms can bloom in relative abundance after disturbance in the most-studied microbiome, the human gut. For example, members of *Enterobacteriaceae* often bloom after antibiotic treatment, and sometimes *Clostridium difficile* can bloom; however, in many of those studies done in mice, the bloom might be only relative, not in absolute numbers (not determined). Again, the reasons for the bloom, whether relative or absolute, are yet unclear. We have not yet identified any biochemical characteristic that is common to the natural pioneer organisms (*Chryseobacterium* in the first run and *Aeromonas* in the second, other studies in our lab revealed *Myroides* or *Aeromonas*) that bloom during the overgrowth phenomenon. That is a target for future study.

### ***Fish Skin Microbiome Alpha Diversity***

A significant issue in community ecology is to know that your experimental sampling is representative of the actual community. If sequencing samples exhibited high coverage and almost all organisms in the skin community were sampling, Good's coverage numbers are expected to be close to 100% and Chao1 numbers are expected to



be very close to the observed numbers of taxa. With poor coverage, Good's coverage would be lower and Chao1 estimates would be much higher than the observed number of taxa. Given the high number of quality sequences in each sample, the high Good's numbers, and the similarity of observed ESVs with Chao1 estimates, the skin microbiomes were well covered in this study.

The total number of ESVs (termed alpha diversity or richness) in all rinsed groups was lowered dramatically. Loss of richness is commonly observed in other microbiome studies following antibiotic treatment or other disruptions. Again, water transfer is a less severe disruption, with a smaller loss of richness since the number of observed ESVs is lower, yet it has the highest observed ESVs from all the groups at 8 hours in recovery. Interestingly, while the total counts return back to pre-treatment levels, the number of observed ESVs does not return to pre-treatment levels in any of the groups, remaining significantly lower. Given that drift also has significantly lower richness (t-test;  $p = 0.021$ ), some of the observed lower richness may be due to the dynamic nature of the skin microbiome (Larsen et al., 2013; Chiarello et al., 2018; Roux et al., 2019). Richness does have an increased trend over time after the rinse, suggesting that the recovery process does include a return of taxa.

As shown on Figure 25, at 240 hours in recovery, there are no differences in the observed ESVs among the groups (Dunn's test;  $p > 0.05$ ) despite being rinsed or not rinsed. The richness of the Pre-Treatment and Drift from the treatment groups at 240 hours in recovery may be due to acclimation time of two weeks in aquarium water; perhaps, if fish were sampled at a much later time, the richness would be the same as all groups have an increasing observed ESV pattern.

As seen on Figure 26, the Pre-Treatment group SDI starts high suggesting a balanced community distribution of ESVs before treatment. Also, treated groups have lower SDI, which is expected because of the rinse protocol and dominance by one taxon. Lower SDI caused by the rinsing method is seen only by the control group, thus supporting that rinsing affects the community drastically. Interestingly, the Not Rinsed group at 8 hours in recovery, despite having lower richness, does not have a different SDI compared to Pre-Treatment group (t-test; p-value = 0.4878). At 240 hours, the Drift group observed ESVs and SDI are not different from Pre-Treatment group observed ESVs and SDI (Dunn's test;  $p > 0.05$ ), showing that taxon richness and distribution is stable in the aquarium water. There is no difference in SDI of treated groups at 240 hours in recovery (Kruskal-Wallis;  $p = 0.176$ ), strongly suggesting a community balance recovery after being disrupted by water transfers. SDI, to some degree, is a measure of evenness, but to quantify how the community is distributed, Simpson's Evenness was used. At 240 hours in recovery, there is no difference among treated groups. These observations suggest that the fish skin microbiome can be easily disrupted, but it has a robust richness resilience.

### ***Community Composition***

The top 10 most abundant ESV by relative abundance is shown in Figure 30. At 8 hours in recovery (pioneer seeding), A8, S8, and B8 groups are dominated by its respective by a different ESV (ESV1, ESV2, ESV14, respectively). Each ESV matched the ID of the added pioneers, supporting that the pioneer species was carried on the fish skin. Interestingly, Figure 30 shows increase of ESV1 in the C8 groups, which was a similar pattern observed in the *E.coli* chapter of the control group at 8 hours in recovery

by dominance of the taxon *Chryseobacterium*. As seen in Figure 31, the natural pioneer is in the genus *Aeromonas*, and differentiation of ESV1 and ESV5 at the genus level cannot be done because both are identified in the genus *Aeromonas*. The genus *Aeromonas* is present in many fish datasets (Butt et al., 2019), and much of the *Aeromonas* seen in this data is probably native *Aeromonas* already present on the fish. From the 16S data, we can infer ESV1 is *A. hydrophilia* (the added pioneer), but we cannot exclude the possibility of *A. hydrophilia* also being classified as other ESVs. Also, at 48 hours in recovery (dominance by natural pioneer), we see some ESV1 and ESV5 as part of the dominant taxa of C48 and N48 groups (never exposed to the introduced pioneer). Furthermore, multiple abundant ESVs (ESV3, ESV4, and ESV 8) are identified as *Aeromonas*, further suggesting that multiple native *Aeromonas* species may be already present in high abundance in the native fish skin microbiome. Therefore, discrimination between introduced and natural strains cannot be determined.

The natural pioneer is the taxon *Aeromonas* because it dominates in relative abundance in all groups at 48 hours in recovery, as shown by Figure 31. Uniquely, *S. rhizophilia* at 48 hours is also present at high abundance, unlike the other two introduced pioneers, suggesting *S. rhizophilia* interacts with *Aeromonas* in a different way than the other genera. Also, *S. rhizophilia* (mostly ESV2) remains a dominant taxon at 240 hours in recovery as seen by Figures 30 and 31. This is the only introduced pioneer observed to “resist” the natural pioneer and to remain abundant after recovery.

The term core microbiota is defined variously across the microbiome field. For this research, the most strict definition was taken, with core being present (relative abundance > 0) in all samples, and as shown by Figure 34, there are only six core ESV,

which is ~0.77% of the richness found across all 75 samples. Within the six ESVs, there are only three genera, *Aeromonas*, *Flavobacterium*, and *Chitinimonas*, and their relative abundance has high variance and no clear pattern across all samples.

### ***Beta Diversity***

The Bray-Curtis distance of all ESVs was calculated in order to visualize sample clustering by NMDS. The “Pre-Treatment” group is a measure of the initial community composition. At 8 hours in recovery, groups greatly disperse on the NDMS, which is expected as they are dominated by the introduced pioneers. Also consistent with the *E.coli* chapter, groups become disperse at 8 hours in recovery. By 48 hours in recovery, groups are dominated by the natural pioneer, where groups become closer to each other. At 240 hours in recovery, despite different treatments, all groups cluster together, suggesting that community composition is very similar across groups and suggesting introduced pioneer species did not affect the recovery of the microbiome. Interestingly, despite clustering of groups at 240 hours in recovery, community composition are different from each other. The “Drift” group is different from “Pre-Treatment” group suggesting that the fish skin microbiome is dynamic even in the aquarium water. Also, the “Drift” sample has less homogeneity, which may be due to loss of fish density in the aquarium tank. Fish skin bacteria are in constant interaction with the water column and can be affected by surrounding water pH (Sylvain et al., 2016). Therefore, differences seen in the fish skin microbiome at 240 hours might be a due to pH differences among Pre-Treatment group, Drift and treated groups. The water chemistry is very similar in all treated groups at 240 hours, which may explain the similar clustering, yet their beta diversity is different. Pre-Treatment and Drift water chemistry is very similar, and their

beta diversity is also different. These results suggest that there might be other factors in shaping microbiome composition. In fact, more studies are finding that host-microbial interactions and even microbial interactions themselves are very dynamic and could have a greater contribution to microbial assemblages in mammals and plants (Copeland et al., 2015; Kaiko & Stappenbeck 2014; LaSarre et al., 2020; Longford et al., 2019; Sommer et al., 2017; Venturelli et al., 2018). Therefore, focusing on microbial interactions should give researchers a more complete understanding of microbial successions.

Additionally, introduction of pioneer species did not inhibit dominance of the natural pioneer *Aeromonas* across all groups, suggesting that domination by one taxon might be predetermined in the starting community. As seen in both series of experiments, the natural pioneer bloom was not affected by the introduced pioneer, whether it was native or not. These series of experiments support succession model B from Connell and Slayer, 1977, where more competitive community members already present at the start are not affected by incoming species. One of the limitations of the first experimental run was that K12 is non-native, putting it at a disadvantage in the fish skin environment, which could be a possible explanation of *Chryseobacterium* taking over the community. However, in the second run, the three introduced pioneer species were all native, yet the recovery communities were still dominated by *Aeromonas*. Note that we can't distinguish between the introduced and the native ESVs of *Aeromonas*. Previous experiments have shown the overgrowth effect of different taxa across different disruptions, suggesting that dominance by one taxon could be somehow predetermined by the initial stable community, further supporting the importance of microbial interactions.

## ***Limitations***

### **16S Gene Copy Number (GCN)**

While the 16S profile method is powerful and has given researchers new insights into microbial diversity, a serious limitation in 16S data is the variation in 16S rRNA gene copy number (GCN) across bacteria. Within published full genomes, bacteria vary from one to 21 copies of the 16S gene (rrnDB, Stoddard et al., 2015). Thus, the normalized abundance of identified sequences in 16S data does not directly convert to abundance of the corresponding genera. The normalized data is biased towards bacteria with high GCN. Tools have been developed that attempt to correct the problem of different GCN and to improve accuracy of microbial surveys, yet it remains an issue and differences in GCN can add significant noise to the data (Kembel et al., 2012; Louca et al., 2017). Previous studies concluded that the sequence databases as of 2017 were still insufficiently complete to accurately adjust community 16S sequence data for GCN variation. Starke and Morais (2019) argue that to identify the noise from GCN variation, standard bacterial mock communities should be included in experiments. A mock community was not included in these experiments, therefore, it is hard to assess noise of 16S gene sequence. Looking within the rrnDB and other published full genomes, we can estimate GCN in our most abundant genera. In the rrnDB, there are 23 entries for *Aeromonas hydrophila*, and of those, 21 have ten copies of the 16S per genome, the others have 11 copies or 9, thus the average GCN is clearly ten. Since in the entire database, the mean GCN is  $5.0 \pm 2.8$  (for 15,829 genomes), the true abundance of *Aeromonas* is likely overrepresented by about double. Small variations in sequence can occur between copies within species, not to mention variations across species, which

explains multiple ESVs representing one genus. *Stenotrophomonas rhizophilia* has only one entry in the database, with two 16S copies. There are 36 genomes within the genus *Stenotrophomonas* in the database, with  $3.58 \pm 0.77$  copies per genome. Thus, this genus may be slightly underrepresented in abundance compared to other genera. There are 11 entries for *Brevibacterium*, and all but two have four 16S copies ( $3.9 \pm 0.7$  copies per genome). Thus, it may also be mildly underrepresented in abundance counts.

*Flavobacterium* is highly diverse as a genus for GCN. The database has 40 entries, with GCN ranging from one to 13, with a mean of  $4.88 \pm 2.58$  copies per genome. So while the mean GCN is near the overall bacterial mean of five, there is not a lot of confidence given the broad range. For reference, *E. coli* strain K12 has seven copies.

### **Fish Stress, Gender, and Heterogeneity**

Another factor not measured was stress and how it could affect fish skin microbiome dynamics. It has been noticed that stress can induce a variety of physiological responses in fish and mammals (Butt et al., 2019; Davis et al., 2016; Sudo, 2014; Tamsyn et al., 2019; Uren et al., 2019). *Gambusia affinis* skin changes in shade (darker) when they are stressed, yet it is only qualitative, and the rinse protocol does induce darkening and stress on the fish. Cortisol levels have been extensively used to assess stress in fish from different tissues and cortisol levels affect the fish gut microbiome and alter mucus composition in the gut, they do not seem to affect skin microbiome composition (Kulczykowska, 2019; Uren et al., 2019).

Gender was not tracked when sampling fish in this study. Some studies have found differences in the gut microbiome composition between males and females in mammals (Freire et al., 2011; Markle et al., 2013; Mueller et al., 2006), yet in Li et al

(2016) there were differences in SDI and richness, but they did not statistically measure beta diversity. Females were most of the samples because of size, but there was no accurate count of gender for this experiment.

Unlike many microbiome models, the fish used in these experiments are wild caught, which increases sample heterogeneity and is a known source of error (Malone et al., 2014). In microbiome studies, it is well understood the role of the immune system affects the interaction of microbes and its host (Nagao-Kitamoto & Kamada, 2017), and it is known that even homogenous populations of mice could have different gut microbiome compositions (Laukens et al., 2017). In fish, skin microbiome seems to be shaped by the host and environmental factors (Larsen et al., 2013; Xavier et al., 2019). In these experiments, the same fish species was used, and fish were initially kept in the same water condition throughout the experiment, yet fish genetic variation can be a source of error that was not accounted for.

### **Water Chemistry and Microbiome Function**

Microbiome function has been increasing in importance in the last few years as more studies shed light on the significance of metabolites produced by microbes (Heintz-Buschart & Wilmes, 2016; HMP, 2012; Lozupone et al., 2012; Milshteyn et al., 2018; Sharon et al., 2014). Bioproducts generated by microbes are recycled and transformed extensively, and as microbial diversity increases, so does metabolic complexity (Morin et al., 2018). Therefore, microbiome studies should be expanded by proteomics and/or metabolomics technologies. Biochemical testing in this study was too limited to yield firm conclusions.



Environmental characteristics measured in these experiments were also limited. As the fish skin microbiome is in constant contact with the water column, it is expected water chemistry may have an influence in shaping the skin (Sylvain et al., 2016). Multiple studies have shown differences in community composition between fish skin microbiome and the surrounding water column (Chiarello et al., 2018; Krotman et al., 2020; Uren et al., 2019). The interactions between the skin microbiome and water chemistry need to be further investigated.

## Conclusion

This series of experiments show that the fish skin microbiome can be easily disrupted. As described by Christian et al (2015), ecological communities can respond to disturbances in four major ways. Resistant communities have no change in composition, resilient communities change and then return to the original state, redundant communities change composition but have the same functions, and altered communities change and do not return. In these series of experiments, fish skin communities are not resistant to disturbance because all treatment groups, including the not rinsed group have compositions significantly different from pre-treatment. The fish skin microbiome is resilient as far as carrying capacity and community diversity (alpha measurements) among groups from different treatments. However, it is not resilient in terms of community composition (beta diversity), as this does not return to the pre-treatment composition under any treatment, even the not rinsed group. The drift group is also distinct despite samples being fed the same amount of food, and not being manipulated in the original aquarium water. Thus, even without an overt disturbance, the skin microbiome is not resistant or resilient to change over time. Insertion of introduced pioneer species do alter final community composition compared to the control. There is not enough data to conclude whether the fish skin microbiome is functionally redundant as the biochemical tests were limited in discrimination. Disturbance did alter the community composition, which did not return to pre-treatment state. Again, functional alteration cannot be reliably assessed. The fish skin microbiome is highly dynamic, reflected by changes in microbiome composition in the drift samples and the small 0.8% shared core microbiome across all samples. Therefore, **hypothesis one** (community

composition is affected by pioneer species) is supported by significant differences in beta diversity between all treated groups at 10d compared to pre-treatment. The richness was also lower in the 10d treated communities compared to the pre-treatment. Note there were no significant differences in CFU level or evenness or Shannon's Diversity Index between the 10d treated groups and pre-treatment samples. This may suggest the microbiome community has alternative stable states. Further, community drift in the same environment also generated a significant difference in composition. **Hypothesis two** cannot be concluded. There were not many changes in the biochemical profile between groups, making interpretation limited, and no clear pattern can be seen across treatments. By not being able to support or reject hypothesis two, **hypothesis three** cannot be concluded either. Full metabolomics profiles may be needed to accurately assess community biochemical profile and possibly predict function of climax community.

For a species to be defined as foundation, it must be abundant and interact with many other species within the community. The three pioneers were all abundant after introduction (at 8 hours), but varied afterwards. *Aeromonas* was 11.1% in relative abundance in the pre-treatment group, and was 3.0% in the *Aeromonas*-exposed group at 10 days, after recovery. It was also 2.0% in the drift and 1.9% in the control rinsed group, yet 8.0% in the *S. rhizo*-exposed group, suggesting some positive interaction. Conversely, the abundance of *Stenotrophomonas* was not increased in the 10d *Aeromonas*-exposed group compared to control. While *Aeromonas* does maintain abundance after the disruption, it cannot be discerned if this is the natural strain from the pre-treatment community or the introduced strain. *Stenotrophomonas* remains abundant

during mid-recovery (66.5% at 48 hours in the exposed group) and at the end (5.5% after 10d). However, *Brevibacterium* does not remain abundant, declining from 74% abundance at 8 hrs to 0.2% at 48 hours to only 0.05% at 10 d. Thus it fails to display this trait of a foundation species. However, addition of all three of these pioneers did result in community compositions significantly different from the control after 10d, suggesting a foundation effect.

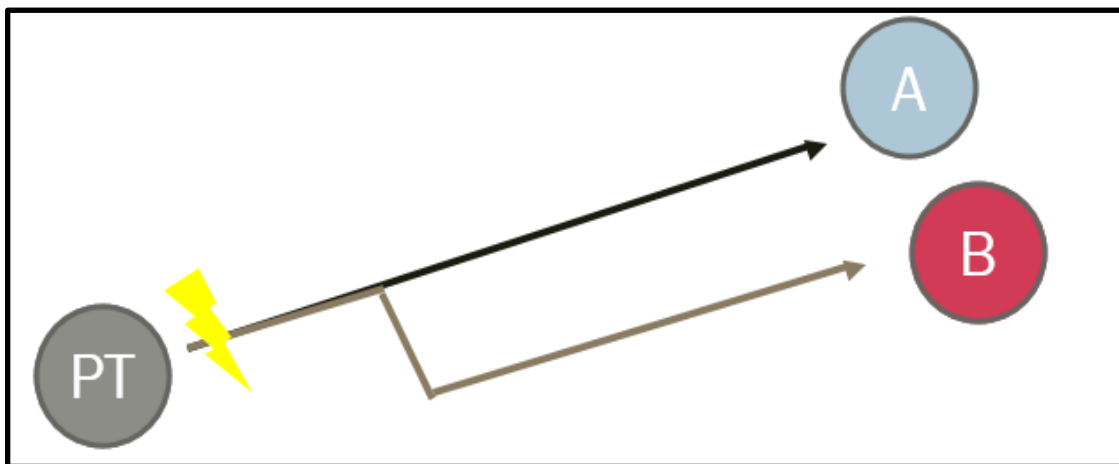


Figure 41 Foundation effect recovery pathway after pioneer species inoculation.

A recovery pathway model (visualized above) may explain these results. The pre-treatment community (PT) has a certain composition and functions. A strong disruption (illustrated as a lightning bolt) lowers total numbers and diversity and begins the process of secondary succession. The community follows a certain pathway of recovery to reach the new climax community (A). If an introduced pioneer is added just after the disruption, that pathway is altered and a different climax community is reached (B). This pathway change may be caused by changes in nutrients caused by the biochemical functions of the introduced pioneer, or by positive/negative interactions of that pioneer with other species in the community, or both. What is evidence from these experiments that relate to this model? First, the introduced pioneer does not have to be abundant in the

recovered community for this community to be different. While *Aeromonas* and *Stenotrophomonas* are abundant above 0.1% in their final communities at 10d, neither *E. coli* nor *Brevibacterium* are, yet the community composition is different from control in each case. This suggests action early in the recovery pathway rather than at the 10d itself. For the environmental parameters measured, no difference was seen between 10d communities between control or any of the three introduced pioneers (Table 21). However, at the 8 hour timepoint, the microbiomes dominated by *Stenotrophomonas* had a much lower ammonia level (0.5 vs 2.0 ppm) than the control. This fits with the metabolic capability of this organism as a denitrifier. By 48 hours, the level of ammonia in both cases is 4.0 ppm. Perhaps that temporary depletion caused a pathway change. This can be tested by experimentally manipulating ammonia concentrations during parallel recovery trials in the future. Future experiments can also monitor potential degradation products of mucin (the predicted major microbial food source), including free amino acids, peptides, and free sugars.

## REFERENCES

- Bauer, M. A., Kainz, K., Carmona-Gutierrez, D., & Madeo, F. (2018). Microbial wars: Competition in ecological niches and within the microbiome. *Microbial cell*, 5(5), 215–219. <https://doi.org/10.15698/mic2018.05.628>
- Bickerton MW, Corleto J, Verna TN, Williges E, Matadha D. (2018). Comparative Efficacy of *Pimephales promelas*, *Fundulus diaphanus*, and *Gambusia affinis* and Influence of Prey Density for Biological Control of *Culex pipiens molestus* Larvae. *J Am Mosq Control Assoc.* Jun;34(2):99-106. doi: 10.2987/17-6718.1.
- Brumlow, C., Luna, R., Hollister, E., Gomez, J., ... Primm, T. P. (2019). Biochemistry not taxonomy drives recovery of skin mucosal microbiome communities after disruption. *Infection and Drug Resistance*.
- Butt, R. L., & Volkoff, H. (2019). Gut Microbiota and Energy Homeostasis in Fish. *Frontiers in endocrinology*, 10, 9. <https://doi.org/10.3389/fendo.2019.00009>.
- Callahan BJ, McMurdie PJ, Rosen MJ, Han AW, Johnson AJA, Holmes SP (2016) “DADA2: High-resolution sample inference from Illumina amplicon data.” *Nature Methods*, 13, 581-583. doi: [10.1038/nmeth.3869](https://doi.org/10.1038/nmeth.3869)
- Cammarota, G., Masucci, L., Ianiro, G., Bibbò, S., Dinio, G., Costamanga, G., ... Gasbarrini, A. (2015). Randomised clinical trial: Faecal microbiota transplantation by colonoscopy vs. vancomycin for the treatment of recurrent *Clostridium difficile* infection. *Alimentary Pharmacology and Therapeutics*, 41(9), 835-843.
- Carlson, J. M., Hyde, E. R., Petrosino, J. F., Manage, A. B. W., & Primm, T. P. (2015). The host effects of *Gambusia affinis* with an antibiotic-disrupted microbiome.

*Comparative Biochemistry and Physiology Part C: Toxicology and Pharmacology*, 178, 163-168. doi.org/10.1016/j.cbpc.2015.10.004

Carlson, J. M., Leonard, A. B., Hyde, E. R., Petrosino, J. F., & Primm, T. P. (2017).

Microbiome disruption and recovery in the fish *Gambusia affinis* following exposure to broad-spectrum antibiotic. *Infection and Drug Resistance*, 10, 143-154. doi:[10.2147/IDR.S129055](https://doi.org/10.2147/IDR.S129055)

Chen, B., Liu K., Zhou, L., Gomes-Silva G., ... & Plath, M. (2018) Personality differentially affects individual mate choice decisions in female and male Western mosquitofish (*Gambusia affinis*). *PLOS ONE* 13(5): e0197197.

<https://doi.org/10.1371/journal.pone.0197197>

Chiarello, M., Auguet, J., Bettarel, Y. et al. (2018). Skin microbiome of coral reef fish is highly variable and driven by host phylogeny and diet. *Microbiome* 6, 147

<https://doi.org/10.1186/s40168-018-0530-4>

Clarke K.,R. (1993). Non-parametric multivariate analyses of changes in community structure. *Austral Ecol.* **18**:117–143.

Cole, J. R., Wang, Q., Fish, J. A., Chai, B., McGarrell, D. M., Sun, Y., Brown, C. T.,

Porras-Alfaro, A., Kuske, C. R., & Tiedje, J. M. (2014). Ribosomal Database Project: data and tools for high throughput rRNA analysis. *Nucleic acids research*, 42(Database issue), D633–D642. <https://doi.org/10.1093/nar/gkt1244>.

Connell, J., and Slatyer, R. (1977). Mechanisms of Succession in Natural Communities and Their Role in Community Stability and Organization. *The American Naturalist*, Vol. 111, No. 982. pp. 1119-1144

- Conrad, T.M., Joyce, A.R., Applebee, M.K. et al. Whole-genome resequencing of *Escherichia coli* K-12 MG1655 undergoing short-term laboratory evolution in lactate minimal media reveals flexible selection of adaptive mutations. *Genome Biol* 10, R118 (2009). <https://doi.org/10.1186/gb-2009-10-10-r118>
- Copeland, J. K., Yuan, L., Layeghifard, M., Wang, P. W., & Guttman, D. S. (2015). Seasonal community succession of the phyllosphere microbiome. *Molecular plant-microbe interaction: MPMI*, 28(3), 274–285. <https://doi.org/10.1094/MPMI-10-14-0331-FI>.
- D'Argenio, V., & Salvatore, F. (2015). The role of the gut microbiome in the healthy adult status. *Clinica Chimica Acta: International Journal of Clinical Chemistry*, 451, 97-102. [doi:10.1016/j.cca.2015.01.003](https://doi.org/10.1016/j.cca.2015.01.003)
- Davis, D. J., Bryda, E. C., Gillespie, C. H., & Ericsson, A. C. (2016). Microbial modulation of behavior and stress responses in zebrafish larvae. *Behavioural brain research*, 311, 219–227. <https://doi.org/10.1016/j.bbr.2016.05.040>.
- Duncan K, Carey-Ewend K, and Vaishnava S. (2019). In situ analysis of mucus residing bacterial community reveals an ecological niche key for gut microbiome stability. *bioRxiv*. doi: <http://dx.doi.org/10.1101/675918>.
- Eck, M., Razack, A., Massart, S., Schmutz, Z., Junge, R., Smits, T. H. M., Jijakli, M. H. (2019). Exploring Bacterial Communities in Aquaponic Systems. *Water*, 11(2), 260. [doi.org/10.3390/w11020260](https://doi.org/10.3390/w11020260)
- El Aidy, S., Van den Abbeele, P., Louis, P., Van de Wiele, T., & Kleerebezem, M. (2013). Intestinal colonization: How key microbial players become established in



- this dynamic process: Microbial metabolic activities and the interplay between the host and microbes. *BioEssays*, 35(10), 913-923. doi.org/10.1002/bies.201300073.
- Ellison, A. M. (2019). Foundation Species, Non-trophic Interactions, and the Value of Being Common. *iScience*, 13, 254-268. <https://doi.org/10.1016/j.isci.2019.02.020>
- Folke, C, Carpenter, S, Walker, B, Scheffer, M, Elmqvist, T, Gunderson, L, Holling, CS. (2004). Regime shifts, resilience, and biodiversity in ecosystem management. *Annu Rev Ecol Evol Syst*. 35(1):557–581.
- Freire, A. C., Basit, A. W., Choudhary, R., Piong, C. W., & Merchant, H. A. (2011). Does sex matter? The influence of gender on gastrointestinal physiology and drug delivery. *International journal of pharmaceutics*, 415(1-2), 15–28. <https://doi.org/10.1016/j.ijpharm.2011.04.069>.
- Gao, J., Santi, F., Zhou, L., Wang, X., Riesch, R., & Plath, M. (2019). Geographical and temporal variation of multiple paternity in invasive mosquitofish (*Gambusia holbrooki*, *Gambusia affinis*). *Molecular ecology*.
- Gaulke, C. A., Martins, M. L., Watral, V. G., Humphreys, I. R., Spagnoli, S. T., Kent, M. L., & Sharpton, T. J. (2019). A longitudinal assessment of host-microbe-parasite interactions resolves the zebrafish gut microbiome's link to *Pseudocapillaria tomentosa* infection and pathology. *Microbiome*, 7(1), 10. <https://doi.org/10.1186/s40168-019-0622-9>.
- Gaurav, K (2019). ranacapa: Utility Functions and 'shiny' App for Simple Environmental DNA Visualizations and Analyses. R package version 0.1.0. <https://github.com/gauravsk/ranacapa>

- Gilbert, J. A., Blaser, M. J., Caporaso, J. G., ,...Knight, R. (2018). Current Understanding of the Human Microbiome. *Nature Medicine*, 24(4), 392-400.  
doi:10.1038/nm.4517
- Gibson, T. E., Bashan, A., Cao, H. T., Weiss, S. T., & Liu, Y. Y. (2016). On the Origins and Control of Community Types in the Human Microbiome. *PLoS computational biology*, 12(2), e1004688. doi:10.1371/journal.pcbi.1004688
- Grabber, A., & Junge, R. (2007). Aquaponic Systems: Nutrient Recycling from Fish Wastewater by Vegetable Production. *Desalination*, 246(1-3), 147-156.  
doi.org/10.1016/j.desal.2008.03.048
- Greenblum S, Turnbaugh P, Borenstein E. (2012). Metagenomic systems biology of the human gut microbiome reveals topological shifts associated with obesity and inflammatory bowel disease. *PNAS* January 10, 2012 109 (2) 594-599;  
<https://doi.org/10.1073/pnas.1116053109>
- Heintz-Buschart, A., & Wilmes, P. (2018). Human Gut Microbiome: Function Matters. *Trends in microbiology*, 26(7), 563–574.  
<https://doi.org/10.1016/j.tim.2017.11.002>.
- Hoffberg, S. L., Troendle, N. J., Glenn, T. C., Mahmud, O., Louha, S., Chalopin, D., Bennetzen, J. L., & Mauricio, R. (2018). A High-Quality Reference Genome for the Invasive Mosquitofish *Gambusia affinis* Using a Chicago Library. *G3 (Bethesda, Md.)*, 8(6), 1855–1861. <https://doi.org/10.1534/g3.118.200101>.
- Holling, CS . 1973. Resilience and stability of ecological systems. *Annu Rev Ecol Syst*. 4:1–24.

- Hou L, Xu H, Ying G, Yang Y, Shu H, Zhao J, Cheng X. (2017). Physiological responses and gene expression changes in the western mosquitofish (*Gambusia affinis*) exposed to progesterone at environmentally relevant concentrations. *Aquat Toxicol.* Nov;192:69-77. doi: 10.1016/j.aquatox.2017.09.011
- Hou LP, Chen H, Tian CE, Liang Y, Wu RR, Zhang XM, Fang XW, Zhang CP, Hu JJ, Song LY, Liang YQ, Schlenk D, Xie L. 2018. Alterations of secondary sex characteristics, reproductive histology and behaviors by norgestrel in the western mosquitofish (*Gambusia affinis*). *Aquat Toxicol.* May;198:224-230. doi: 10.1016/j.aquatox.2018.03.014
- Hui, C (2006). Carrying capacity, population equilibrium, and environment's maximal load. *Ecological Modelling.* 192 (1–2): 317–320.  
doi:10.1016/j.ecolmodel.2005.07.001
- Jensen F. B. (1996). Uptake, elimination and effects of nitrite and nitrate in freshwater crayfish (*Astacus astacus*). *Aquat. Toxicol.* 34:95–104. 10.1016/0166-445X(95)00030-8
- Jorth, P, Turner, KH, Gumus, P, Nizam, N, Buduneli, N, Whiteley, M. 2014. Metatranscriptomics of the human oral microbiome during health and disease. *MBio.* 5(2):01012–e01014.
- Kaiko, G. E., & Stappenbeck, T. S. (2014). Host-microbe interactions shaping the gastrointestinal environment. *Trends in immunology*, 35(11), 538–548.  
<https://doi.org/10.1016/j.it.2014.08.002>

- Kayama, H., & Takeda, K. (2016). Functions of innate immune cells and commensal bacteria in gut homeostasis. *Journal of biochemistry*, 159(2), 141–149.  
<https://doi.org/10.1093/jb/mvv119>
- Kembel, S. W., Wu, M., Eisen, J. A., & Green, J. L. (2012). Incorporating 16S gene copy number information improves estimates of microbial diversity and abundance. *PLoS computational biology*, 8(10), e1002743.  
<https://doi.org/10.1371/journal.pcbi.1002743>
- Kennedy, K., Hall, M. W., Lynch, M. D., Moreno-Hagelsieb, G., & Neufeld, J. D. (2014). Evaluating bias of illumina-based bacterial 16S rRNA gene profiles. *Applied and environmental microbiology*, 80(18), 5717–5722.  
<https://doi.org/10.1128/AEM.01451-14>.
- Krotman, Y., Yergaliyev, T.M., Alexander Shani, R. *et al.* (2020). Dissecting the factors shaping fish skin microbiomes in a heterogeneous inland water system. *Microbiome* 8(9). <https://doi.org/10.1186/s40168-020-0784-5>.
- Kulczykowska E. (2019). Stress Response System in the Fish Skin-Welfare Measures Revisited. *Frontiers in physiology*, 10, 72.  
<https://doi.org/10.3389/fphys.2019.00072>.
- Larsen, A., Tao, Z., Bullard, S. A., & Arias, C. R. (2013). Diversity of the skin microbiota of fishes: evidence for host species specificity. *FEMS microbiology ecology*, 85(3), 483–494. <https://doi.org/10.1111/1574-6941.12136>.
- LaSarre, B., Deutschbauer, A. M., Love, C. E., & McKinlay, J. B. (2020). Covert cross-feeding revealed by genome-wide analysis of fitness determinants in a synthetic

bacterial mutualism. *Applied and environmental microbiology*, AEM.00543-20.

Advance online publication.

Laukens, D., Brinkman, B. M., Raes, J., De Vos, M., & Vandenabeele, P. (2016).

Heterogeneity of the gut microbiome in mice: guidelines for optimizing experimental design. *FEMS microbiology reviews*, 40(1), 117–132.

<https://doi.org/10.1093/femsre/fuv036>.

Legrand, T., Catalano, S. R., Wos-Oxley, M. L., Stephens, F., Landos, M., Bansemer, M.

S., Stone, D., Qin, J. G., & Oxley, A. (2018). The Inner Workings of the Outer Surface: Skin and Gill Microbiota as Indicators of Changing Gut Health in Yellowtail Kingfish. *Frontiers in microbiology*, 8, 2664.

<https://doi.org/10.3389/fmicb.2017.02664>

Lee F, Simon KS, Perry GLW. 2017. Increasing agricultural land use is associated with the spread of an invasive fish (*Gambusia affinis*). *Sci Total Environ*. 2017 May 15;586:1113-1123. doi: 10.1016/j.scitotenv.2017.02.101

Lee, S. M., Donaldson, G. P., Mikulski, Z., Boyajian, S., Ley, K., & Mazmanian, S. K. (2013). Bacterial colonization factors control specificity and stability of the gut microbiota. *Nature*, 501(7467), 426–429. doi:10.1038/nature12447

Leo Lahti, Sudarshan Shetty et al. (2017). Tools for microbiome analysis in R. Microbiome package version 1.9.95. *Bioconductor*.

Li, X., Yan, Q., Ringø, E., Wu, X., He, Y., & Yang, D. (2016). The influence of weight and gender on intestinal bacterial community of wild largemouth bronze gudgeon (*Coreius guichenoti*, 1874). *BMC microbiology*, 16(1), 191. <https://doi.org/10.1186/s12866-016-0809-1>.

- Longford, S.R., Campbell, A.H., Nielsen, S. *et al.* (2019). Interactions within the microbiome alter microbial interactions with host chemical defenses and affect disease in a marine holobiont. *Sci Rep* (9), 1363. <https://doi.org/10.1038/s41598-018-37062-z>
- Louca, S., Doebeli, M. & Parfrey, L.W. (2018). Correcting for 16S rRNA gene copy numbers in microbiome surveys remains an unsolved problem. *Microbiome* (6), 41. <https://doi.org/10.1186/s40168-018-0420-9>
- Lozupone, CA, Stombaugh, JI, Gordon, JI, Jansson, JK, Knight, R. 2012. Diversity, stability and resilience of the human gut microbiota. *Nature*. 489(7415):220–230.
- Mach, N., Berri, M., Estelle, J., Levenez, F., Lemonnier, G., Denis, C., ... Lepage, P. (2015). Early life establishment of swine gut microbiome and impact on host phenotypes. *Environmental Microbiology Reports*, 7(3), 554-569. doi:10.1111/1758-2229.12285
- Magurran, A. E. (1988). Ecological Diversity and its Measurement. Princeton University Press, Princeton, NJ.
- Malone, D. C., Hines, L. E., & Graff, J. S. (2014). The good, the bad, and the different: a primer on aspects of heterogeneity of treatment effects. *Journal of managed care & specialty pharmacy*, 20(6), 555–563. <https://doi.org/10.18553/jmcp.2014.20.6.555>
- Marcobal, A., Southwick, A. M., Earle, K. A., & Sonnenburg, J. L. (2013). A refined palate: bacterial consumption of host glycans in the gut. *Glycobiology*, 23(9), 1038–1046. <https://doi.org/10.1093/glycob/cwt040>

- Markle, J. G., Frank, D. N., Mortin-Toth, S., Robertson, C. E., Feazel, L. M., Rolfe-Kampczyk, U., von Bergen, M., McCoy, K. D., Macpherson, A. J., & Danska, J. S. (2013). Sex differences in the gut microbiome drive hormone-dependent regulation of autoimmunity. *Science (New York, N.Y.)*, 339(6123), 1084–1088. <https://doi.org/10.1126/science.1233521>.
- McMurdie PJ, Holmes S (2013). “phyloseq: An R package for reproducible interactive analysis and graphics of microbiome census data.” *PLoS ONE*, 8(4), e61217. <http://dx.plos.org/10.1371/journal.pone.0061217>.
- Miller, E. A., Beasley, D. E., Dunn, R. R., & Archie, E. A. (2016). Lactobacilli Dominance and Vaginal pH: Why Is the Human Vaginal Microbiome Unique?. *Frontiers in microbiology*, 7, 1936. <https://doi.org/10.3389/fmicb.2016.01936>
- Milshcheyn, A., Colosimo, D. A., & Brady, S. F. (2018). Accessing Bioactive Natural Products from the Human Microbiome. *Cell host & microbe*, 23(6), 725–736. <https://doi.org/10.1016/j.chom.2018.05.013>.
- Modi SR, Collins JJ, Relman DA. Antibiotics and the gut microbiota. *J Clin Invest*. 2014;124:4212–8. <https://doi.org/10.1172/JCI72333>.
- Morin, M., Pierce, E. C., & Dutton, R. J. (2018). Changes in the genetic requirements for microbial interactions with increasing community complexity. *eLife*, 7, e37072. <https://doi.org/10.7554/eLife.37072>.
- Moya A and Ferrer M. (2016). Functional Redundancy- Induced Stability of Gut Microbiota Subjected to Disturbance. *Trends in Microbiology*, May 2016, Vol. 24, No. 5 <http://dx.doi.org/10.1016/j.tim.2016.02.002>
- Mueller, S., Saunier, K., Hanisch, C., Norin, E., Alm, L., Midtvedt, T., Cresci, A., Silvi, S., Orpianesi, C., Verdenelli, M. C., Clavel, T., Koebnick, C., Zunft, H. J., Doré,

- J., & Blaut, M. (2006). Differences in fecal microbiota in different European study populations in relation to age, gender, and country: a cross-sectional study. *Applied and environmental microbiology*, 72(2), 1027–1033.  
<https://doi.org/10.1128/AEM.72.2.1027-1033.2006>.
- Nagao-Kitamoto, H., & Kamada, N. (2017). Host-microbial Cross-talk in Inflammatory Bowel Disease. *Immune network*, 17(1), 1–12.  
<https://doi.org/10.4110/in.2017.17.1.1>.
- Nobel, Y. R., Cox, L. M., Kirigin, F. F., & Bokulich, N. A. (2015). Metabolic and metagenomic outcomes from early-life pulsed antibiotic treatment. *Nature Communications*, (6), 1-15.
- Oksanen, J F. Guillaume Blanchet, Michael Friendly, Roeland Kindt, Pierre Legendre, Dan McGlinn, Peter R. Minchin, R. B. O'Hara, Gavin L. Simpson, Peter Solymos, M. Henry H. Stevens, Eduard Szoecs and Helene Wagner. (2019). vegan: Community Ecology Package. R package version 2.5-6. <https://CRAN.R-project.org/package=vegan>
- Pantoja-Feliciano, I. G., Clemente, C. J., ... & Dominguez-Bello, G. M. (2013). Biphasic assembly of the murine intestinal microbiota during early development. *ISME J*, (6):1112-5. doi:10.1038/ismej.2013.15.
- Pyke G. H. (2008). Plague minnow or mosquito fish? A review of the biology and impacts of introduced *Gambusia* species. *Annu. Rev. Ecol. Evol. Syst.* 39: 171–191. 10.1146/annurev.ecolsys.39.110707.173451.



- Ratzke, C., Barrere, J. & Gore, J. (2020). Strength of species interactions determines biodiversity and stability in microbial communities. *Nat Ecol Evol*.  
<https://doi.org/10.1038/s41559-020-1099-4>
- Razali, N., Wah, Y. (2011). "Power comparisons of Shapiro–Wilk, Kolmogorov–Smirnov, Lilliefors and Anderson–Darling tests". *Journal of Statistical Modeling and Analytics*. 2 (1): 21–33.
- Roux, N., Lami, R., Salis, P. *et al*. Sea anemone and clownfish microbiota diversity and variation during the initial steps of symbiosis. *Sci Rep* **9**, 19491 (2019).  
<https://doi.org/10.1038/s41598-019-55756-w>
- Scher JU, Ubeda C, Artacho A, Attur M, Isaac S, Reddy SM, et al. Decreased bacterial diversity characterizes the altered gut microbiota in patients with psoriatic arthritis, resembling dysbiosis in inflammatory bowel disease. *Arthritis Rheumatol*. 2015;67:128–139. doi: 10.1002/art.38892.
- Sharon, G., Garg, N., Debelius, J., Knight, R., Dorrestein, P. C., & Mazmanian, S. K. (2014). Specialized metabolites from the microbiome in health and disease. *Cell metabolism*, 20(5), 719–730. <https://doi.org/10.1016/j.cmet.2014.10.016>.
- Shi, N., Li, N., Duan, X., & Niu, H. (2017). Interaction between the gut microbiome and mucosal immune system. *Military Medical Research*, 4, 14.  
<https://doi.org/10.1186/s40779-017-0122-9>.
- Singh, R. K., Chang, H. W., Yan, D., Lee, K. M., Ucmak, D., Wong, K., ... Liao, W. (2017). Influence of diet on the gut microbiome and implications for human health. *Journal of translational medicine*, 15(1), 73. doi:10.1186/s12967-017-1175-y

- Sommer, F., Anderson, J. M., Bharti, R., Raes, J., & Rosenstiel, P. (2017). The resilience of the intestinal microbiota influences health and disease. *Nature reviews. Microbiology*, 15(10), 630–638. <https://doi.org/10.1038/nrmicro.2017.58>.
- Spees, A. M., Wangdi, T., Lopez, C. A., Kingsbury, D. D., Xavier, M. N., Winter, S. E., Tsolis, R. M., & Bäumler, A. J. (2013). Streptomycin-induced inflammation enhances *Escherichia coli* gut colonization through nitrate respiration. *mBio*, 4(4), e00430-13. <https://doi.org/10.1128/mBio.00430-13>
- Starke, R. and Morais, D. (2019). Gene Copy Normalization of the 16S rRNA Gene Cannot Outweigh the Methodological Biases of Sequencing, *Biorxiv*. <https://doi.org/10.1101/813477>.
- Stoddard S.F, Smith B.J., Hein R., Roller B.R.K. and Schmidt T.M. (2015) rrnDB: improved tools for interpreting rRNA gene abundance in bacteria and archaea and a new foundation for future development. *Nucleic Acids Research* 2014; doi: 10.1093/nar/gku1201
- Sudo N. (2014). Microbiome, HPA axis and production of endocrine hormones in the gut. *Advances in experimental medicine and biology*, 817, 177–194. [https://doi.org/10.1007/978-1-4939-0897-4\\_8](https://doi.org/10.1007/978-1-4939-0897-4_8)
- Sylvain, F., Cheaib, B., Llewellyn, M. *et al.* (2016). pH drop impacts differentially skin and gut microbiota of the Amazonian fish tambaqui (*Colossoma macropomum*). *Sci Rep* 6, 32032. <https://doi.org/10.1038/srep32032>
- Tachedjian, G., Aldunate, M., Bradshaw, C. S., Cone, R. A. (2017). The role of lactic acid production by probiotic *Lactobacillus* species in vaginal health. *Research in Microbiology*, 168(9-10), 782-792. [doi.org/10.1016/j.resmic.2017.04.001](https://doi.org/10.1016/j.resmic.2017.04.001)

- The Human Microbiome Project Consortium. (2012). Structure, function and diversity of the healthy human microbiome. *Nature*, 486(7402), 207-214.  
doi:10.1038/nature11234
- Theriot, C. M., & Young, V. B. (2015). Interactions between the gastrointestinal microbiome and *Clostridium difficile*. *Annual Review of Microbiology*, 69, 455-461. doi:10.1146/annurev-micro-091014-104115
- Tilman, D., Downing, J. (1994). Biodiversity and stability in grasslands. *Nature* 367, 363–365. <https://doi.org/10.1038/367363a0>
- Uren Webster, T. M., Consuegra, S., Hitchings, M., & Garcia de Leaniz, C. (2018). Interpopulation Variation in the Atlantic Salmon Microbiome Reflects Environmental and Genetic Diversity. *Applied and environmental microbiology*, 84(16), e00691-18. <https://doi.org/10.1128/AEM.00691-18>.
- Uren Webster, T., M., U., Rodriguez-Barreto, D., Consuegra, S., Garcia de Leaniz., C. (2019). Cortisol-induced signatures of stress in the fish microbiome. *bioRxiv*. doi: <https://doi.org/10.1101/826503>.
- Van Best, N., Hornef, M. W., Savelkoul, P. H. M., & Penders, J. (2015). On the origin of species: Factors shaping the establishment of infant's gut microbiota. *Birth Defects Research, Part C: Embryo Today: Reviews*, 105(4), 240-251.  
doi.org/10.1002/bdrc.21113
- Venturelli, O. S., Carr, A. C., Fisher, G., Hsu, R. H., Lau, R., Bowen, B. P., Hromada, S., Northen, T., & Arkin, A. P. (2018). Deciphering microbial interactions in synthetic human gut microbiome communities. *Molecular systems biology*, 14(6), e8157. <https://doi.org/10.15252/msb.20178157>.

- Waddington C. H. (1957). *The Strategy of the Genes: A Discussion of Some Aspects of Theoretical Biology*. London: Allen & Unwin.
- Walker, L. R. & del Moral, R. (2011). Primary Succession. *In eLS*, (Ed.).  
doi:10.1002/9780470015902.a0003181.pub2
- Wang, L., Zhu, L., & Qin, S. (2019). Gut Microbiota Modulation on Intestinal Mucosal Adaptive Immunity. *Journal of immunology research*, 2019, 4735040.  
<https://doi.org/10.1155/2019/4735040>
- Wickham, H. (2016). *ggplot2: Elegant Graphics for Data Analysis*. Springer-Verlag New York.
- Wiles, T. J., Jemielita, M., Baker, R. P., Schlomann, B. H., Logan, S. L., Ganz, J., Melancon, E., Eisen, J. S., Guillemin, K., & Parthasarathy, R. (2016). Host Gut Motility Promotes Competitive Exclusion within a Model Intestinal Microbiota. *PLoS biology*, 14(7), e1002517.  
<https://doi.org/10.1371/journal.pbio.1002517>
- Wright, E. (2016). Using DECIPHER v2.0 to Analyze Big Biological Sequence Data in R. *The R Journal*, 8(1), 352-359.
- Wu, G. D., Chen, J., Hoffmann, C., Bittinger, K., Chen, Y. Y., Keilbaugh, S. A., ... Lewis, J. D. (2011). Linking long-term dietary patterns with gut microbial enterotypes. *Science* (New York, N.Y.), 334(6052), 105–108.  
doi:10.1126/science.1208344.
- Xavier, R., Mazzei, R., Pérez-Losada, M., Rosado, D., Santos, J. L., Veríssimo, A., & Soares, M. C. (2019). A Risky Business? Habitat and Social Behavior Impact

Skin and Gut Microbiomes in Caribbean Cleaning Gobies. *Frontiers in microbiology*, 10, 716. <https://doi.org/10.3389/fmicb.2019.00716>.

Zeng, M. Y., Inohara, N., & Nuñez, G. (2017). Mechanisms of inflammation-driven bacterial dysbiosis in the gut. *Mucosal immunology*, 10(1), 18–26. <https://doi.org/10.1038/mi.2016.75>

Zhu, W., Winter M. G., Byndloss, M. X., Spiga, L., ... & Winter, S.E. (2018). Precision editing of the gut microbiota ameliorates colitis. *Nature* 553: 208-211.

## VITA

**Javier Angel Gomez**

### EDUCATION

---

2018-2020(Expected) **M.S. in Biology**

Sam Houston State University

Huntsville, TX 77341

Mentor: Dr. Todd P. Primm

2012-2017 **B.S. in Biomedical Sciences**

Sam Houston State University

Huntsville, TX 77341

### SKILLS

---

<i>Programing Skills</i>	<i>Proficiency</i>
The R Project for Statistical Computing	Competent
Python	Competent
<i>Sequencing Technology</i>	
Illumina (MiSeq)	Competent

### EMPLOYMENT

---

2018- Present Teaching Assistant

Department of Biological Sciences

Sam Houston State University

Huntsville, TX 77341

Courses: Intro to Cell Bio and Adv. Cell Bio

2015-2018 Resident Assistant

Department of Residence Life

Sam Houston State University

Huntsville, TX 77445

### ACTIVITIES

---

<i>Scientific Presentations</i>	
Feb 2020	“Pioneer Species Act as Foundation Species Affecting Climax Community Structure on the Fish Skin Microbiome of <i>Gambusia affinis</i> ” <b>Oral</b> Presentation at Texas Academy of Science, Nacogdoches, TX

Feb 2020“Pioneer Species Affect Recovery of Microbial Communities”

**Oral** Presentation at 3-Minute Thesis Competition, Huntsville, TX

Mar 2019“*E. coli* as Pioneer Species Affects Climax Community Composition and Biochemical Profile on the Mucosal Surface of *Gambusia affinis*”

**Oral** Presentation at ASM Texas Branch Spring Meeting, New Braunfels, TX

Nov 2018“Pioneer Species Affect Community Composition and Function During Recovery from Physical Disruption of the Mucosal Microbiome of *Gambusia affinis*”

**Poster** Presentation at ASM Texas Branch Fall Meeting, Corpus Christi, TX

Mar 2018“Microbial Overgrowth Following Disruption is Microbial not Host Driven”

**Poster** Presentation at ASM Texas Branch Spring Meeting, New Braunfels, TX

Apr 2016“Is the Cambrian Explosion Real?”

**Poster** Presentation at SHSU 9<sup>th</sup> Undergrad Research Symposium, Huntsville, TX

### ***Awards***

Spring 2020The Graduate School Aspire Student Scholarship

\$750

Fall 2019The Graduate School Aspire Student Scholarship

\$750

Spring 2019The Graduate School Aspire Student Scholarship

\$750

Fall 2018The Graduate School Graduate Mentoring Scholarship

\$750

Fall 2018College of Science and Engineering Technology Graduate Achievement Scholarship

\$1000

### ***Organizations***

2020–PresentMember of the Texas Academy of Science (TAS)

2018–PresentA.S.P.I.R.E. Scholar

2018–PresentMember of the American Society for Microbiology (ASM).

2018– PresentMember of the American Society for Microbiology (ASM) Texas Branch.

2017– PresentMember of Biological Science Graduate Student Organization (BSGSO)

## **PUBLICATIONS**

---

**Gomez, J.A.**, Cowdrey, M. B., Khuu, M., Primm, T. Foundation Effect on the Fish Skin Microbiome of *Gambusia affinis*. *In preparation*.

**Gomez, J.A.**, & Primm, T. A Review on Fish Skin Microbiomes. *In preparation*

**Gomez, J.A.**, Lopez, L., Means, G., Russell, A., Lynne, A., Bechelli, J. Bacterial Community Profiling of *Ixodes scapularis* ticks from Western New York. *In preparation*

Brumlow, C. E., Luna, R. A., Hollister, E. B., **Gomez, J. A.**, Burcham, L. A., Cowdrey, M. B., & Primm, T. P. (2019). Biochemical but not compositional recovery of skin mucosal microbiome communities after disruption. *Infection and drug resistance*, 12, 399–416. <https://doi.org/10.2147/IDR.S185992>

## TEACHING EXPERIENCE

---

### *Courses Taught*

2019-Present                      Molecular Biology LabBIOL4480  
     Introductory Cell Biology LabBIOL2440  
 (Head TA)  
 Introductory Cell Biology Honors Lab BIOL2440

2018-2019                      Advanced Cell Biology      Lab BIOL4490  
     Introductory Cell Biology Lab   BIOL2440

### *Guest Lectures*

Mar 2018                      Introduction into the Human Genome Project  
     Intro to Cell Biology              BIOL2440

## FUNDING

---

Graduate Student Travel Funds  
 SHSU Office of Graduate Studies  
 March 2018                      \$500  
 Presented at 2018 Spring ASM Texas Branch Meeting in New Braunfels, TX

Graduate Student Travel Funds  
 SHSU Office of Graduate Studies  
 November 2018              \$500  
 Presented at 2018 Fall ASM Texas Branch Meeting in Texas A&M-Corpus Christi, TX